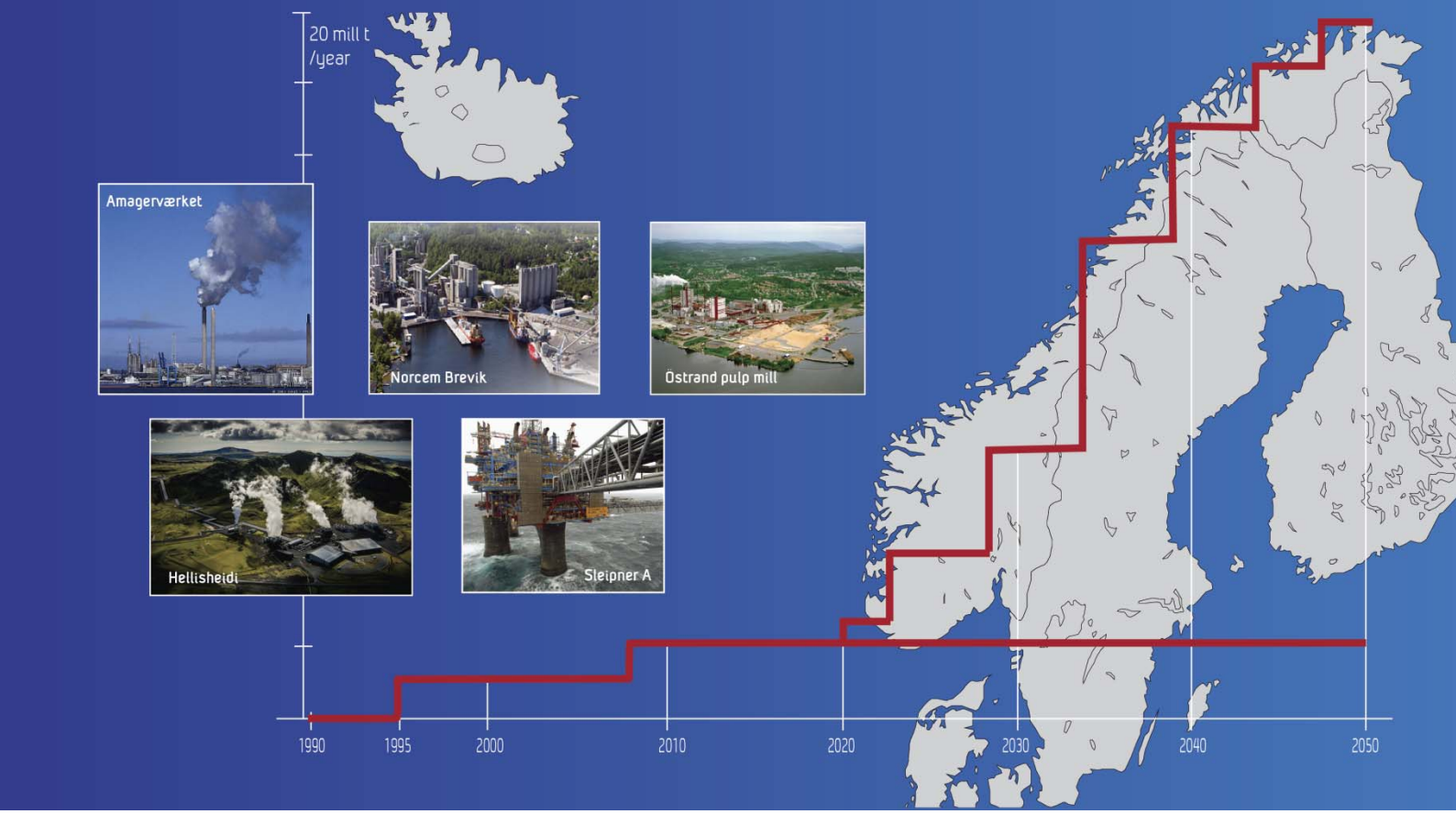

Updated estimate of storage capacity and evaluation of Seal for selected Aquifers (D26)

Ane Lothe, Benjamin Emmel, Per Bergmo,
Gry Möl Mortensen, Peter Frykman

NORDICCS Technical Report D 6.3.1401 (D26)

January 2015

norden
Top-level Research Initiative

nordiccs
Nordic CCS Competence Centre

CO2

NORDICCS concept:

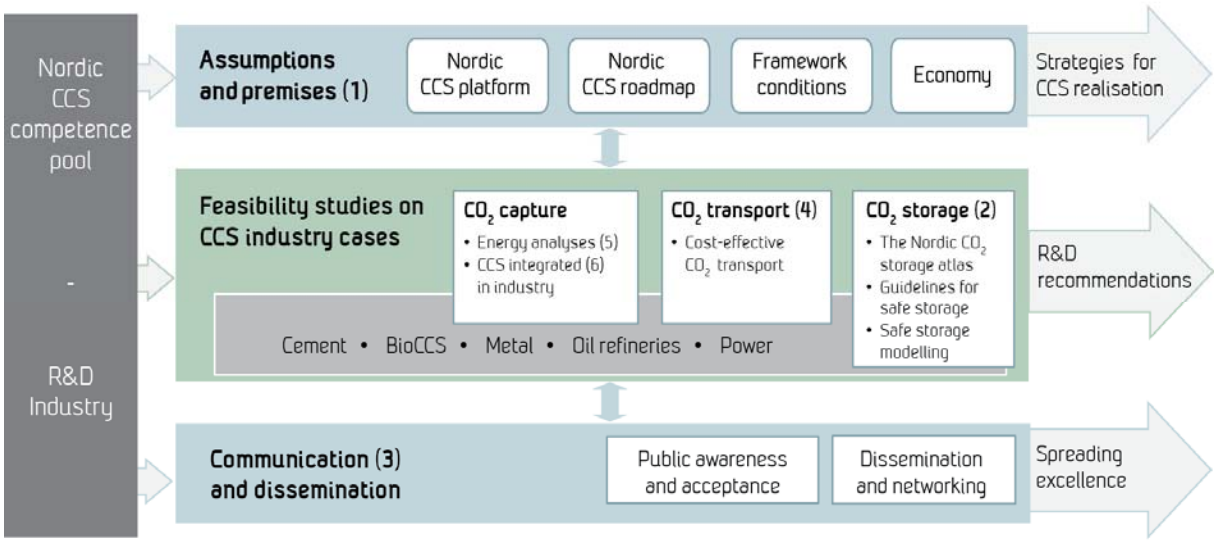

Partners:

VTT · CHALMERS UNIVERSITY OF TECHNOLOGY · IVL Swedish Environmental Research Institute · SGU Sveriges geologiska undersökning Geological Survey of Sweden · GEUS · Orkuveita Reykjavíkur · SINTEF · NTNU · UiO : University of Oslo · tel-tek · University of Iceland · Statoil · GASSCO · NORCEM HEIDELBERGCEMENT Group · VATTENFALL · TECHNOLOGY CENTRE MONGSTAD

Contact: Centre Director Nils A. Røkke • + 47 951 56 181 • Nils.A.Rokke@sintef.no
www.sintef.no/NORDICCS

Summary

In order to quantify the CO_2 storage capacity dynamic modelling has been carried out for different formations including: the Gassum Formation in the Skagerrak area (Norway and Denmark), the Garn Formation at the Trøndelag Platform (Norway), the Faludden sandstone in south-west Scania (Sweden) and the Arnager Greensand Formation in south-east Baltic Sea (Sweden)

The open dipping Gassum Formation has an estimated pore volume of ca. 4.1·1011 m3. Assuming the same storage efficiency for the larger area as in the simulation model would give a storage capacity of 3.7 Gt CO_2 for the north-eastern part of the Gassum Formation. This represent a storage efficiency of 1.6% (plus ~25% dissolved CO_2) in the open dipping aquifer. Dynamic models for the Hanstholm structure, offshore Denmark give a storage capacity of ca. 1.17 Gt. The capacity for the Vedsted structure is c. 0.125 Gt.

The Garn Formation on the Trøndelag Platform offshore middle Norway has in the structural closures a storage capacity of ca. 2.0 Gt to 5.2 Gt. This estimate is made assuming no migration loss and a very low dissolution rate in the traps. Scanning of safe injection sites revealed several locations where CO_2 with a rate of 1 Mt/year could be injected without migrating out of the working area. These sites were verified using different modelling approaches.

The Faludden sandstone can store in structural traps at least 561 Mt CO_2 whereby the storage capacity below 800 m with 10 Mt is drastic lower. The dynamic models indicate that 250 Mt CO_2 can be injected into the sandstone with only 4.1 % migrating to shallow depth below 600 m. For the Arnager Greensand Formation at least 26 Mt CO_2 can be stored in traps whereby the storage capacity below 800 m is reduced to only 10 Mt. The dynamic migration modelling suggests that ca. 225 Mt CO_2 can be injected whereby only 3.3 % would migrate to depths less than 800 m.

Keywords Storage capacity, Dynamic modelling, Norway, Denmark, Sweden

Authors Ane Lothe, Sintef, Norway, Ane.Lothe@sintef.no
Benjamin U. Emmel, SINTEF, Norway, BenjaminUdo.Emmel@sintef.no
Per Bergmo, SINTEF Petroleum Research, Norway, Per.Bergmo@sintef.no
Gry Møl Mortensen, Geological Survey of Sweden, Sweden, Gry.Mol.Mortensen@sgu.se
Peter Frykman, GEUS, Denmark, pfr@geus.dk

Date January 2015

norden
Top-level Research Initiative

About NORDICCS

Nordic CCS Competence Centre, NORDICCS, is a networking platform for increased CCS deployment in the Nordic countries. NORDICCS has 10 research partners and six industry partners, is led by SINTEF Energy Research, and is supported by Nordic Innovation through the Top-level Research Initiative.

For more information regarding NORDICCS and available reports, please visit http://www.sintef.no/NORDICCS.

Project 11029

Table of contents

1.Introduction

This report, D6.3.1401 "Update estimate of storage capacity and evaluation of Seal for selected Aquifers" is an updated and expanded version of report D 6.3.1302 "A first estimation of storage potential for selected aquifer cases (D25)". The aim with this report is to present storage capacity for selected aquifers in Norway, Sweden and Denmark.

The simulation in Chapter 3 (Gassum Formation, Skagerrak) is carried out by Per Bergmo (SINTEF), Chapter 4 (Trøndelag Platform) by Benjamin Emmel, Per Bergmo and Ane Lothe (all SINTEF), Chapter 5 and 6 (Hanstholm and Vedsted) by Peter Frykman (GEUS). Gry Møl Mortensen (SGU) wrote the geological description of the Faludden sandstone and Amager Greenstone in Chapter 7 and 8, while the corresponding simulations have been carried out by Benjamin Emmel and Per Bergmo (both SINTEF).

2. Overview of the selected sites in Norway, Sweden and Denmark

Here is an overview of possible storage candidates for Norway, Denmark and Sweden.

2.1 Norway

Several units are potentially well suited for CO_2 storage in the North Sea (Halland 2012), Norwegian Sea (Bøe et al. 2005, Lundin et al. 2005, Halland et al. 2013a) and in the Barents Sea (Halland et al. 2013b). During the last years SINTEF PR has been carrying out reservoir modelling in several areas:

- For the Gassum Formation, in the Norwegian and partly also Danish part of Skagerrak (Bergmo et al. 2011, Bergmo et al. 2013).
- The Johansen Formation, east of Troll, is a potential storage site that has been investigated by several (e.g. Eigestad et al. 2009, Bergmo et al. 2009).
- Utsira Formation (e.g. Zweigel et al. 2004, Lindeberg et al. 2009) and Utsira South (Bergmo et al. 2009)
- For the Garn Formation at the Trøndelag Platform, offshore Mid-Norway SINTEF PR has carried out migration modelling using SEMI (Rinna et al. 2013, Lothe et al. 2013, Grøver et al. 2013, Lothe et al. 2014).

Another possible site could be the

- Skade and Utsira Fm together, this is mapped by the Norwegian Petroleum Directorate (NPD) as a very promising storage formation). However, at present we do not have access to this data in the NORDICCS project.

A recent publication by Anthonsen et al. (2014), gives an overview of the ten most prospective storage formations in Norway, based on a ranking criteria presented in the same article (Table 2-2a and b).

Based on data availability, scanning of sites and ranking it was agreed to carry out capacity estimate using dynamic simulations for the Gassum Formation, Skagerrak area and the Trøndelag Platform area, offshore Norway. Additionally dynamic modelling CO_2 storage capacities were estimated for areas in south-east Baltic and Scania, Sweden. The results are presented in the Chapter 3 to 8.

Table 2-1 Overview of possible aquifers in Norwegian Part of the North Sea. From NPD Storage Atlas.

Evaluated Aquifers	Avg depth	Bulk volume	Pore volume	Avg K	Open/ Closed	Storage eff	Density	Storage capacity
	m	m^3	m^3	mD		%	t/Rm^3	Gtons
Utsira Formation and Skade	1000	2.49E+12	5.26E+11	>1000	Half Open	4	0.75	15.77
Bryne/Sandnes Formations	1700	5.04E+12	4.41E+11	150	Half Open	4.5	0.69	13.6
Sognefjord Delta East	1750	5.54E+11	1.08E+11	300	Half Open	5.5	0.69	4.09
Statfjord Formation East	2400	1.13E+12	1.21E+11	200	Half Open	4.5	0.66	3.59
Gassum Formation	1700	6.53E+11	7.61E+10	450	Half Open	5.5	0.68	2.85
Farsund Basin	2000	8.55E+11	8.21E+10	150	Half Open	4	0.7	2.3
Johansen and Cook Fm.	1700	N/A	9.14E+10	300	Faults	3	0.65	1.78
Fiskebank Formation	1600	1.00E+11	2.50E+10	1000	Half Open	5.5	0.7	0.96
Stord Basin, Jurassic model	1450	2.70E+11	1.62E+10	5-20	Half Open	0.8	0.71	0.1
Hugin East	1700	1.93E+10	2.42E+09	500	Half Open	5.5	0.7	0.09

Table 2-2a The ten most prospective storage units in Norway, Part I. From Anthonsen et al. (2014), references therein.

Ranking criteria	Sognefjord Fm. (unit) North Sea	Krossfjord Fm. (unit) North Sea	Utsira Fm. (unit) North Sea	Skade Fm. (unit) North Sea Bøe et al. (2002)	Heimdal Fm. (unit)
Ranking score (max. 45)	45	45	44	44	44
Storage Capacity (Mt)	11465	3977	21300	7560	5112
Reservoir properties					
Age / primary reservoir fm.	Late Jurassic Sognefjord Fm.	Middle Jurassic Krossfjord Fm.	Late Middle Miocene to Upper Pliocene Utsira Fm.	Early Miocene Skade Fm.	Palaeocene Heimdal Fm.,
Depth, top (msl.)	1400-2000*	1650-2250*	450 to 1500 m. Central Viking Graben 500-750 m	850-1140	2000-2100
Porosity (%)	18-25*	25	21	35	25-30
Permeability (mD)	150-300*	400	1000	?	800-1000
Heterogeneity (N/G)	0.9	0.8	0.7	0.7	0.85
Facies	Wave dominated asymmetric deltaic coast (Dreyer et al., 2005)	Shallow marine, wave- to tide dominated shoreface deposits (Holgate et al.,2013)	Marine environment with reworked sheet sands (Eidvin et al. 2002, Gregersen & Rundberg, 2007)	Marine turbidite deposits with thin claystone interbeds (Eidvin et al. 2002, Gregersen & Rundberg, 2007)	Viking Graben: Submarine fans (Isaksen & Tonstad 1989)
Pore pressure**	<hs	<hs	<hs	<hs	<hs
Net sand thickness (m)	55-180*	65-135*	max. 350	120	50-295
Seal properties					
Primary seal fm.	Draupne Fm. in the Horda Platform	Heather Fm	Upper Nordland Gr.	Hordaland Gr.	Lista Fm.
Thickness (m)	Several hundred meters**	1000m in graben	500-1500 m (Bøe et al. 2002)	100 m	50-several hundred meters (Isaksen & Tonstad 1989)
Lithology	claystone	Siltstone and silty claystone	claystone	claystone	shale
Fault intensity	low	low	low	low	medium
Lateral extend	continuous	continuous	continuous	widespread	widespread
Multiple seals	yes	yes	no	yes	yes, Sele and Balder Fm.
Safety					
Seismicity	low	low	low	low	low
Groundwater contamination	no	no	no	no	no

Data coverage					
Wells	Several, type well 31/2-1**	Several, type well 31/2-1**	Several, type well 16/1-1	Type well 24/12-1	Type well 24/4-1
Seismic survey	2D, 3D	2D and 3D	2D and 3D	2D and 3D	2D and 3D

*Different fault blocks
** Vollset & Dore 1984

Table 2-2b The ten most prospective storage units in Norway, Part II. From Anthonsen et al. (2014), references therein.

Ranking criteria	Fensfjord Fm. (unit) North Sea	Frigg Fm. North Sea	Garn Fm. Norwegian Sea	Johansen Fm.	Statfjord Group North Sea
Ranking score (max. 45)	44	44	43	42	42
Storage Capacity (Mt)	4100	1164	8003	861	1850
Reservoir properties					
Age primary reservoir fm.	Middle Jurassic Fensfjord Fm.	Early Eocene Frigg Fm.	Middle Jurassic Garn Fm.	Lower Jurassic Johansen Fm.	Late Triassic-Early Jurassic Statfjord Gr.
Depth, top (msl.)	1550-1850	1800	1200-1750	2000-2700	1800-2750
Porosity (%)	25	30	20-25	0.1	22
Permeability (mD)	150	1000	400-500	400	200
Heterogeneity (N/G)	0.8	0.85	0.2-0.5	0.8	0.5
Facies	Shallow marine, wave- to tide dominated shoreface deposits (Holgate et al.,2013)	Submarine fans with stacked channels, lobe and interchannels sandstone interval with shales in between (Bowman 1998; Heritier et al, 1980)	Progradation of braided river systems and delta front (Dalland et al., 1988)	Wave dominated asymmetric deltaic coast (Sundal et al. submitted)	Transition from continental to shallow marine (Vollset & Dore 1984)
Pore pressure**	Moderate	<hs	<hs	Some parts have overpressure	Parts are overpressured
Net sand thickness (m)	42-170	155, max thickness 300 in block 25/1 (Bøe et al. 2002)	100-185	95-130	95-286
Seal properties					
Primary seal fm.	Heather Fm.	Hordaland Gr.	Viking Gr.	Drake Fm. (above Cook Fm.)	Dunlin Group
Thickness (m)	1000 m in graben (Vollset & Dore 1984)	Several hundred	Approx.	80-100	Several hundred

		metres	1000 m		metres
Lithology	Siltstone and silty claystone	claystone	shale and mudstone	Claystone and shale	Shale's and siltstones
Fault intensity	low	low	low	moderate	low
Lateral extend	wide	wide	wide	wide	wide
Multiple seals	yes	?	yes	yes	?
Safety					
Seismicity	low	low	low	low	low
Groundwater contamination	no	no	no	no	no
Data coverage					
Wells	Many, Type well 31/2-1	Many, Type well 25/1-1	Several, type well 6407/1-3	Several, type well 31/2-1	Several, type well 33/12-2
Seismic survey	2D and 3D	2D and 3D	2D Trøndelag Platform, 2D and 3D in Halten Terrace area	2D and 3D	2D and 3D

2.2 Denmark

As summed up in NORDICCS report D6.2.1201, since 1993 several CO_2 screening and exploration programs have evaluated the Danish CO_2 storage potential. Table 2-3 summarises the storage capacity calculated in the respective exploration programmes through the years.

Table 2-3 Overview of all Danish storage sites evaluated in exploration programs.

Storage sites	Project	Capacity	Remarks
Bunter Sandstone Formation	Joule II	2900 Mt	Storage efficiency factor 6% Storage in traps
Tønder Formation	Joule II	977 Mt	Storage efficiency factor 6% Storage in traps
Gassum Formation	Joule II	1195 Mt	Storage efficiency factor 6% Storage in traps
Haldager Formation	Joule II	325 Mt	Storage efficiency factor 6% Storage in traps
Frederikshavn Formation	Joule II	199 Mt	Storage efficiency factor 6% Storage in traps
Gassum Structure	GESTCO	242 Mt	Storage efficiency factor 40%
Hanstholm Structure	GESTCO Dynamis Skagerrak Project	2752 Mt Max. 3107 Mt Min. 250 Mt	Storage efficiency factor 40%

Havnsø Structure	GESTCO CO2STORE	923 Mt Min. 1028 Mt	Storage efficiency factor 40% Reservoir information from Stenlille natural gas storage.
Horsens Structure	GESTCO	490 Mt	Storage efficiency factor 40% The structure has later been reinterpreted as three minor structures.
Pårup Structure	GESTCO	90 Mt	Storage efficiency factor 40%
Rødby Structure	GESTCO	151 Mt	Storage efficiency factor 40%
Stenlille Structure	GESTCO	62 Mt	Storage efficiency factor 40% Presently natural gas storage.
Thisted Structure	GESTCO	11187 Mt	Storage efficiency factor 40%
Tønder Structure	GESTCO	93 Mt	Storage efficiency factor 40%
Vedsted Structure	GESTCO Vedsted Demo-project	161 Mt 100 Mt	Storage efficiency factor 40% Initial reservoir modelling result. No public data.
Voldum Structure	GESTCO	288 Mt	Storage efficiency factor 40%
Røsnæs Structure	CO2STORE	227 Mt	Storage efficiency factor 40%
Skagerrak Area 2	Climit NORDICCS	Min. 250 Mt 3700 Mt	Gently dipping open aquifer Based on modelling
SNS 1 SNS 2 SNS 3	NORDICCS	135 Mt 1458 Mt 98 Mt	Storage efficiency factor 40% Storage efficiency factor 40% Storage efficiency factor 40%
WBS 1 WBS 2 WBS 3 WBS 4 WBS 5 WBS 6 WBS 7 WBS 8 WBS 9	NORDICCS	245 Mt 305 Mt 26 Mt 328 Mt 149 Mt 236 Mt 51 Mt 187 Mt 14 Mt	Storage efficiency factor 40% Storage efficiency factor 40% Storage efficiency factor 40% Storage efficiency factor 40% Storage efficiency factor 40% Storage efficiency factor 40% Storage efficiency factor 40% Storage efficiency factor 40% Storage efficiency factor 40%
Oil & Gas fields	Joule II GESTCO GeoCapacity	590 Mt 628 Mt 810 Mt	Data from 16 fields Data from 11 fields Data from 17 fields

2.3 Sweden

In Sweden eight potential storage units and one trap have been identified (Mortensen 2014, Anthonsen et al. 2013, Erlström et al. 2011, Erlström & Sivhed 2012). According to a ranking procedure in the frame of NORDICCS (Bergmo 2013; Aaagaard et al. 2014)(Table 2-4) the three most promising sites were selected and are represented as follows:

- The Faludden sandstone in the south-east Baltic Sea
- The Arnager Greensand Formation in the south-west Scania
- The Höganäs-Rya sequence (equiv. Gassum Fm.) in the south-west Scania

We have done capacity estimate based on dynamic modelling for two formations. Chapter 7 shows the result for the Faludden Sandstone and Chapter 8 summary the modelling results for the Arnager Greensand Formations.

Table 2-4 Overview of potential storage sites in Sweden, ranked according to NORDICCS (Bergmo 2014)

Storage unit (u) or trap (t)			**Reservoir properties**						**Seal properties**					**Safety/ risk**		Maturity /data coverage	
Name	Storage capacity in Mt	Total Score	Depth	Porosity	Permeability	Heterogeneity	Pore pressure	Thickness/	Thickness	Fault intensity	Lateral extend	Multiple seals	Lithology	Seismicity	Groundwater	Well data	Seismic
Faludden (u)	745	40	3	2	3	3	2	2	3	3	3	3	2	3	3	3	2
Arnager Greensand (u)	521	39	3	3	3	3	3	2	3	2	3	2	2	3	2	3	2
Höganäs-Rya (u)	543	39	3	3	3	3	3	2	3	2	3	3	2	3	2	3	1
L.Cretaceous sands, unit A (u)	330	39	3	3	3	3	3	2	3	2	3	3	2	3	2	3	1
Dalders structure (t)	22	38	3	2	2	3	2	2	3	3	3	3	2	3	3	3	1
När (u)	426	37	3	2	2	3	3	2	3	3	1	3	2	3	3	3	1
Bunter Sandstone (u)	165	37	3	2	2	3	3	2	3	2	3	3	2	3	2	3	1
Viklau (u)	553	36	3	1	2	3	3	2	3	3	1	3	2	3	3	3	1
L.Cretaceous sands, unit B (u)	115	36	3	3	3	3	3	3	3	2	3	3	2	2	1	3	1

3. Simulations for the Gassum Formation, Skagerrak area

The Upper Triassic Gassum Formation is deposited in the whole Skagerrak-Kattegat area (see Figure 3-1). Three reservoir models have been built and the results from the simulations will be presented and discussed.

The work presented here for this formation is carried out built on data and earlier work from a Climit programme (Project number 194492), sponsored by Gassnova and industry. It has been updated and published in D6.3.1203 and Bergmo et al. (2011), in addition as NORDICCS deliverable

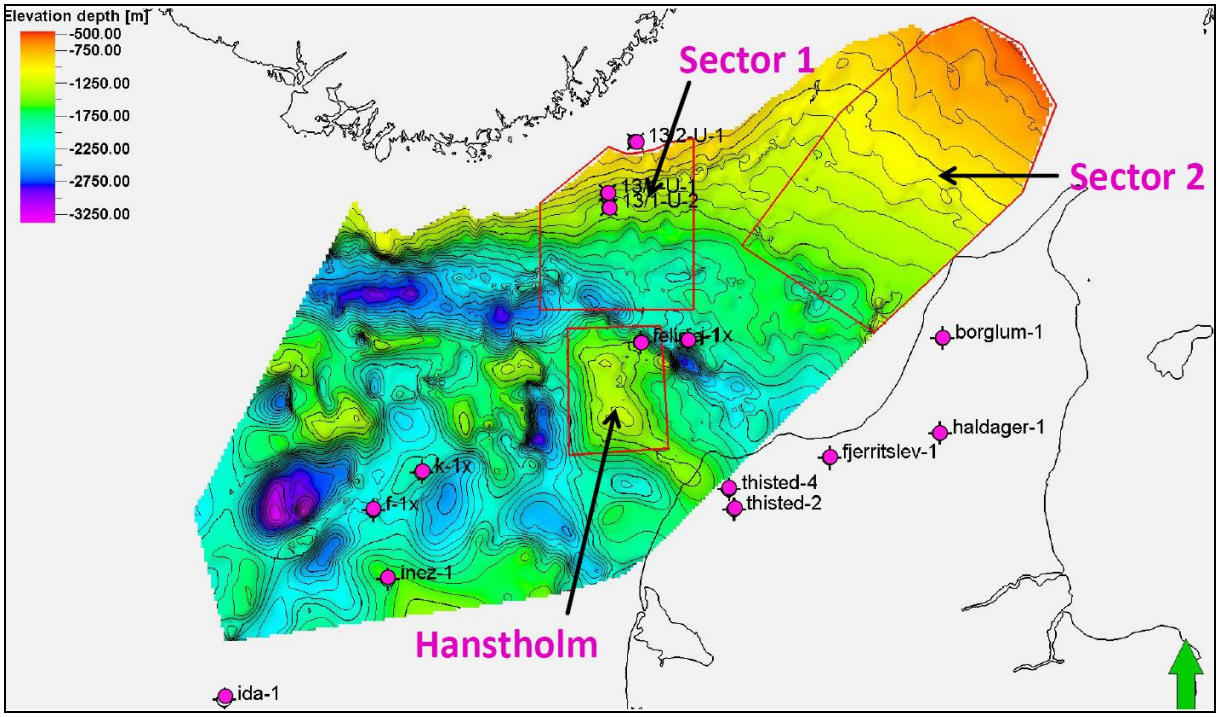

Figure 3-1 **Overview map for the top Gassum Formation surface in the Skagerrak area. The modelled areas are marked as Model 1, Model 2 and the southern Hanstholm area. Colour scale in meters.**

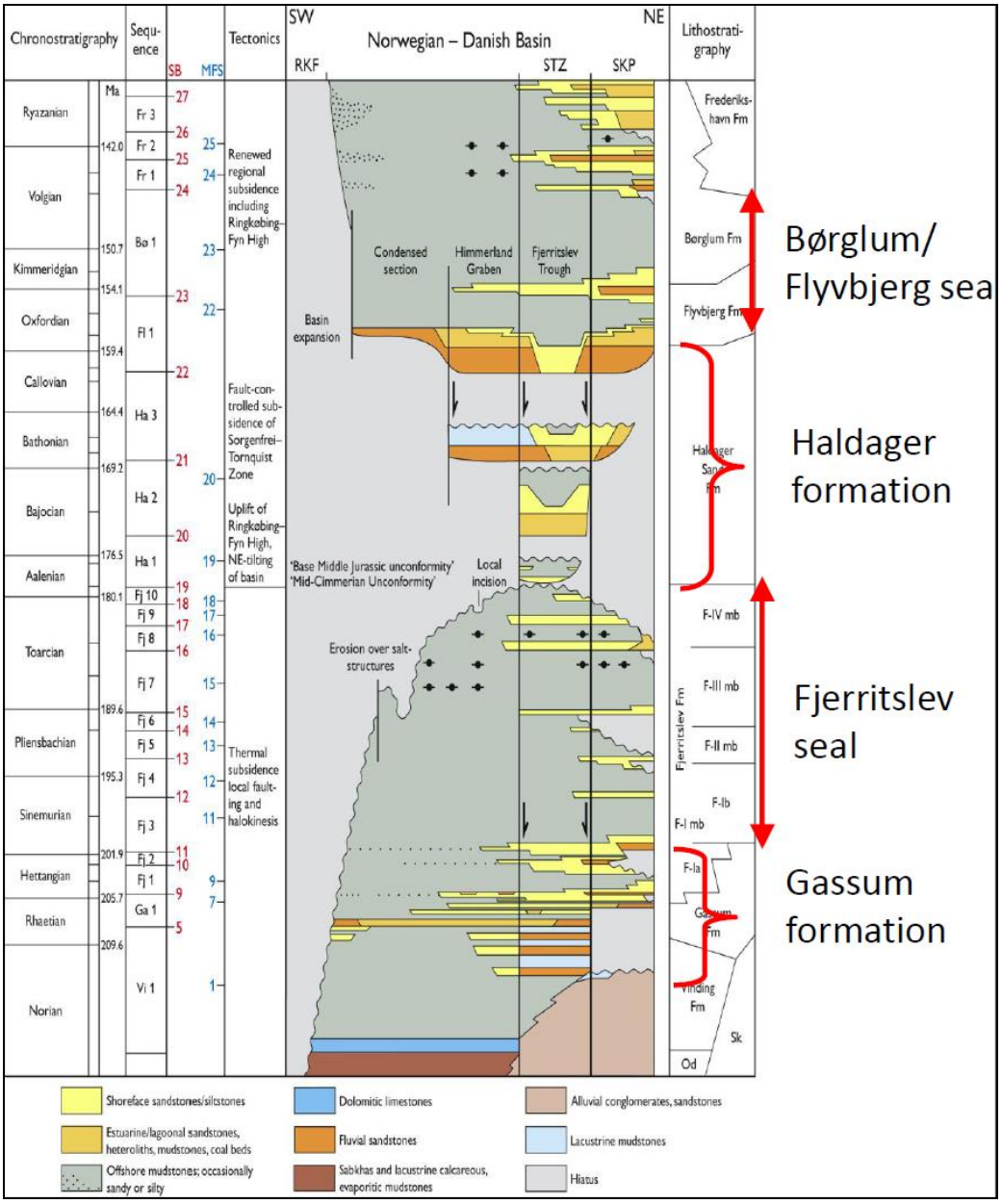

Figure 3-2 Lithostratigraphic column from the Norwegian-Danish Basin (Nielsen 2003).

3.1 Background

The Skagerrak-Kattegat area between Denmark, Sweden and Norway has no previous record of oil exploration or other activities which could have resulted in extensive mapping of the sub-surface. The data coverage is therefore scarce compared to regions in the North Sea and the density of data is decreasing as one moves eastward in Skagerrak. An initial screening of possible CO_2 storage sites in the region has been performed based on published work, new interpretations of seismic lines and interpretation of available well logs.

The screening has revealed large open/semi-closed dipping aquifers in the Upper Triassic Gassum (Fawad et al. 2011), which is evaluated for CO_2 storage. This work presents reservoir simulations of CO_2 injection into

the Gassum in the area north and north-east of the Fjerritslev Trough. In addition a model of the Hanstholm structure, offshore Denmark has been constructed on which initial simulations have been performed for estimating storage capacity.

The Gassum Formation is overlain by thick marine mudstones of the Fjerritslev Formation, which is characterized by large lateral continuity, forming a highly competent cap rock unit probably making the Gassum Formation one of the most promising reservoirs for CO_2 storage in the study area (Figure 3-2). Here we only present results from simulations of CO_2 injection into the Gassum Formation and it is assumed that the Fjerritslev Formation is sealing.

3.2 Model set up

Three locations in the Skagerrak region have been investigated for CO_2 injection in this study (Figure 3-1). Two open dipping aquifer models in the Gassum Formation (Model 1, Model 2) with homogenous net thickness were made. In addition a model of the Hanstholm structure just south of Model 1 has been constructed on which initial simulations were performed for estimating storage capacity.

Location of Model 1 and Model 2 was decided based on the concept of storing CO_2 in an open dipping trap. The injection points should therefore be located down flank of a gentle dipping formation. The main short term mechanism for trapping CO_2 is assumed to be capillary trapping of CO_2 as residual phase. In addition, the long migration distance of the injected CO_2 will enhance the dissolution of CO_2 into the formation water. The Hanstholm structure is assumed to be a closed structure and was chosen for its size. The main short term trapping mechanism is assumed to be capillary trapping by the assumed sealing cap rock.

Reservoir properties are based on petrophysical logs from 12 Danish wells (including 6 offshore wells). No wells penetrate the model areas and average properties of the wells have been used. No thickness maps of formations were available when the reservoir models were built and a constant effective thickness was assumed. The model thicknesses are equal to the average net thickness in the well logs (not weighted) giving 50 meter thickness for Gassum Formation. Average effective porosity from the well logs is 23%, but a linear correlation to depth was applied based on average porosity and depth points in the wells. The range of porosity in the two models is between 21% and 29%. Permeability was correlated to porosity by a relationship developed by GEUS for this study based on their regional database. Permeability varies between 200 and 650 mD. Average net permeability from wells is 210 mD.

The open dipping trap models (Model 1 and Model 2) cover a large depth range and hence one can expect a relatively large variation in temperature and salinity of the formation water. A salinity gradient of 75.6 ppm NaCl per meter and a temperature gradient of 31°C/m were assumed based on regional models and well data. In order to model the effect of this on density and viscosity of the formation water and solubility of the injected CO_2, 6 pVT regions (having constant temperature and salinity) were generated for Model 1 and Model 2.

Viscosity and density of the formation water was calculated for each region based on Spivey et al. (2004) and Kestin et al. (1978). The solubility of CO_2 in brine is calculated from a correlation by Spycher et al. 2005. The density of CO_2 is based on an equation of state for CO_2 developed by Span and Wagner (1996). The viscosity of CO_2 was calculated from a correlation by Fenghour et al. (1998).

Due to the relatively large grid block sizes linear relative permeability curves for brine and CO_2 phases were used. Residual CO_2 was set to 20% and residual brine was set to 7%. Measurement on cores from the Utsira Sand at the Sleipner CO_2 injection site (unconsolidated sand stone) indicates residual CO_2 saturation of 25% (Akervoll et al. 2008). Assuming 20% might be on the low side (i.e. will underestimate trapped CO_2) but no measurements were available for the Gassum sandstone.

Initial hydrostatic conditions were assumed, with open/semi-closed boundaries up-dip towards north (Model 1) and northwest (Model 2). The open boundaries to the north were modelled by production wells producing at constant pressure giving amount of CO_2 migrating out of the model as produced CO_2.

3.3 Results

In all three models, a total of 250 million tonnes of CO_2 is injected down-flank using three horizontal injection wells over a period of 25 years. Total simulated time is 4000 years.

Model 1 and Model 2

Injection took place by 3 horizontal injection wells perforated in the bottom layer with distance between injection wells 8 – 10 km. The wells have perforation intervals of 800-1000 meters. Injection depth was approximately 2410 m (Model 1) and 1708 m (Model 2). The well injection rate was 3.33 Mt/year = 4.88·106 Sm3/day/well giving a total of 10 Mt/year.

The results of the simulations on the open dipping traps are shown in Figure 3-3 and Figure 3-4 as distribution of CO_2 saturation. For Model 1, CO_2 reaches the northern border after 400 years, and after 4000 years 7.5% has escaped. The rest is capillary trapped (~74.5%) or dissolved (~18%). Figure 3-3 shows CO_2 saturation in Model 1 after 25 years (stop of injection), after 400 years and after 4000 years when the first CO_2 has reached the open boundary to the North. The open boundary is modelled with constant hydrostatic pressure. Figure 3-4 shows the plume development for Model 2 first after 25 years, secondly after 4000 years. We see that the plume has not spread much, and has not reached the boundaries to the model.

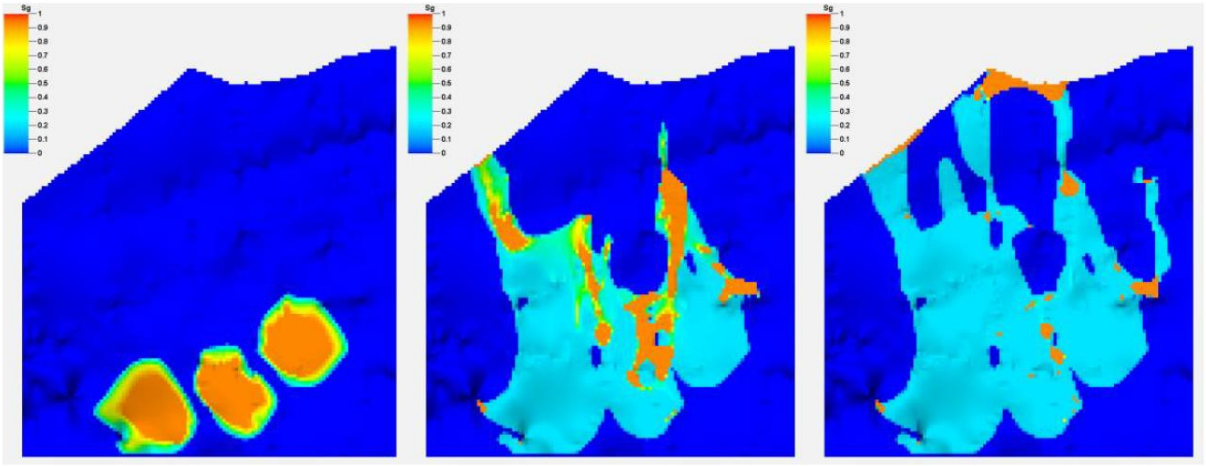

Figure 3-3 Plume development, shown as CO_2 saturation, for Model 1 after 25, 400, and 4000 years after injection stop. The model area is ca. 40 x 50 km.

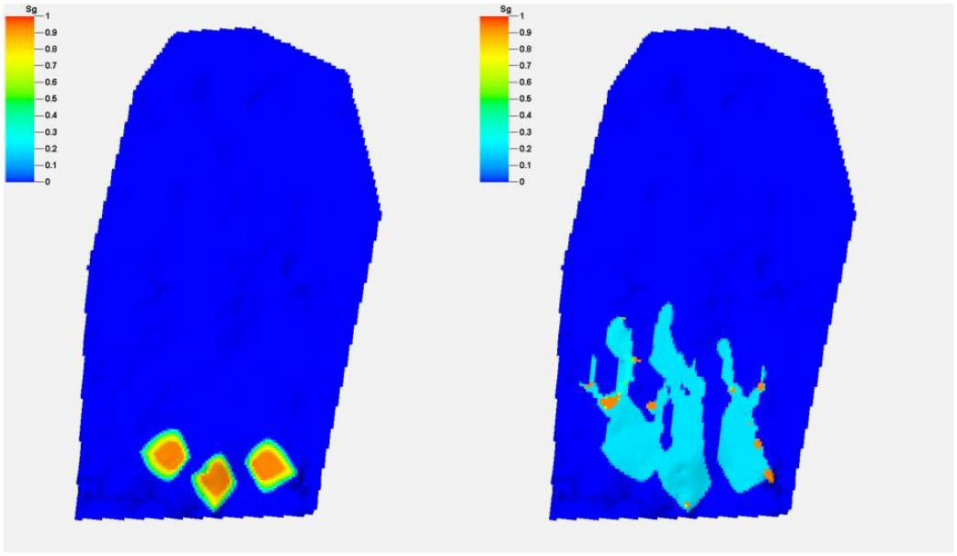

Figure 3-4 Plume development, shown as CO_2 saturation, for Model 2 after 25 year (figure left) and 4000 years (figure right) after injection stop. The model area is ca. 50 x 100 km.

Hanstholm study area

The results of simulation of CO_2 injection in the Hanstholm structure is shown in Figure 3-5. Three horizontal injection wells were located down flank on the western and north-western side of the structure. The injected CO_2 migrates towards the top of the structure and 12.5% is dissolved into the formation water after 4000 years. Figure 3-5 shows CO_2 distribution after 25, 400 and 4000 years.

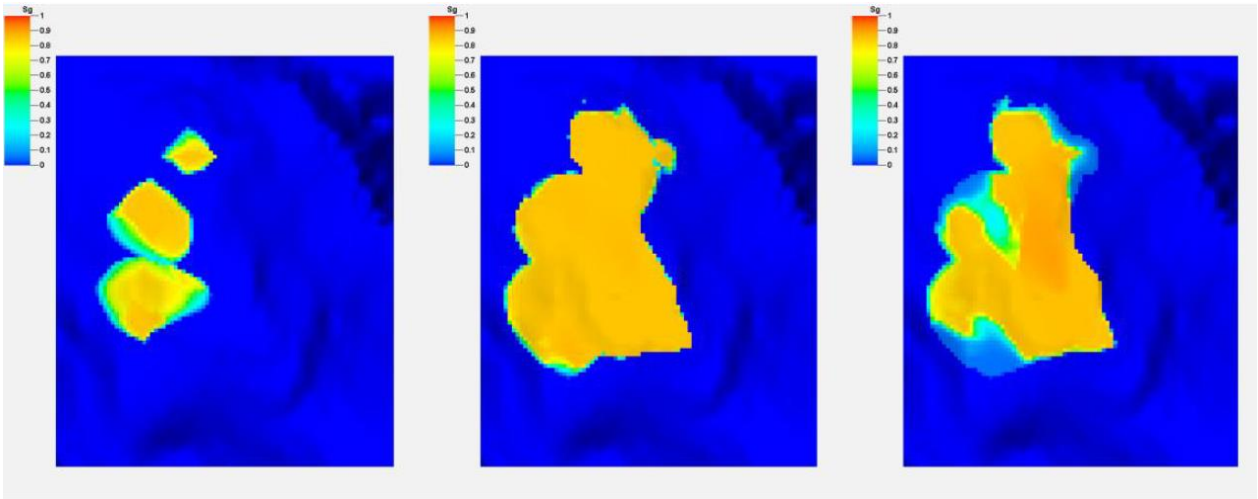

Figure 3-5 Distribution of injected CO_2 in the Hanstholm structure after 25, 400, and 4000 years (from left to right). The model is approximately 34 by 42 km.

3.4 Discussion

The injectivity is mainly a function of the permeability in the regions close to the injection wells. If the injectivity is low the bottom hole pressure (BHP) of the injection well will be high since a higher pressure is needed to push the injection phase at a given rate into the reservoir. Typical parameters affecting

permeability for sand stone reservoirs are burial history and depth (diagenesis), shale content and porosity. A general observation is that the injectivity reduces with increasing depth and increasing shale content.

The increase in BHP for the three horizontal injection wells for Model 1 and Model 2 is around 90 bars in both cases. A safe pressure with respect to fracturing of the cap rock is assumed to be around 75% of the lithostatic pressure but a detailed characterisation of the overburden is needed to estimate this. Estimating a safe pressure increase has not been performed at this stage but the difference between hydrostatic and lithostatic pressure increase with depth enabling a higher safe pressure increase with depth. A first estimate of safe pressure below the cap rock can be calculated by assuming an average density of the overlying formations. An estimate for Model 1 and Model 2 gives safe pressure increases of approximately 108 and 76 bars respectively if assumed sea depth is 100 meter and overburden density is 2000 kg/m3. No maps of sea depth in the injection areas were available but increasing sea depth to 400 meter gives corresponding safe pressure increases of 86 and 54 bars.

If the pressure increase is too high several options exists to reduce it. Increase number of injection wells, produce formation water (will need production wells). The present simulations indicate that the open dipping traps in the Gassum Formation can permanently store 250 Mt CO_2 by residual trapping. More detailed mapping of reservoir and overburden is required for better estimate of safe pressure, required number of injection (and production) wells and better estimates of CO_2 migration in the trap.

The bottom hole pressure increase in the Hanstholm structure are approximately 140 bars when using 3 horizontal injection wells. This is too high although the pressure increase below the cap rock (some distance away from the well perforations) will be lower. The option of increasing the number of injection wells and/or introduce water production wells down flank should therefore be considered. As for the other models a more detailed characterization of the cap rock and overburden is required to determine the safe pressure increase. The structure is however large enough to contain 250 Mt CO_2 assuming the cap rock is sealing.

Parameter sensitivities

In the open dipping traps of Model 1 and Model 2 the lateral migration speed of CO_2 is important for estimating capacity and safety of the storage site. A series of simulations on a synthetic tilted model were performed to investigate migration speed and dissolution rate as function of grid block resolution and capillary pressure. The synthetic model is 1500 by 10 000 meters and has a thickness of 50 m. The tilt of the model is 2° and the top of the model is at 1000 meter depth (shallow part). Porosity and horizontal permeability is 22.5% and 210 mD respectively. Vertical to horizontal permeability ratio is 0.1 and the injection is down flank in one vertical well perforating the bottom layers. Injection rate was 100 000 tonnes of CO_2 per year for three years, total pore volume of the model is around 1.7×10^6 m^3. Grid resolution and capillary pressure were varied in the sensitivity simulations.

Capillary pressure will affect the migration speed and thickness of the CO_2 front. No capillary pressure measurements were available and capillary pressure measured on Utsira sand was used as basis for sensitivity simulations. The Utsira capillary entrance pressure (no gas saturation) equals to 0.01 bars. Simulations were performed with varying capillary pressure by multiplying the measured capillary pressure curve by factors 2, 4, 8, 16, and 32. It is assumed that the capillary pressure in Gassum will be higher than the capillary pressure in Utsira due to the reservoir's grain-size, sorting and assumed cementation (smaller pore throats).
The effect of increasing the capillary pressure on CO_2 distribution is shown in Figure 3-6a for the model with a grid block size of 100 by 100 meters and layer thickness below the top equal to 0.5 meter. It can be seen that an increase in the capillary entry pressure will reduce the total migration distance of the injected CO_2. This is because the migrating CO_2 has to overcome the capillary entry pressure before it can flow into a neighbouring grid block. Thickness of the migrating CO_2 front will thus be larger if the grid layering is fine

enough to capture this. Capillary effects are a pore scale phenomenon and since large scale models have to be coarsely gridded the effect of the capillary pressure is scaled into the grid block size and the critical gas saturation (i.e. the minimum gas saturation necessary for the gas to be mobile). No simulation tests have been performed on how the distribution of CO_2 will depend on critical and residual gas saturation.

The injected CO_2 will due to buoyancy forces migrate along the top of the model. The thickness of the migrating front will in the simulations depend on grid layer thickness and critical gas saturation. These should be balanced to represent the effect of capillary pressure. However, both of these parameters are unknown. Figure 3-6b displays the effect of refining the layers below the top of the model from 5 to 0.5 meter layer thickness. Increasing the layer thickness will reduce the plume length. This is due to increased thickness of the front (one layer in the grid) and because the increased size of the grid blocks will require a larger volume of CO_2 in each grid block to overcome the critical gas saturation. This will slow down the speed of the migrating front. No sensitivity on the gas distribution by refining the areal grid block size has been investigated. Having smaller grid blocks will reduce the gas volume required to overcome the critical gas saturation but this effect will be minor if the coarsest grid resolution is sufficient to resolve the shape of the migrating CO_2.

Dissolution of CO_2 into the formation water is a function of the contact area between the CO_2 phase and under-saturated formation water. In practice this will depend on how large volume CO_2 has swept because almost all the dissolved CO_2 is present in the residual non-mobile water. An increase in migration distance will result in an increase in dissolved CO_2.

Simulations with refined layer thickness below the top were performed for Model 2. Base case simulations which had 5 meter layer thickness would correspond to a very high capillary entry pressure. Results of refining the layers at the top to 1 and 2 meters are shown in Figure 3-7. The migration distance for the refined models is increased but the injected CO_2 is still within the boundaries of the model. Similar increase in migration distance should be expected for Model 1 with the consequence that more CO_2 migrates out of the boundaries of the model.

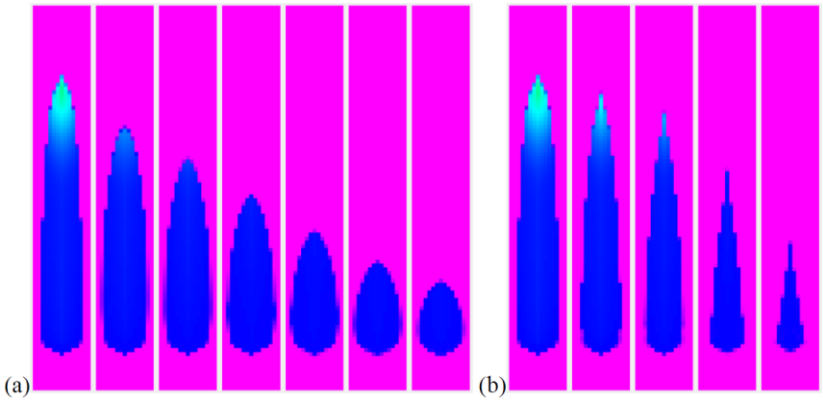

Figure 3-6 **(a) Effect of capillary pressure on migration distance. Capillary entrance pressure in the different simulations was (from left to right): 0 (no capillary pressure), 0.01, 0.02, 0.04, 0.08, 0.16 and 0.32 bar. (b) Plots show CO_2 distribution after migration has stopped. The layer thickness has been varied (from left to right): 0.5 m, 0.75 m, 1 m, 2 m, and 5 m layer thickness.**

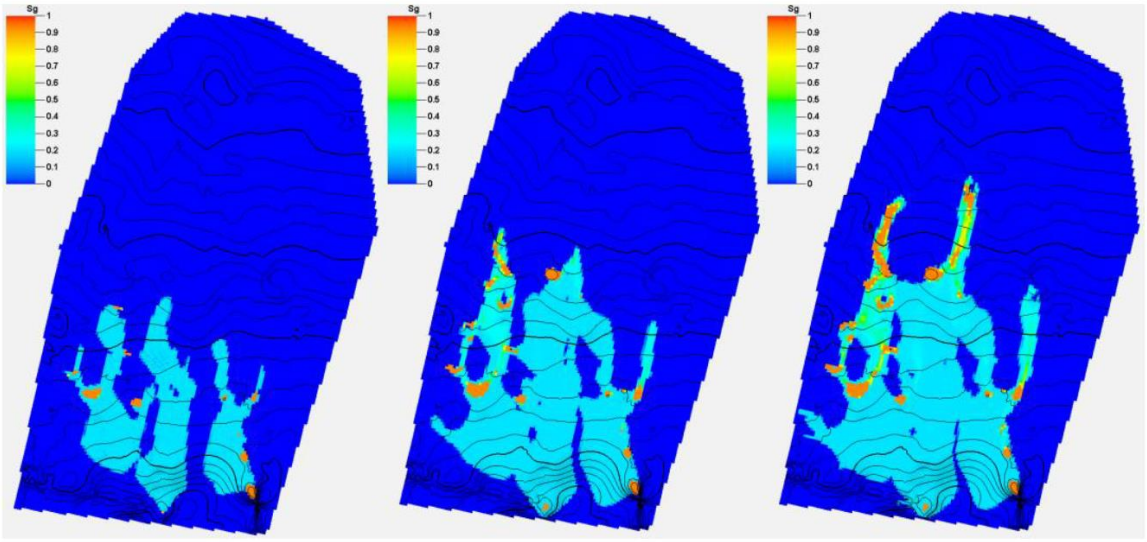

Figure 3-7 Distribution of injected CO_2 after 4000 years for the base case model with uniform layer thickness of 5 m in the whole model (left) and for refined layer thickness below the top equal to 2 m (middle) and 1 m (right).

3.5 An updated Model 2 with facies distribution and faults

Simulations using an updated reservoir model where facies distribution from Nielsen (2003) is included have been performed (Figure 3-8). The new interpretation is built on facies and porosity logs from Børglum-1 and J-1x wells. The major faults are included from seismic.

The NE-SW elongation of the facies bodies are derived from the interpretation of the depositional environment as mainly fluvial to estuarine, with trends perpendicular to the assumed NW-SE trending coastline.

No capillary pressure in the saturation functions is used. The capillary effect is scaled into relative permeability end points and grid resolution. The relative permeability end-points are for irreducible water saturation S_{wir} = 0.07 and critical gas saturation S_{gc} = 0.2. A linear relative permeability functions is used and no hysteresis is included.

The injection rate was set to 10 Mt CO_2 per year for 25, 50 and 100 years. Three horizontal injection wells and three horizontal production wells are used in the simulations (Figure 3-9). Open boundary conditions were set to the North.

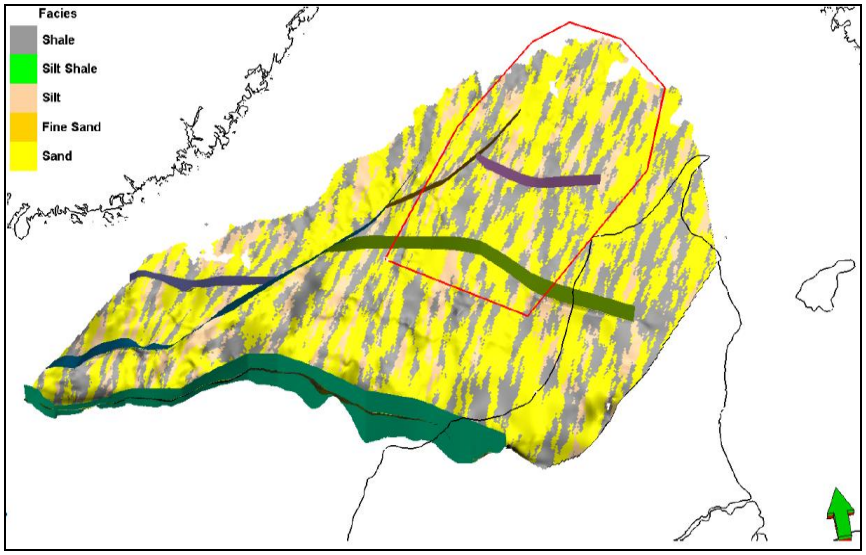

Figure 3-8 **The figure shows facies model for the North-Eastern Gassum Formation. The main facies are sand, silt and shale.**

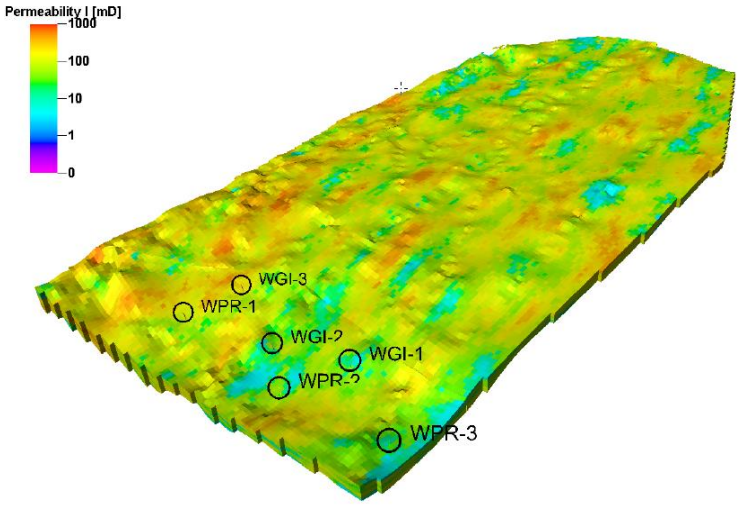

Figure 3-9 **The figure shows estimated permeability distribution for the Gassum Formation in study area model 1, with model updates. The well positions are marked. WGI = injection wells, WPR = Production wells.**

3.6 Results of simulations using new facies model and faults

For model 2, an updated reservoir model was made, based on facies heterogeneities and with faults included. Simulations were carried out on this model with injection of 10 Mt CO_2 per year for 25, 50 and 100 years (250, 500 and 1000 Mt). The simulation results show little spread in the injected gas during injection (see Figure 3-10). Figure 3-11 shows the same amount of injected CO_2 after 4000 years. Actually, we see the same evolving distribution patterns for 250, 500 and 1000 Mt CO_2, but naturally larger areas with highly saturated CO_2 is seen with the largest amount of CO_2 injected and some CO_2 has migrated towards the eastern part for the case with 1000 Mt injected. After 6000 years (Figure 3-12) 3 Mt (e.g. 3‰) has migrated

out of the model through the open boundary in the case when 1000 Mt CO_2 is injected. The other two cases show no CO_2 migration out of the model.

If one compares modelling results for the homogenous model and the heterogeneous model for study area 2, with 500 Mt CO_2 injection after 4000 years, one can observe approximately the same migration pattern for both runs. The difference is that the heterogeneous facies distribution seems to favour slower migration and more CO_2 dissolved and capillary trapped in the deeper part of the formation (see Figure 3-13).

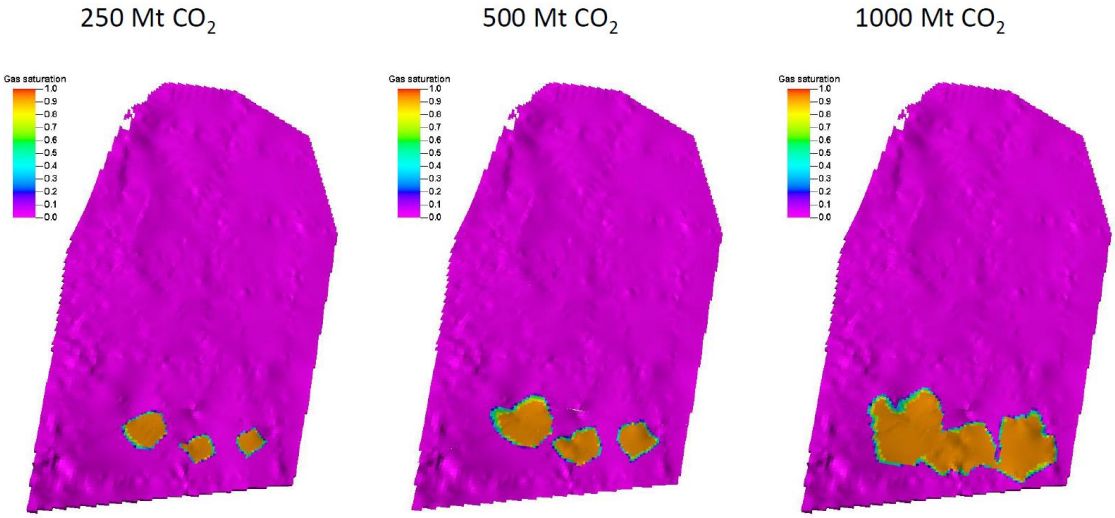

Figure 3-10 The maps shows the initial distribution of CO_2 after the injection period, for 250 Mt, 500 Mt and 1000 Mt CO_2 injected. The injection rate is 10 Mt CO_2 per year. The colour scale shows gas saturation where 1 is fully saturated.

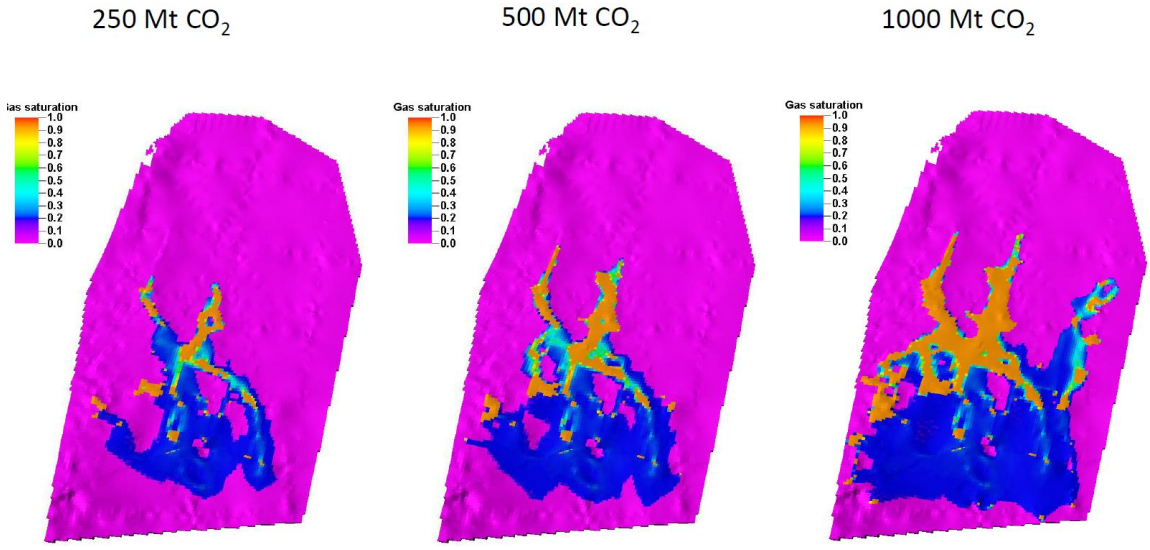

Figure 3-11 The maps shows distribution of CO_2 after 4000 years, for 250 Mt, 500 Mt and 1000 Mt CO_2 injected. The injection rate is 10 Mt CO_2 per year. The colour scale shows gas saturation where 1 is fully saturated.

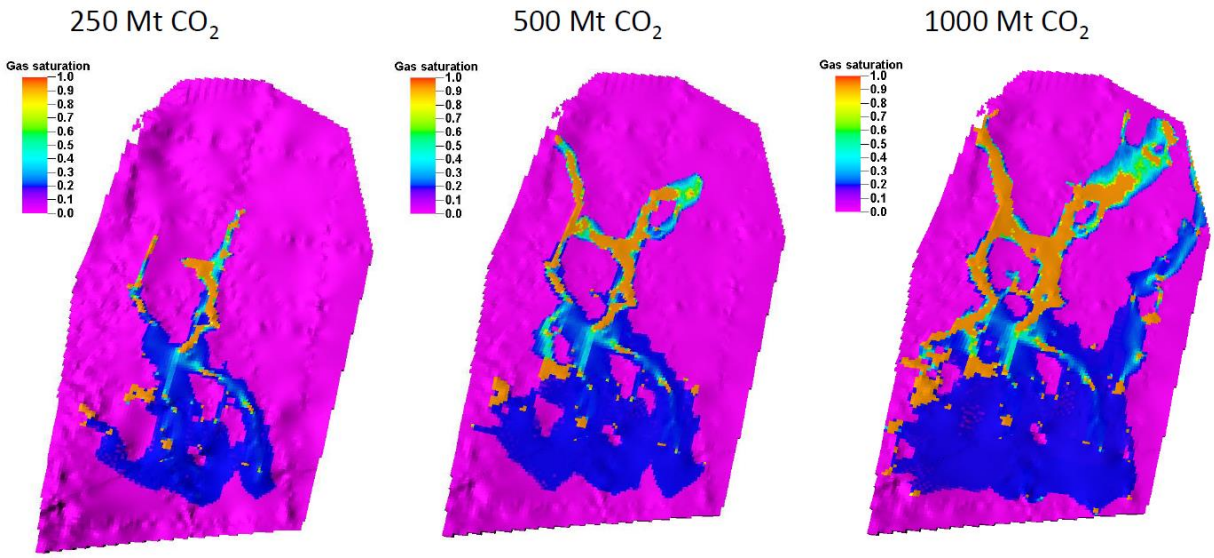

Figure 3-12 The maps shows distribution of CO_2 after 6000 years, for 250 Mt, 500 Mt and 1000 Mt CO_2 injected. The injection rate is 10 Mt CO_2 per year. The colour scale shows gas saturation where 1 is fully saturated.

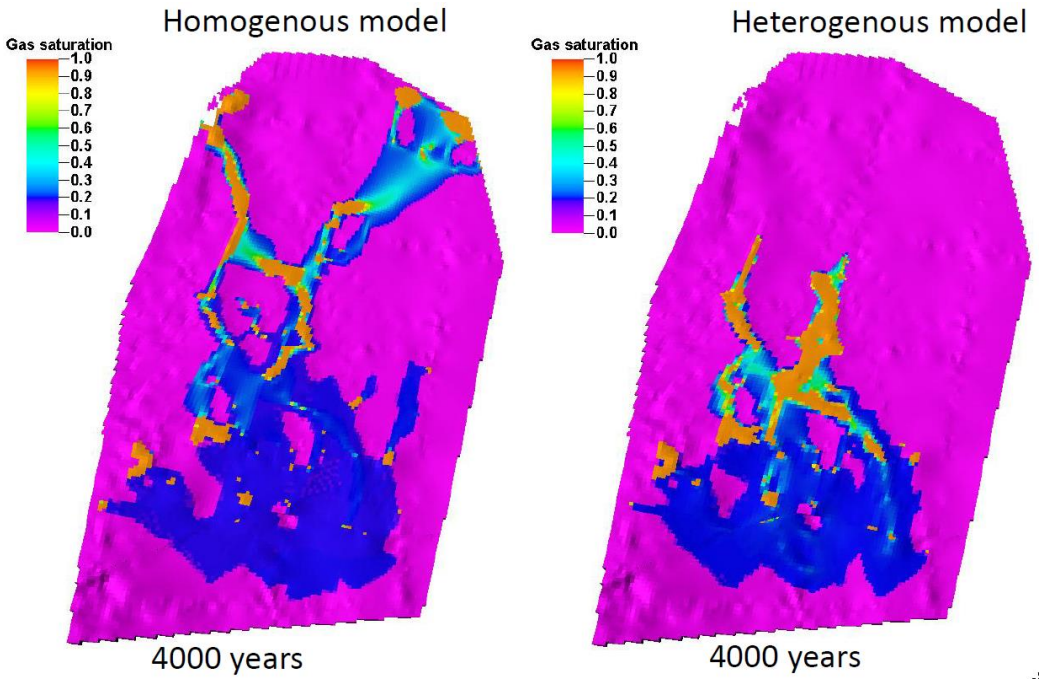

Figure 3-13 CO_2 distribution after 4000 years after injection of 500 Mt CO_2. Left figure show the homogenous model and the right figure show the heterogeneous model.

Simulations on the heterogeneous model indicate that one can permanently store 1 Gt CO_2 without migration out of the formation. The injected CO_2 occupies approximately 1.6 % of the pore volume and in addition 25% of the injected CO_2 is dissolved after 6000 years. The estimated pore volume in the open dipping Gassum Formation North-East of the main fault zone (see Figure 3-8) is $4.1 \cdot 10^{11}$ m^3. The pore

volume of the simulation model is $1.1 \cdot 10^{11}$ m^3 and assuming the same storage efficiency for the larger area as in the simulation model would give a storage efficiency of 3.7 Gt CO_2 for the North-Eastern part of the Gassum Formation.

3.7 Conclusions

Simulations on the homogenous model indicate that the Late Triassic Gassum Formation has the capacity for storing at least the 250 million tonnes of CO_2 from the mapped industrial sources in the Skagerrak-Kattegat area but it must be emphasized that there are large uncertainties in the constructed models due to scarcity of data. The most critical factors for safe storage are the frustration pressure of the sealing cap rock and the parameters controlling lateral migration of the injected CO_2. The induced pressure increase in the Hanstholm model is higher than the estimated safe pressure increase for the cap rock integrity, but the formation may still be suitable for storage by increasing the number of injection and water production wells. Further characterization of the cap rock and overburden is required to give a better estimate of frustration pressure in all three target areas. Sea bottom depth may be a limiting factor for the open dipping traps since a thinner overburden will reduce the frustration pressure of the cap rock.

Simulations on the heterogeneous model indicate that up to 1 Gt CO_2 can be stored in the modelled area. Extrapolating this result to include the whole North-Eastern part of the Gassum Formation (see Figure 3-8) would give a maximum storage capacity of 3.7 Gt CO_2. However, different topography, heterogeneity and dip in the regions not simulated will affect this estimate.

The main results indicate that the north-eastern part of the Gassum formation on the Danish side is the most promising target for injection of CO_2. This is based on the observation that all the injected CO_2 is capillary trapped or dissolved within the model boundaries; the injection pressure is thought to be in the safe pressure range. The location is still worth investigating further since small changes in flow parameters can change the maximum plume size of the injected CO_2. These parameters are at the present uncertain and more data is needed for better characterization of the target formation.

The Hanstholm structure has a domal closure that can hold the injected amount of CO_2 but simulation results from the current model indicate injectivity problems with the applied high injection rates. Introducing a larger number of injection wells and/or production wells could change this and if it is possible to build confidence in the sealing properties of the cap rock, Hanstholm could be the preferred target. Further characterization of the target formations and the overburden could also change the ranking of the models (cap rock integrity and safe pressure increase).

4. Simulation of the Garn Formation at the Trøndelag Platform, offshore Mid-Norway

The Trøndelag Platform, offshore Norway covers an area of more than 50,000 km² (Figure 4-1). It is roughly rhomboid in shape and is situated between 63°N - 65°50'N and 6°20'E - 12°E (Blystad et al., 1995). The platform has been a large stable area since the Jurassic and it is covered by relatively flat-lying and mostly parallel-bedded strata that dip gently towards the north-west. The investigated central Platform is confined to the Halten Terrace in the west by the Bremstein Fault Complex, to the Helgeland Basin in the north by the Ylvingen Fault Zone, to the Froan Basin the south-east by the Vingleia Fault complex, and bounded to the east by Caledonian crystalline basement (Figure 4-1). Both the Helgeland and the Froan Basin have been recognized as subsidiary elements of the Trøndelag Platform.

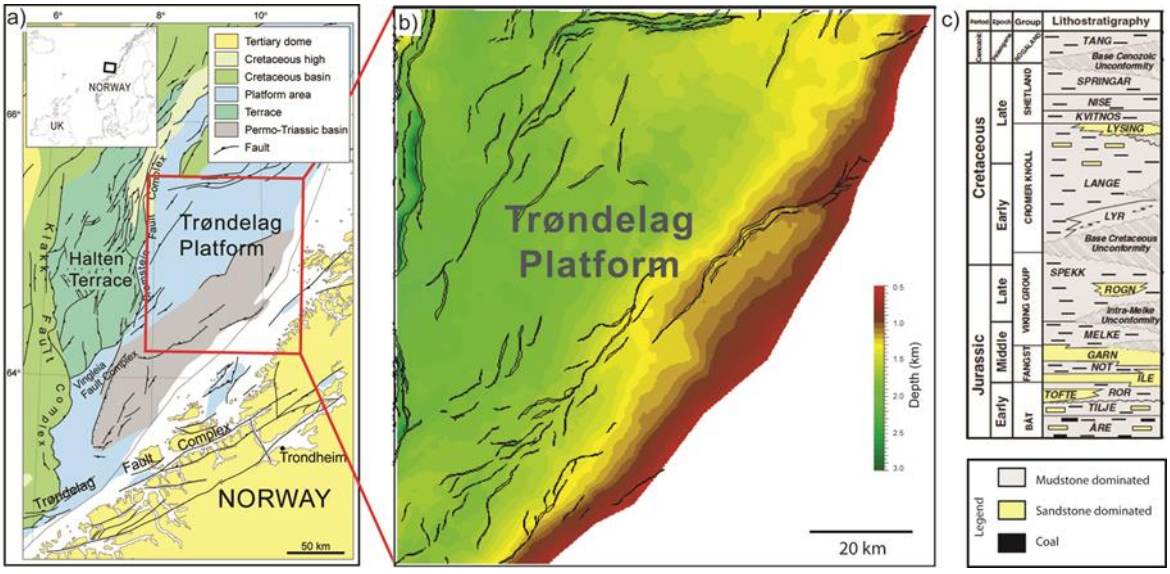

Figure 4-1 **(a) Main structural elements offshore Mid-Norway. The working area within the Trøndelag Platform is marked by the red box [modified from 14, 21]. (b) Depth map (km) of the top Garn Fm. (c) Lithostratigraphy of Mid-Norway (from Dalland et al., 1988).**

4.1 Available knowledge of the site

During the last two decades the Halten Terrace area, offshore mid-Norway (Figure 4-1) has become a rather mature exploration area for the oil and gas industry with currently 13 fields under production. Data from the area is available from the Norwegian Petroleum Directorate homepage (www.npd.no) and from the literature (e.g. Martinius et al. 2005). Major oil companies including Statoil have also collected and compiled a wealth of data from the region. These data are primarily used for oil exploration, but during recent years they have also been utilised for CO_2 storage studies. The results of these studies are of proprietary character and have not been published. However, several other projects have worked in this area such as the GESTCO project (Bøe et al., 2002) and the CO2STORE (Bøe et al. 2005). GESTCO concluded that the Lysing Fm., Rogn, Garn and Ile are the most promising aquifers for storage of CO_2 in the Halten area. The best oil fields would be Norne, Heidrun, Åsgard, Draugen and Njord (Bøe et al., 2002). Lundin et al. (2005)

presented reservoir simulations of part of the Froan Basin on the Trøndelag platform. They concluded that the Jurassic rocks are well suited for industry scale CO_2 storage (see also Bøe et al. 2005).

The Garn Formation is considered as the best reservoir candidate for CO_2 storage. It is widely laterally deposited, nearly all over the Halten Terrace and the Trøndelag Platform and it also has a sufficient thickness. The Garn Formation has been interpreted as homogenous sandstone, with a lateral extent of 10s of km. However, Gjelberg et al. (1987) demonstrated a facies diachroneity of the Garn and Melke Formations on regional scale, and Corfield et al. (2001) support this view on a local scale (Smørbukk area). The Garn Formation consists of medium to coarse grained, moderately to well-sorted sandstones (Dalland et al., 1988). Mica-rich zones are also represented. The porosity presents important variations related to the burial depth. Quartz cementation in the Garn Formation is a controlling factor of its porosity. The Garn Formation is in the Norne Field, buried to 2.6 - 2.7 km and has a porosity of 13 - 16%, while in Kristin Field the Garn Formation is buried to 4.6-4.7 km has 26 - 31% porosity (Storvoll & Bjørlykke 2004).

4.2 Site Concept

The area has been chosen for this CO_2 study for a number of reasons. First two promising potential storage units of significant thickness are present within the middle Jurassic sedimentary layers, the Ile and the Garn Formation (Figure 4-1). Second, these formations have good to excellent storage characteristics, since they are the main oil and gas bearing reservoirs on the Halten Terrace. For CO_2 storage it is also of great importance that the formations are relatively shallow buried (<2000 m) e.g. Figure 4-1. The Trøndelag Platform has a large lateral extension and the overall storage volume is likely also large. The overlying low-permeable clastic rocks, which cover the whole investigated area and have a reported thickness up to 1650 m, will most likely provide an effective seal (Figure 4-1). However, they are thinning towards east and intersecting with Quaternary sections close to the Norwegian coast so possible migration routes in the storage unit are very important to study (Figure 4-1).

4.3 Method

In order to apply and verify a basin modelling approach we used an updated version of the SEMI software (Sylta, 2004; Grøver et al., 2013) and compared final results to outcome of the commercial reservoir simulation software ECLIPSE 100.

4.3.1 Basin Modelling - SEMI

The basin modelling tool SEMI has been developed to model quantitative hydrocarbon migration and exploration risk (Sylta, 2004). It includes all 'standard' migration processes and can handle multi-carrier secondary migration and entrapment on geological time scales. It uses a ray-tracing technique to migrate CO_2 within a carrier bed just below a sealing cap-rock. This carrier unit can also act as a storage unit. The technique uses the dip of the carrier to determine pathway directions (Figure 4-2). The phase pressure, volume, and temperature properties are computed as properties for each trap during simulations. Secondary migration losses are computed during the ray-tracing according to volumes lost in dead-ends and micro traps, in addition to the required saturation of the pore space of the migration stringers. This saturation requirement can be computed from Darcy permeability grids and relative permeability relationships.
The methodology for SEMI adapted as a tool for CO_2 storage simulations was presented in Grøver et al. (2013) where two loss mechanisms were introduced: (i) Migration loss (trapping of CO_2 along migration pathway) (ii) Dissolution of CO_2 at gas-water-contact within trap entities. Gas is here referring to the CO_2 phase independent of its supercritical or not supercritical state.

CO_2 dissolution is modelled mainly at the gas-water phase contact within a trap. In our implementation the dissolution by convective mixing is assumed to be the dominant term, and for simplicity, the only term included. After onset of convection, dimensional analysis and numerical flow simulations suggest that this rate of dissolution by convective mixing (C_c) at the gas water contact (in $[m/s]$) is given by equation (1):

$$(1)\quad C_c = \frac{k_v}{\mu_w}\Delta\rho_{dis} g \psi(\zeta)$$

Thereby, k_v is the vertical permeability ratio, μ_w is the viscosity of water, $\Delta\rho_{dis}$ is the water density change during CO_2 dissolution, g is gravity and $\psi(\zeta)$ is a dimensionless intrinsic function estimated in flow simulations (Wessel-Berg, 2013). The ζ is proportional to the permeability ratio (kv/kh) (Elenius and Gasda, 2012). In the software we have introduced a CO_2 dissrate-factor as the inverse value of the intrinsic function.

The simulator workflow starts with finding every migration path within the carrier unit and correspondently identifies all drainage areas (each with a distinct trap structure). The injected CO_2 will then be migrated towards its nearest trap structure along the identified paths. If the CO_2 volume is greater than the trap structure capacity, the surplus volume of CO_2 will be spilled along a distinct spill path towards neighbouring trap structure (Figure 4-2). These steps are performed until there is no more CO_2 volume left to migrate.

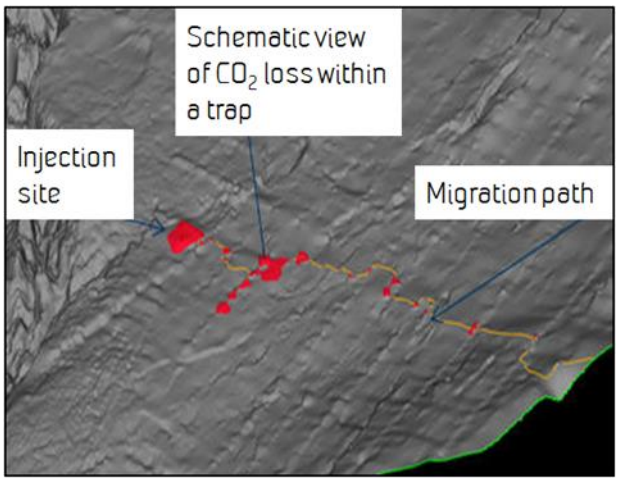

Figure 4-2 Schematic overview of how CO_2 will migrate from injection site to traps and maybe also out of the reservoir (orange and green line).

4.3.2 Reservoir Modelling – ECLIPSE

Dynamic modelling of CO_2 injection into deep saline aquifers is performed using the industry standard reservoir simulator ECLIPSE 100 from Schlumberger. ECLIPSE 100 is a fully-implicit, three phase, three dimensional, general purpose black oil simulator which accounts for all trapping mechanisms involved in CO_2 storage except mineral trapping.

4.4 Input parameter and modelling set-up

For the basin modelling approach, an interpreted seismic horizon at top Garn Fm., the today's seabed and an interpreted fault map at top Garn Fm. are used as input. The parameters are set as shown in Table 4-1.

A 3D reservoir model of the Trøndelag platform has been constructed based on data from well logs and interpretation of top Garn Fm. from seismic. Porosity and permeability was estimated to vary between 15-40 % and 0.5-10 D (Table 4-1). Salinity was set to 3 wt% TDS and a uniform temperature gradient of 40 °C/km and surface temperature of 4 °C were assumed.

Table 4-1 Parameters used for the SEMI modelling of CO_2 migration. The total injected amounts of CO_2 as well as the values for the intrinsic function were varied for the selected injection sites.

Parameters	SEMI model	ECLIPSE 100
Thermal gradient	40 [ºC/km]	40 [ºC/km]
Entry pressure	5000 [Pa]	
Water depth	Present day seabed [m]	Present day seabed [m]
Pressure	Hydrostatic conditions [MPa]	Hydrostatic conditions [MPa]
Average net permeability	1 [D]	0.5-10 D, a log linear relation between porosity and permeability
CO_2-diss-rate factor	Variable [dimensionless]	
Total injection	Variable [Mt]	700 Mt
Porosity	Compaction curve from [24] calibrated vs. data from [20].	15-41% (depth dependent); [20] with cut-off at 41%
Thickness maps*	Garn Fm. 127 m	Garn Fm. 127 m
Top reservoir map	Interpreted top Garn Fm. seismic map (surface)	Interpreted top Garn Fm. seismic map (surface)
Fault map	Interpreted fault map at top Garn Formation	

*Well data from six wells: 6407/6-3, 6407/6-5, 6407/6-4, 6407/6-1, 6407/9-7 and 6408/4-1

4.4.1 Basin modelling set up

The horizontal grid dimension is set to 200 m x 200 m. Two set-ups are used for the basin modelling approach. To estimate the total trap storage capacity a "pseudo" CO_2 layer below the reservoir layer where introduced (Figure 4-3a). Secondly, injections were carried out in 38 injection sites distributed over the whole working area (Figure 4-3b).

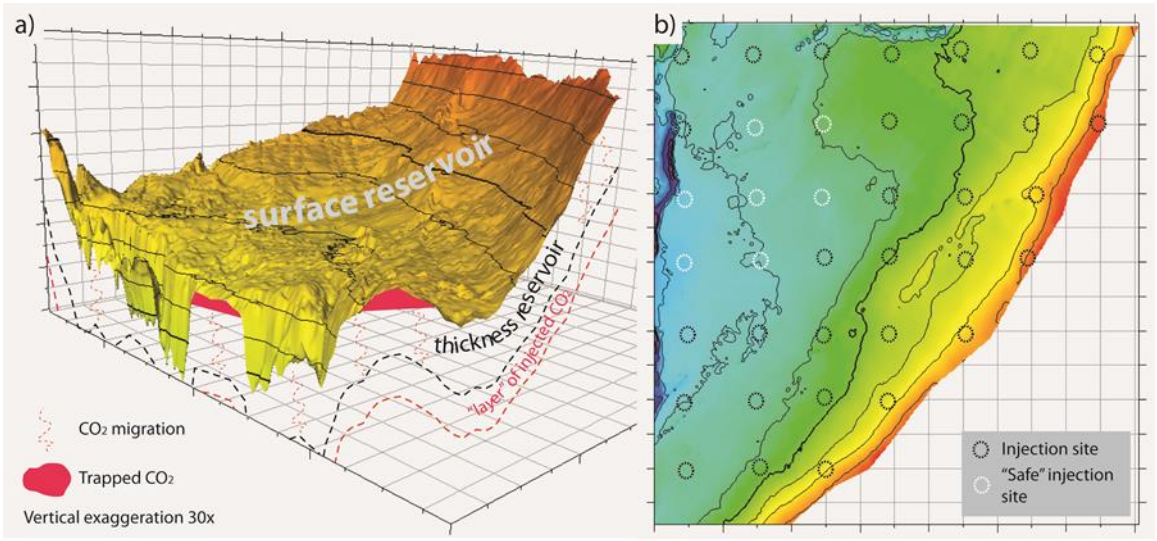

Figure 4-3 Concept for the basin modelling approach. (a) At first, the total trap storage capacity was estimated by flooding the reservoir with CO_2. This is technically done by adding a "layer" of CO_2 under the reservoir unit. (b) Secondly, simulations were carried out using 38 CO_2 injection sites. The simulations showed that injection into 7 sites did not cause migration out of the Garn Fm., shown as "safe" injection sites.

4.4.2 The reservoir model set up

The grid dimension is set to 500 m x 500 m. Vertical grid layer thickness is refined below the top. Average vertical layer thickness is 16 m. Faults are implemented as geometrical features, but with no transmissibility modifications. Net-to-gross values are set to 1-0.85 with a random assigned algorithm for the reservoir layer.

4.5 Results

4.5.1 Modelling of total trap storage capacity for the Garn Formation

The total trap-storage capacity was estimated assuming the parameters given in Table 4-1 and using the modelling set-up described in section 4.4.1. An important assumption is that the whole platform is overlain by sealing layers. An infinite amount of CO_2 was "injected" into the carrier unit, migration loss and dissolution in the traps was disabled. Two scenarios were tested (a) no faults or open faults (b) all faults are sealing (Figure 4-4). The modelling results suggest a total maximum trap storage capacity of ca. 2.0 Gt for the no faults scenario and a significantly higher value of 5.2 Gt if sealing faults were taken into account (Figure 4-4).

Some traps show significant differences for the two scenarios, e.g., trap 1 does not exist if faults are neglected whereas up to 716 Mt of CO_2 can be stored in the trap if all faults are sealing. In general, the traps in the faulted northern part of the working area give higher capacities for the fault scenario (e.g., traps 1, 2, 3). In contrast, traps located in the centre of the working area show similar results for both scenarios (e.g., traps 4, 5, 7).

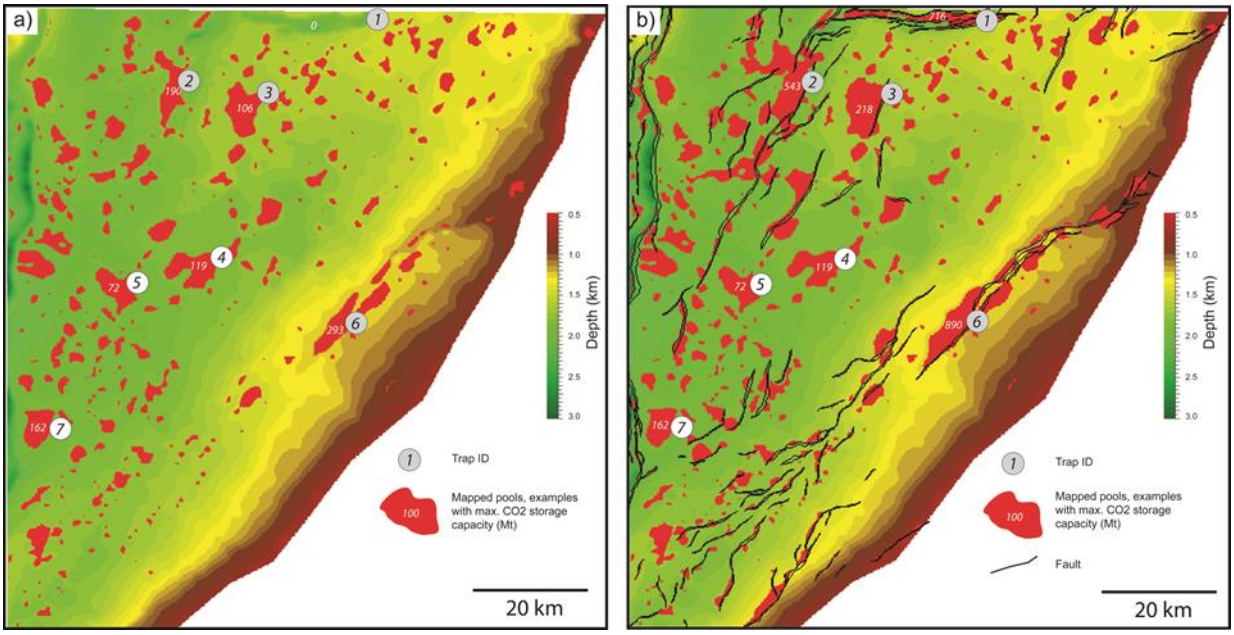

Figure 4-4 **Modelled CO_2 accumulations projected onto the Garn Fm. depth map using the basin modelling approach. In order to estimate a total trap-storage capacity for the Garn Fm. the whole area was "flooded" with CO_2 and all traps were filled to a maximum. CO_2 dissolution during migration and within the trap entities was disabled. (a) For the scenario without faults a total trap storage capacity of ca. 2.0 Gt was modelled. (b) The second scenario assuming sealing faults gave a total trap storage capacity of ca. 5.2 Gt.**

4.5.2 Varying the CO_2 dissolution rate factor

The CO_2 dissrate-factor was varied for a base case with open faults, multi injection sites and with a total injection of 1000 Mt CO_2. The amount of dissolved CO_2 was dependent on the dissrate-factor (Figure 4-5). The factor was calibrated versus migration distance simulated by reservoir models for Gassum Formation, Skagerrak area (Bergmo et al., 2013) and core measurement of residual CO_2 saturation (c. 25%) from the unconsolidated Utsira Sand at the Sleipner CO_2 injection site (Akervoll et al., 2008). From this calibration, a dissrate-factor of 250 was used further in the basin modelling approach.

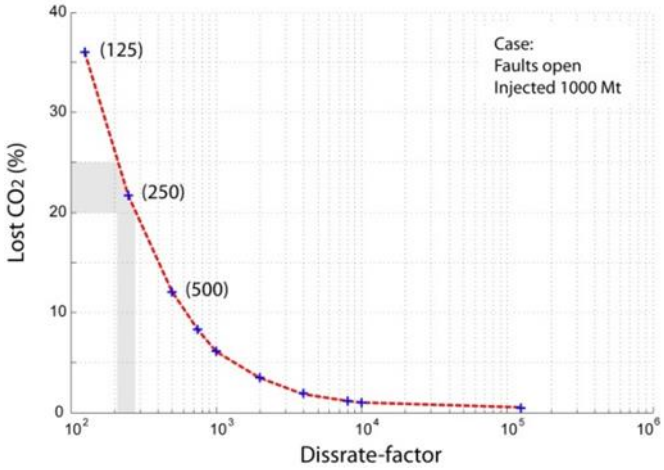

Figure 4-5 Scatter plots highlighting the impact of the CO_2 dissolution rate-factor on SEMI modelling results. Assuming high CO_2 dissolution at gas-water-contact has a significant impact on the calculated total CO_2 loss in the SEMI software. Grey shaded area depicts the most realistic values for our models.

4.5.3 Mapping possible injection sites for the Garn Formation

In a second approach SEMI was used for a systematic mapping of possible "safe" injection sites. At first, 38 CO_2 injection sites with constant plume radii's of ca. 1.6 km were distributed with equal spacing (ca. 20 km) over the area of interest (Figure 4-3). Thereby, very high amounts of CO_2 (up to 3.8 Gt) were injected over a period of 100 year assuming a CO_2 dissrate-factor of 250 (Figure 4-5) for a no faults scenario and a sealing fault scenario. Subsequently, injection sites which caused CO_2 migration out of the boundary of the working area were excluded. Our modelling results indicate 7 injection sites which fulfil the criteria for safe CO_2 storage (Figures 4-3 and 4-6).

The final 7 injection sites were used as input to the reservoir model and a simulation injecting a total of 700 Mt CO_2 over 100 years was performed. Simulating CO_2 loss over 3000 years took approximately 23 hours (CPU-time) on a standard desktop single processor. A total of 35% of the injected CO_2 was dissolved after 3000 years and the remaining CO_2-phase was capillary trapped below the sealing cap rock or as residual phase in the pores. CO_2 saturation after 3000 years is shown in shown in Figure 4-6.

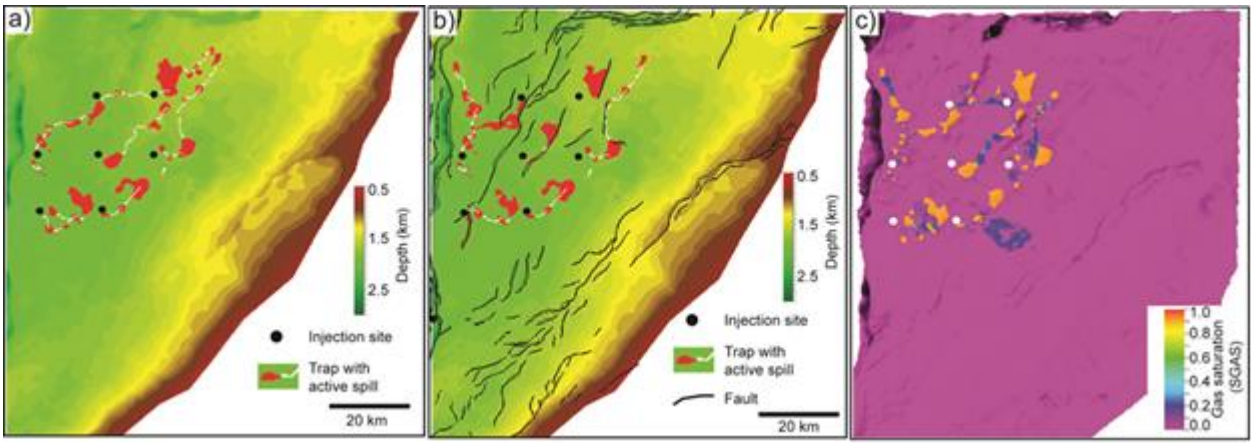

Figure 4-6 **Basin modelling results of the systematic mapping for "safe" CO_2 injection sites compared with reservoir modelling results. Map view of the top Garn Fm. horizon with pools of CO_2 accumulations and active spill paths 100 yrs after the injection. (a) For the no faults scenario a total trap storage capacity of ca. 447 Mt was modelled. (b) For the simulations taking sealing faults into account a total trap storage capacity of ca. 477 Mt was estimated. (c) CO_2 saturation below the top of the storage unit in the reservoir model after 3000 years.**

4.6 Discussion

The method used to simulate the total trap storage capacity, with a pseudo CO_2 layer below the storage unit, is a very simplified approach. However, it gives a maximum estimate of how much CO_2 can be trapped if all the traps are filled. The simulation results show a large range from 2.0 Gt with no faults to 5.2 Gt with faults included (Figure 4-4). A reservoir model for the Garn/Ile aquifer by Halland et al. (2013) gave a maximum storage capacity of up to 8 Gt CO_2 assuming a half open system (contact with a larger aquifer). In a second model set-up they used a closed system which indicates a drastic lower storage capacity of only 0.4 Gt.
In a trap-scale the basin modelling approach can give a rapid overview of which structures might be good candidates for planning CO_2 injection. For example, traps 4 and 7 (Figure 4-4), can store large volumes both with and without sealing faults. Other traps like 2 and 3 show significant differences in the storage capacity of CO_2 e.g., trap 2 with a capacity of 543 Mt taking sealing faults into account and a significantly lower capacity of 190 Mt without faults (Figure 4-4). These modelling results illustrate the significance of the chosen model assumptions on the final storage capacities.

4.6.1 CO_2-dissrate factor

CO_2 storage capacity estimate in the SEMI approach focus on reservoir capacities and thus the CO_2 dissolution is modelled mainly at the gas-water phase contact within a trap. By running several simulations, varying the dissrate-factor from minimum 125 to 10000 (Figure 4-5), the corresponding loss of CO_2 can be evaluated. The simulations show that SEMI's migration and storage estimates strongly correlate with the dissrate-factor (Figure 4-5). The equation (1) illustrates the strong dependency of the dissrate-factor. In principle, this factor represents the lateral and vertical heterogeneous lithologies within the trap, and its impact on the dissolution rate (Bergmo et al., 2013). Unfortunately, for the Garn Fm. lithological variations are not mapped and thus a homogenous sediment model was applied. Core measurement of residual CO_2 saturation from the unconsolidated Utsira Sand at the Sleipner CO_2 injection site gave values of CO_2 loss of c. 25% (Akervoll et al., 2008). Applied to our modelling area, such a value would indicate a dissrate-factor of c. 250 which was applied in the final model for the 7 selected injection sites.

4.6.2 Effect of fault on migration pathways and traps

In a brittle undeformed, homogeneous sedimentary strata overlaying by a sealing unit, buoyancy forces would cause CO_2 migration from the bottom towards the top of the layer and finally migrating along the top towards the highest points. Faults interrupt this general migration path and can cause deflection from the estimated migration paths depending on their properties and spatial distribution. In our approach the faults were modelled as an open conduit per se (Allan, 1989) or as sealing. For all modelled cases with sealing faults the regional fault distribution has a significant influence on the lateral migration pathways and on the trap capacities (Figures 4-4, 4-6). Here we only presented end-member models for sealing or open faults which visualised the drastic impact on final trap storage capacities. In nature, fault permeability's will vary substantially and a rigorous testing is necessary for CO_2 storage estimates. This might be achieved by using Monte Carlo simulation testing various fault models.

4.6.3 Mapping of "safe" injection sites

In the mapping of "safe" injection sites, we followed strict limitations such as that no migration out of the storage unit should occur, for both scenarios (with and without faults). Finally, 7 sites showed no migration spill out of the Garn Fm.

For the selected 7 injection sites two fault scenarios (with or without faults), were modelled injecting a total amount of 700 Mt CO_2 and applying a dissrate-factor of 250 (Figure 4-5). The selected injection sites are mainly located in the centre of the working area following an SW-NE trending axis. Our model results indicate that the spatial distribution of sealing faults has a significant influence on CO_2 storage capacities. For both cases the injected CO_2 remains in the working area but migration pathways and CO_2 accumulations in traps differ significantly. For the no fault scenario the spill paths follow a general SE-NW trend (Figure 4-6a). In contrast assuming sealing faults would deflect some of the spill path in an S-N trend following the strike of the faults (Figure 4-6b). Moreover, total CO_2 as well as migration losses are with ca. 30 Mt and 1.9 Mt lower than in the non-fault case (40 Mt and 3.1 Mt). The general low migration losses point to the main weakness of the basin modelling approach. SEMI simulates migration using the ray-tracing (flow path) technique and migration loss is spatially very limited. In proper reservoir simulator software CO_2 flows along a migration front and covers a larger area. This gives more reliable results on the migration loss and migration paths. The results for the reservoir models show a similar distribution for the CO_2 saturation in the working area (Figure 4-6a-c). However, the reservoir model gives more realistic estimates for the total CO_2 loss (ca. 35% or 245 Mt; 3000 years after injection).

4.7 Conclusion

According to our modelling estimates the Garn Fm. of the Trøndelag Platform has in structural closures, a total trap storage capacity in the range of 2.0 Gt for the non-fault scenario and 5.2 Gt with faults included. This estimate is made assuming no migration loss and a very low dissolution rate in the traps and can be interpreted as a maximum estimate. Seven locations for "safe" CO_2 injection have been mapped and results are validated by an ECLIPSE reservoir model. Compared to conventional reservoir simulators, the basin modelling approach allows fast simulations (minutes instead hours/days) which can be utilized for testing several scenarios in a short time-period. Thus, this approach offers a possibility for a rigorous statistical testing of different parameters.

5.Simulations of the Hanstholm structure, NW Denmark

5.1 Background and study area

The informal name "Hanstholm structure" is used for an offshore domal closure at Gassum Formation level situated approximately 40 km northwest of the city of Hanstholm (Figure 5-1). The water depth at the site of the structure is approximately 30 m. The structure is situated close to the edge of the Fjerritslev Fault of the Sorgenfrei-Tornquist zone (Figure 5-2). The main sediment input during the Triassic–Jurassic was from the northeast. The structure is caused by uplift due to post depositional salt tectonics. The structure is a huge domal closure covering 603 km². The depth to top reservoir is approximately 890 m below msl. and the last closing contour is at approximately 1330 m. The spill point is situated at the south-eastern flank of the structure leading into the Thisted domal structure (Figure 5-1).

The following description of modelling input and procedures is valid for the porosity-permeability model of date April 30 2008. This model has been used for several simulation studies. The model was constructed from sparse reservoir data, and therefore surrounded by significant uncertainties. Studies of the structure and injection strategy have been performed within the DYNAMIS project and some of the results were presented at the IFP Scientific Conference "Deep Saline Aquifers for Geological Storage of CO_2 and Energy" (Maurand et al. 2009).

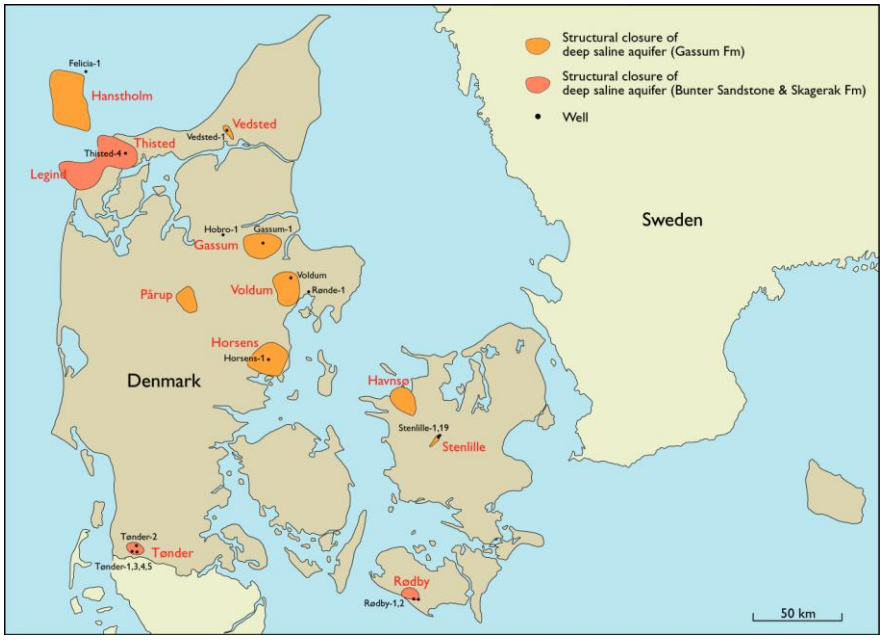

Figure 5-1 **Map showing the position and outline of structural closures. Black dots indicate the position of some of the deep exploration wells used in the evaluation of the reservoir formation. For the Hanstholm structure was used 3 additional wells from the offshore area.**

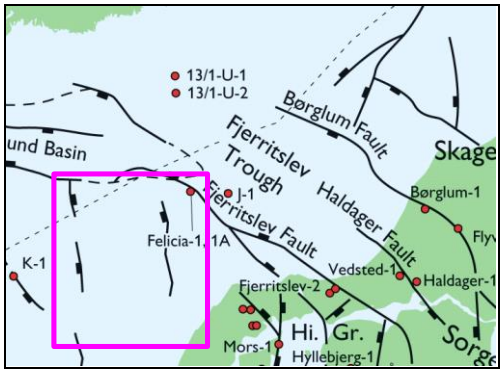

Figure 5-2 Map showing the approximate location of the Hanstholm structure and the nearby wells of K-1, Felicia-1 and J-1, northwest Denmark.

5.2 General geological setting

The structure is situated close to the edge of the Fjerritslev Fault of the Sorgenfrei-Tornquist zone (Figure 5-2). The main sediment input during the Triassic–Jurassic was from the northeast. The structure is caused by uplift due to post depositional salt tectonics.

5.3 Gassum Formation (Upper Triassic–Lower Jurassic)

The Gassum Formation consists of fine- to medium-grained, locally coarse-grained sandstones interbedded with heteroliths, claystones and locally thin coal beds (Michelsen & Clausen 2002, Nielsen *et al.* 2003). The sandstones were deposited by repeated progradation of shoreface and deltaic units forming laterally continuous sheet sandstones separated by offshore marine claystones. Fluvial sandstones dominate in the lower part of the formation in the Fennoscandian Border Zone.

5.3.1 Well database

The structure itself has not been drilled. Well information is extrapolated from the three nearby wells Felicia-1, J-1 and K-1 (Figure 5-2). It should be noted however, that Felicia-1 is drilled at the crest of a rotated fault block, and shows an extraordinary large thickness of the Gassum Formation including a thick mudstone in the middle part, which could reflect topographic influence during deposition from the nearby salt pillow and association with a rim syncline. This may result in marked differences in reservoir properties between the well and the formation on the undrilled structure. Only the upper third of the Gassum Fm. in the Felicia-1 well is included in the present modelling. Due to the well Felicia-1 not being representative of the main reservoir units on the structure, the well J-1 some 30-40 km to the NE has been used as a template for the sand/shale sequence and for guiding the N/G ratio.

5.3.2 Structural maps

The structure is interpreted from the depth structure map of the "Top Triassic" as defined by Japsen and Langtofte (1991) (Figure 5-3). The "Top Trias" map has been used as a template for defining top and bottom of reservoir with uniform thickness.

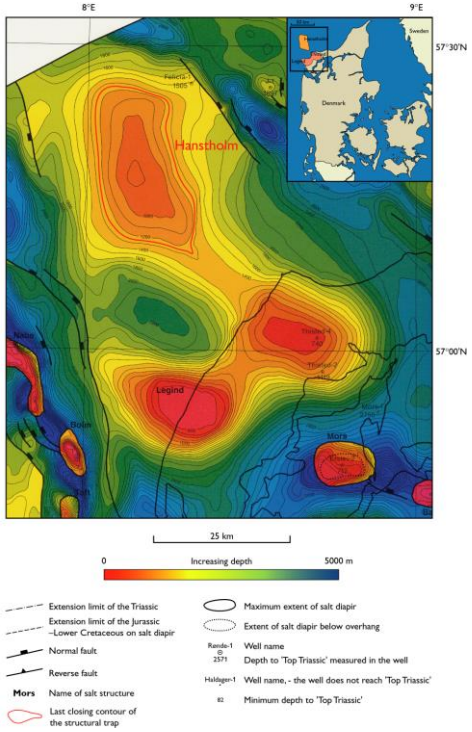

Figure 5-3 Outline of the structural trap defining the potential storage site at Hanstholm. The structure is interpreted from the depth structure map of the "Top Triassic" as defined by Japsen and Langtofte (1991).

5.3.3 Storage reservoir unit

Sandstones of the Upper Triassic – Lower Jurassic Gassum Formation form the main reservoir unit of the structure. The present reservoir model has been extended to include a few meters of caprock lithology from the Fjerritslev Fm. above the Gassum Fm., and additionally approximately 30 meter section below the Gassum Fm. from the Vinding/Skagerrak Fm. (Figure 5-4). This results in an N/G of 0.64 for the J-1 well and a value of 0.21 for the Felicia-1 well for the reservoir section.

5.3.4 Storage seal

The claystones of the Fjerritslev Formation form the top seal of the aquifer. The Fjerritslev Formation is expected to be approximately 500 m thick above the Hanstholm aquifer.

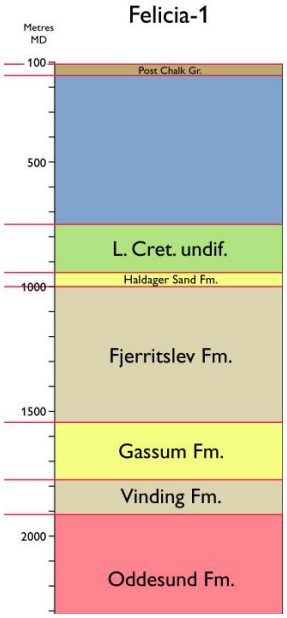

Figure 5-4 Stratigraphic-depth section of the Felicia-1A well showing the lithostratigraphic units and their thickness (<2.5 km). The main reservoir is sandstones of the Gassum Formation. The lithostratigraphic units and definition of formation boundaries in the deep wells are based on Nielsen & Japsen (1991).

5.4 Model setup

The following description of input and procedures is valid for the porosity-permeability model dated April 30 2008. The model was constructed from sparse data, and therefore includes significant uncertainties, especially regarding thickness and extent of reservoir layers over the undrilled structure, and regarding the porosity data originating from old and flawed well log data. Later re-visit of well-log data points to obvious revisions of the porosity model, and these are included as suggestions in the following chapters.

5.5 Grid

The model covers an area of 34.4 x 41.6 km (Figure 5-5). The fairly large area of the model has promoted the use of a coarse grid resolution with cell size of 400x400 m. Uniform thickness of 104 m is assumed.

The "Top Trias" map as defined by Japsen and Langtofte (1991) has been used as a template for defining top and bottom of reservoir, adjusting to the well information and the desire to include additional section to the Gassum Fm.

Cells (nI x nJ x nK) 86 x 104 x 52, cell size 400x400x2 m.

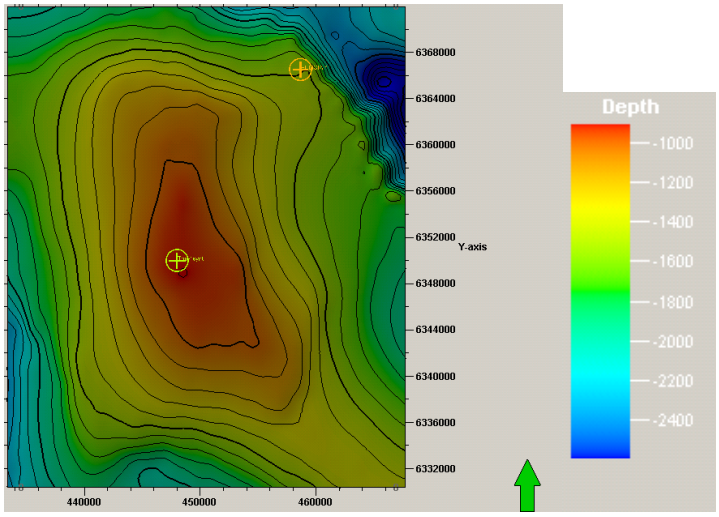

Figure 5-5 Map of top reservoir showing position of the well Felicia-1 in the NE corner and the introduced synthetic well Top-1synt on the top of the structure.

5.5.1 Well data for conditioning

The lack of reliable well log data for interpretation of porosity in the first stage of the work has resulted in the use of only target histograms for simulation of porosity model for the sand and shale facies.

5.5.2 N/G mapping

A trend map is constructed based on an average value of 0.41 from the J-1 template, and a minimum area with 0.21 around the Felicia-1 well (Figure 5-6 and Figure 5-7). This trend map is used as secondary input during the facies modelling.

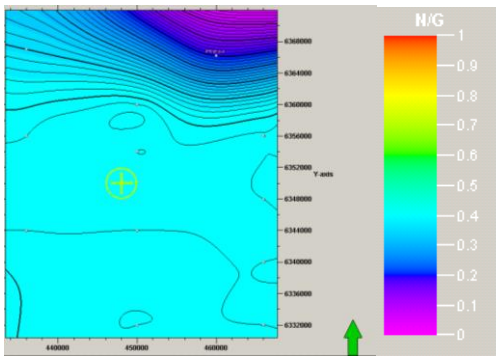

Figure 5-6 Map for N/G trend interpolated from the Felicia-1 data point and support points with the average value of 0.41.

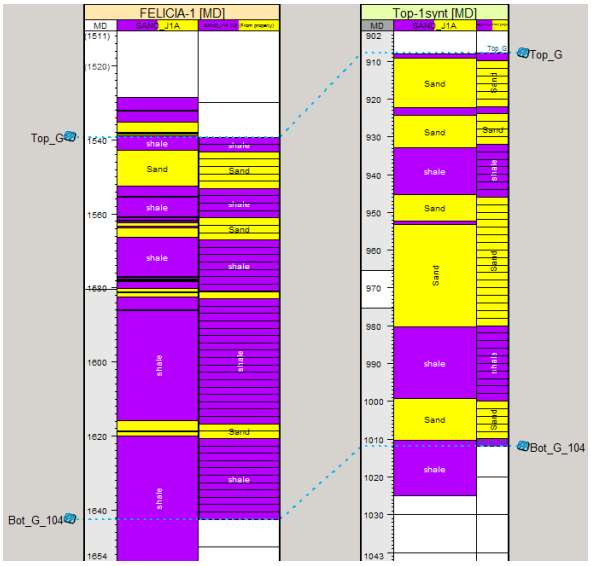

Figure 5-7 Well sections for Felicia-1 and Top-1synt for the reservoir section showing the difference in N/G.

5.5.3 Facies modelling

The facies modelling is carried out with stochastic placement of large rounded ellipses, 20x40 km areal extent, 4-12 m thick, and with a slight angle to NW-SE (Figure 5-8). This is used as a simple proxy for sheet-like shoreface deposits of large areal extent. The background facies is the marine muddy lithology from offshore deeper water deposition.

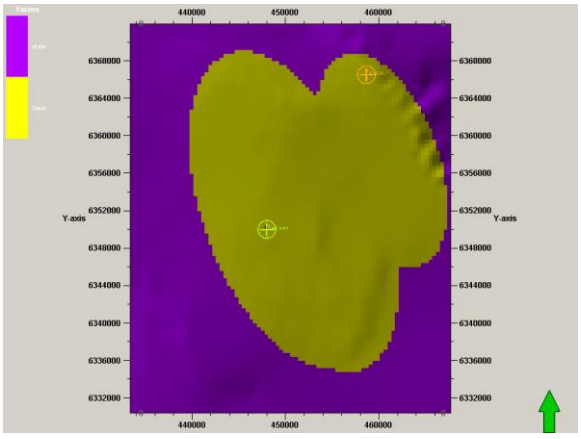

Figure 5-8 Map of a single layer in the facies model showing the rounded ellipses used for modelling of the shallow-marine to near shore sand sheets.

5.5.4 Petrophysical modelling

After the facies modelling, the total porosity PHIT is simulated with SGS, using no well data for conditioning but only target histograms being different for the sand and shale lithologies. These histograms have been derived from other studies of sand/shale sequences and are not fully adjusted to the local porosity information.

From the porosity PHIT (see Figure 5-9) the fluid permeability is calculated by using macro with equations separating the sand/shale lithologies, and limiting the maximum permeabilities to 1000 and 600 for the sand/shale respectively as shown in Figure 5-10. The large span on porosity and permeability for the shale lithology is due to the difficulty in discriminating the two lithologies based on the available well log data. Therefore the shale lithology should be viewed as a generally poor-reservoir category.

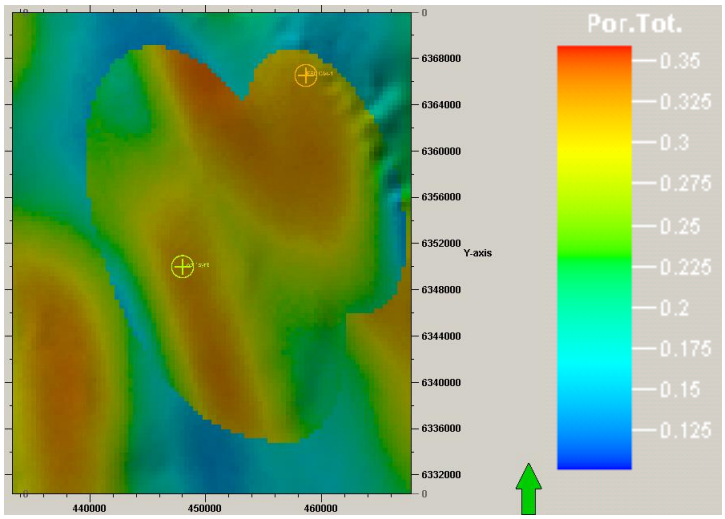

Figure 5-9 Porosity PHIT for a single layer in the model.

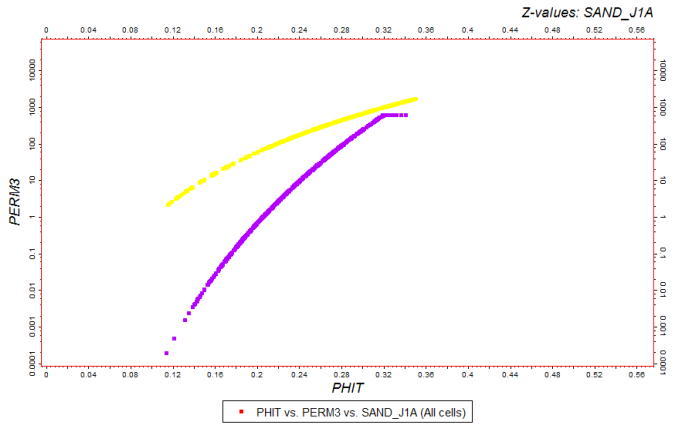

Figure 5-10 Porosity/permeability relations for the sand and shale lithologies

5.5.5 Export of grid

The grid data for the model is exported as Generic ECLIPSE style (ASCII) properties with cell origin in I=0, J=0, K.

The facies designation is exported as integer values 1/0 for sand/shale, and can be used for assigning properties and saturation functions for the 2 lithologies when the model grid is set up in a reservoir simulator using SATNUM for the saturation table input (Figure 5-11).

PHIE - effective porosity is exported to be used as porosity in the reservoir simulation, since this measure is restricted to the mobile water present in the model as the clay-bound water has been excluded. This therefore serves as a better property when looking into the amount of mobile water that might be replaced by the CO_2 injection.

5.6 Dynamic modelling

The dynamic simulation was carried out with the commercial simulator ECLIPSE100. ECLIPSE 100 is a black-oil simulator that can handle up to four flowing phases. Only the oil and gas phases were used in the present simulations. The simulator oil phase was given PVT and phase data corresponding to the assumed brine composition in the reservoir, and the simulator gas phase was given properties corresponding to CO_2 (PVT and solubility data and viscosities are represented in input-tables for the simulator). This allows both solubility properties and density versus depth data to be consistently represented, as pressure variation in the model is dominated by the hydrostatic pressure gradient throughout the simulation. The phase behaviour is described by black-oil PVT tables and CO_2 densities for the PVT table were calculated by the Soave-Redlich-Kwong equation-of-state as modified by Peneloux (Peneloux et al 1982).

5.6.1 Grid and Reservoir Parameters

The flow simulation grid is Cartesian with same grid cell size as in the geological model. 400x400 x 2 m.

5.6.2 Boundary conditions

The total pore volume in the model is too small to prevent the average reservoir pressure to build up during the CO_2 injection. For compensation of this in the simulations, cells with extremely large virtual pore volume were placed at the 4 vertical end-faces surrounding the reservoir, which via rock and fluid compressibility prevents boundary effects and violent pressure increase. In a physical sense this modification serves as a very large aquifer around the model volume. To obtain this effect the pore volume of normal cells at the margin of the model was multiplied in Eclipse 10,000 times using the MULTPV keyword.

This boundary condition modification is to some degree simulating the condition if a family of water extraction wells were placed around the structure for managing the overpressure in the storage site and for moderating the pressure effects in the neighbouring region and any adverse effects on adjacent operations in the subsurface.

The caprock compressibility is set to $5x10^{-5}$ 1/bar. This value has been adopted from other published studies, although a recent study by Mbia et al. (2013, 2014) has pointed out that caprock compressibility could be a factor 10 lower, i.e. more stiff than previously assumed. Initial hydrostatic conditions were assumed.

5.6.3 Saturation functions

The curves (Figure 5-11) are inspired by analyses from Bennion and Bachu 2006(1). For the wells, linear relative permeability curves for brine and CO_2 phases were used.

For capillary pressure were used 2 different curves having 0.1 and 1 bar threshold pressure for the reservoir/shale respectively.

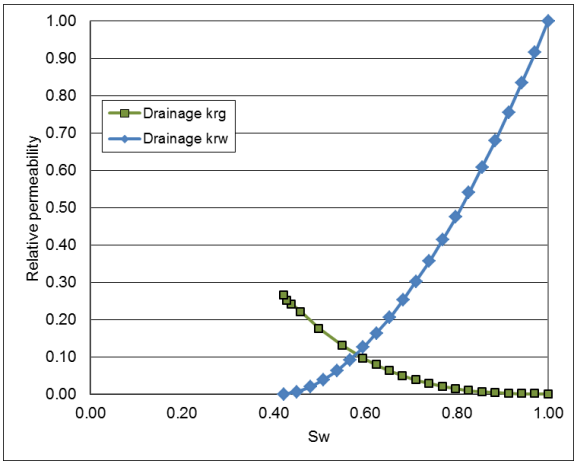

Figure 5-11 Relative permeability used for the 2 lithologies.

5.6.4 Initial Conditions

The temperature at mid Gassum level is estimated as 49 Centigrade. From a general salinity/depth relationship a salinity of 16% is assumed.

Assuming hydrostatic pressure leads to a Gassum datum pressure of

$P_{D,Gassum}$ = 154 bar, at the datum depth $D_{D,Gassum}$ = 1500 m.

The PVT description is described in the input tables:

pvt-han_PVTO.tab

pvdg-han_PVDG.tab

5.7 Injection conditions

By trial and error decision was reached for 7 wells to effectively fill most of the structure (Figure 5-12).

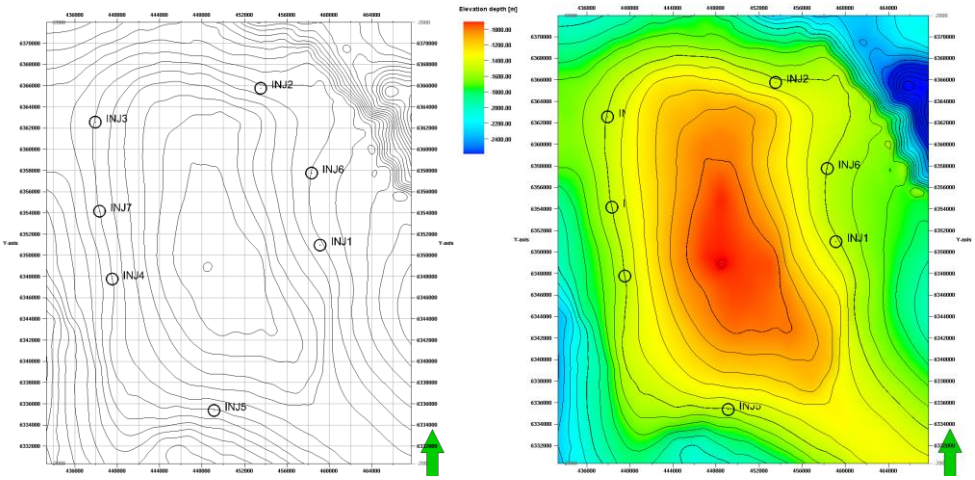

Figure 5-12 Maps with depth contours for the top reservoir level and the position of the 7 injection wells.

The CO_2 was injected at a constant rate of 6,000,000 Sm3/day per well resulting in 4.2 Mt per well per year. The dynamic simulations account for the injection period of 40 years (Figure 5-13 and 5-14).

5.8 Filling of structure

This described injection scenario results in a total injection mass of 1170 Mtons = 1.17 Gt capacity.

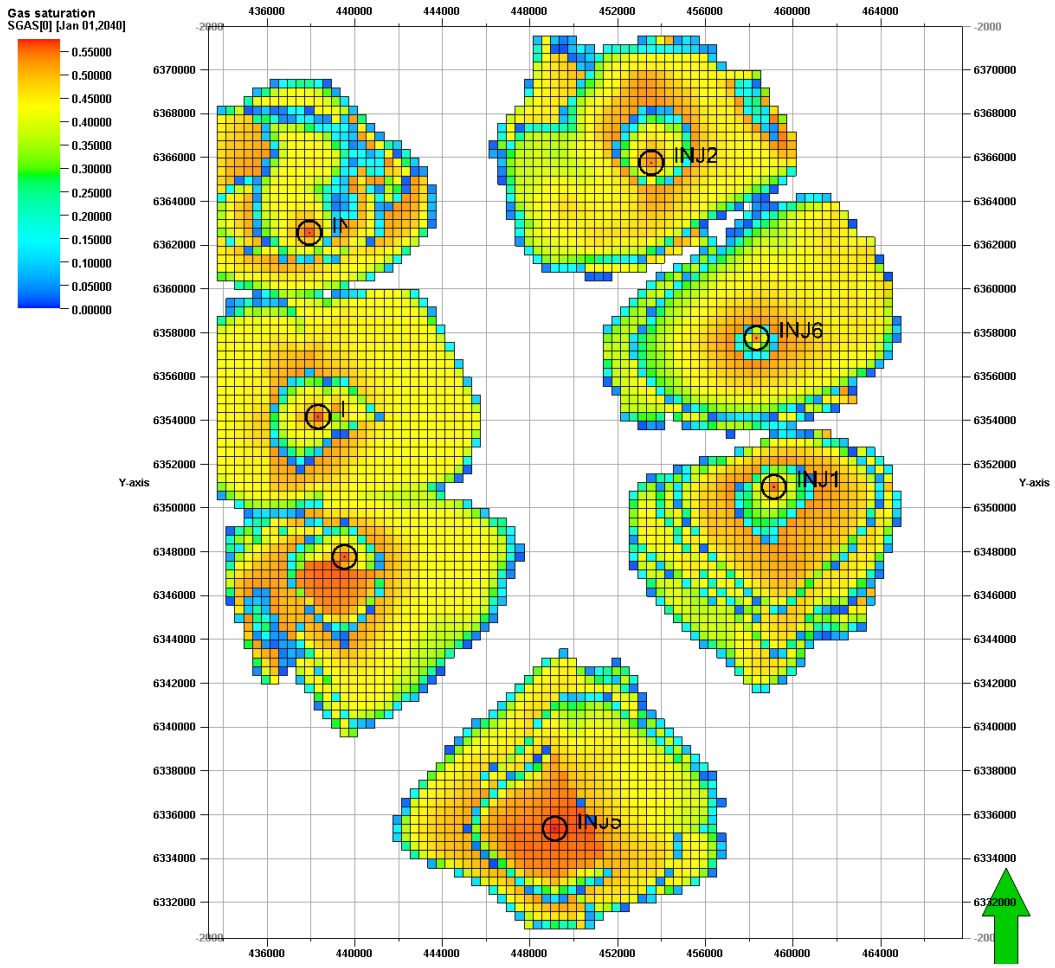

Figure 5-13 Map of extent of all layers with CO_2 saturation. HH14_7W_RATE_40M_40Y. Injection scenario after 40 years injection. The margins of some of the individual plumes reach the model margin and dissolves in the rim cells with artificially high pore volumes. The mass lost is minor compared to the injected and is therefore not subtracted explicitly in the capacity, but raises a concern about optimising the placement of the wells and regulation of the injection rate distribution for the wells.

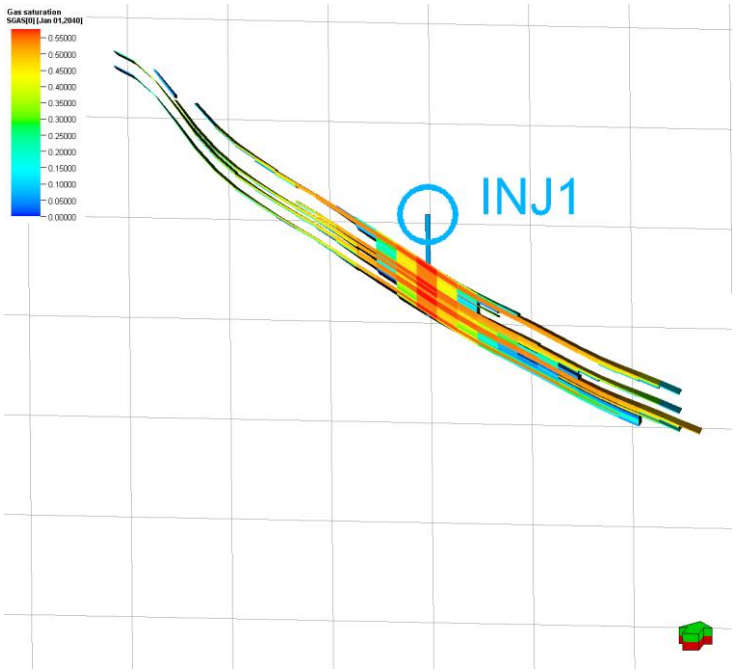

Figure 5-14 Vertical section West-East through injection well no. 1 showing the extent of the plume of 11.5 km laterally

Without any geological information, it was considered that the engineering safety margin on the cap rock will allow a pressure increase up to about 85% the lithostatic pressure. Changing this safety rule will of course influence the evaluation of the storage capacity and has to be discussed in relation to risk factors regarding cap rock integrity (Figure 5-15).

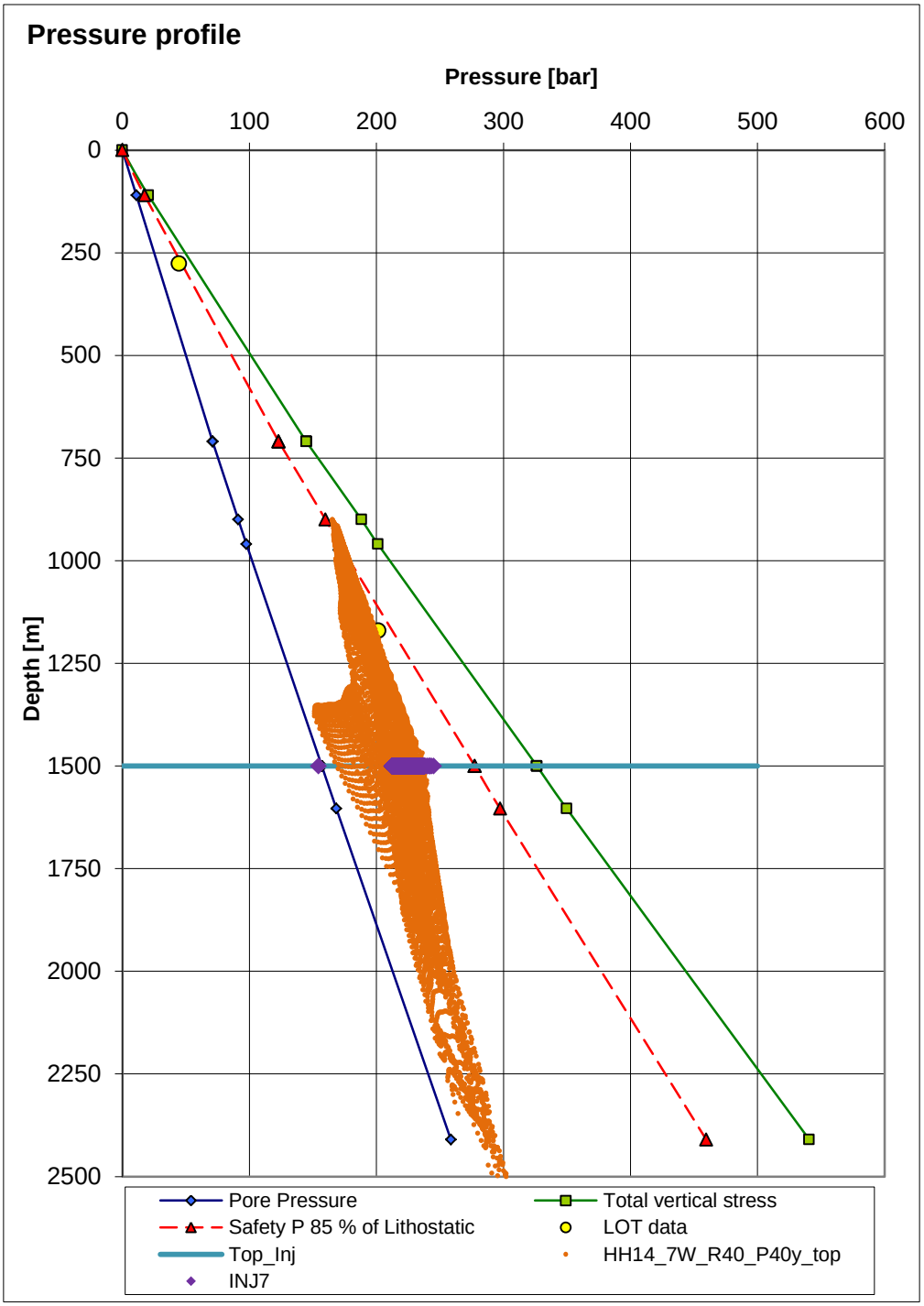

Figure 5-15 **Evaluation chart for pressure extracted from the uppermost reservoir layer at the 40 year time step (orange points) and the well BHP (purple points) at 1500 m depth. The hydrostatic and lithostatic gradients are calculated from brine and rock densities for the different formations overlying the reservoir. The safety margin for pressure at 85% of the lithostatic pressure is shown as red dashed line.**

5.9 Results

This described injection scenario results in a total injection mass of 1170 Mtons = 1.17 Gt capacity. This can be compared to previous estimates based on the static model characteristics and an assumed efficiency factor, in this case 40% as described by Larsen et al. (2003)(Table 5-1 and Figure 5-16).

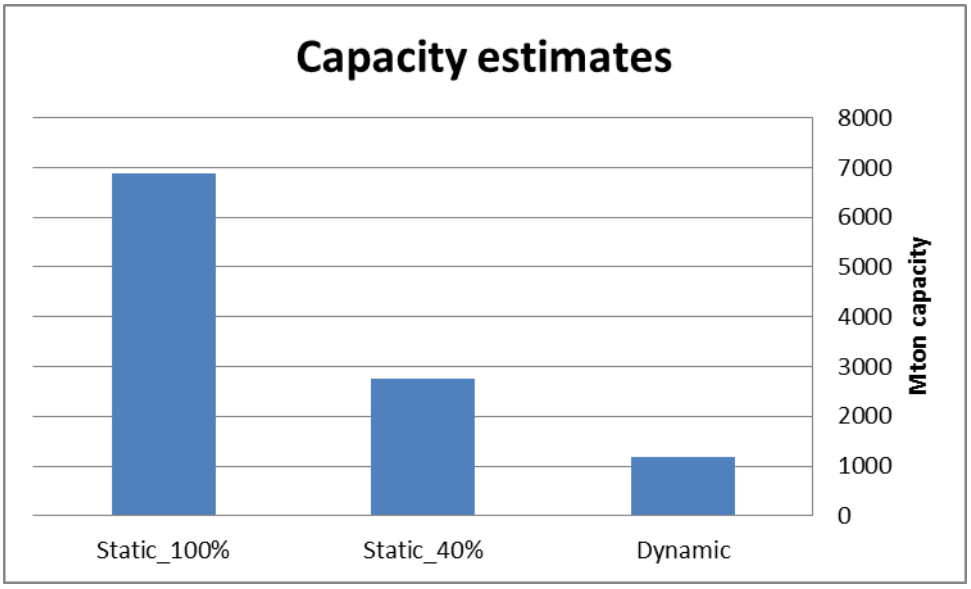

Figure 5-16 Comparison of different capacity estimates including value from dynamic simulation of optimum filling of the structure.

It should be obvious that the single scenario analysed here should be refined and subjected to various optimisation methods concerning injection strategy. The number of wells, location, operational injection rate over time, and other factor could be varied in order to optimise the estimate of capacity. Despite this treatment, it should also be noted that the underlying uncertainty for the geological model, often based on sparse data, will limit credibility of the capacity estimation study. Therefore this study should be seen as an example of a workflow which can be applied as a first-order treatment of structural closures for storage purposes.

Table 5-1 The table includes values derived from previous projects dealing with only static simply capacity estimates (GESTCO, GeoCapacity).

Evaluated Aquifers	Avg depth	Bulk volume	Pore volume	Avg K	Open/ Closed	Storage eff	Density	Storage capacity
	m	m^3	m^3	mD		%	t/Rm^3	Gtons
Vedsted	1800		0.638E+9	100	Closed	40	633	0.162
Hanstholm	1100		11.1E+9	400	Closed	40	620	2.753

6. Modelling of the Vedsted structure, Northwest Denmark

6.1 Structural outline and geology of the Vedsted area

The study area is the Vedsted site (Figure 6-1), an anticlinal structural closure, in northern Denmark (about 25 km east of the city of Aalborg) located in the Fjerritslev Trough as a subbasin in the Sorgenfrei-Tornquist Zone (Nielsen 2003). The main storage reservoir is represented by the regional Upper Triassic – Lower Jurassic Gassum Sand Formation (Dalhoff et al. 2011). The Gassum Formation is about 250 m thick in the Vedsted area and contains two sandy intervals divided by about 75 m thick interval of marine shales of the Fjerritslev Formation. This shale unit contains different sandstone layers of low thickness and is overlain by marine sandstones of 5 m thickness. The lower 140 m of the Gassum Formation is interpreted as fluvial sandstone interbedded with lacustrine mudstones upward grading into shallow marine sandstones interbedded with marine mudstones, while the upper 50 m of the formation are interpreted as marine shoreface sand (Nielsen 2003). Available well information indicates net to gross of 0.74 and sandstone porosity up to 20% is estimated from core material (Dalhoff et al. 2011, Larsen et al. 2003). Existing oil exploration wells from the 1950s (Vedsted-1 and Haldager-1), Top Gassum Formation map and available 2D seismic data allowed Frykman et al. (2009) to implement a 3D structural geological model.

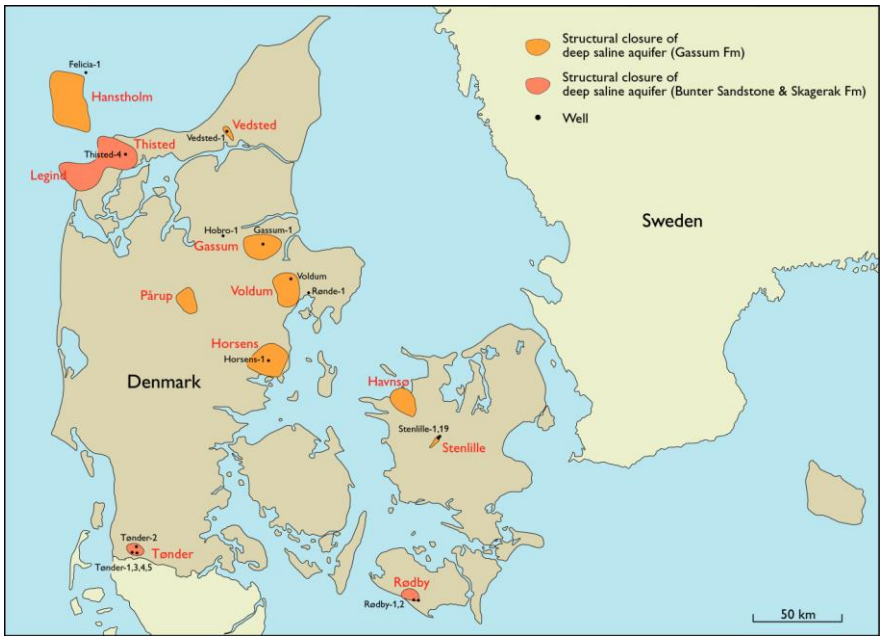

Figure 6-1 Map showing the position and outline of structural closures. Black dots indicate the position of some of the deep exploration wells used in the evaluation of the reservoir formation. The Vedsted structure is onshore Northern Denmark.

The primary caprock of the reservoir located in the Gassum Formation is the regional marine mudstones of the Fjerritslev Formation with a 525 m thickness at the study area. The Flyvbjerg Formation is the seal of the second reservoir (Haldager Formation), with a thickness of 25 m to 50 m consisting of marine mudstones with intercalated siltstones and sandstones. This formation is then followed by a thick succession of about 780 m of mainly marine mudstones of the Børglum, Frederikshavn and Vedsted Formations. The top of the model is represented by the Chalk Group of 400 m thickness and the Quaternary of relatively low thickness (Dalhoff et al. 2011, Larsen et al. 2003).

6.2 Dynamic flow simulations

Integrated dynamic fluid flow simulations studies were carried out for the Vedsted site by Frykman et al. (2009 and 2011) to assess CO_2 storage potentials and pressure perturbation in the two main reservoirs of the Vedsted structure. The very early work on capacity (Larsen et al. 2003) was re-evaluated, and according to Dalhoff et al. (2011) the total CO_2 storage potential was estimated to about 160 Mt considering a sweep efficiency of 40% at reservoir conditions. The dynamic simulation results could be fed directly into the development of a monitoring plan. Simulations using the ECLIPSE 100 black-oil simulator as undertaken by Nielsen et al. (2012) demonstrated that regional pressure propagation resulting from CO_2 injection can be mitigated by formation fluid production and that the structural filling is also enhanced by the integrated pressure management concept.

The present study will focus on a workflow for assessing the dynamic storage capacity from numerical simulations, incorporating the geometry of the mapped faults and their possible effects on filling pattern.

6.3 Model setup

The model area covers 12 x 16 km, with the long axis approximately aligned to fault zones mapped in the area (The rectangular model turned 25 degrees – NW)(Figure 6-2). The faults are included in the structural model. The updated Top_Gassum Map from the 2D seismic mapping has been imported into Petrel. Uniform thickness of the reservoir within the model area has been assumed. The main faults have been included in the gridding of the 3D model, although as vertical features and with zigzag geometry in the grid to minimise gridding irregularity.

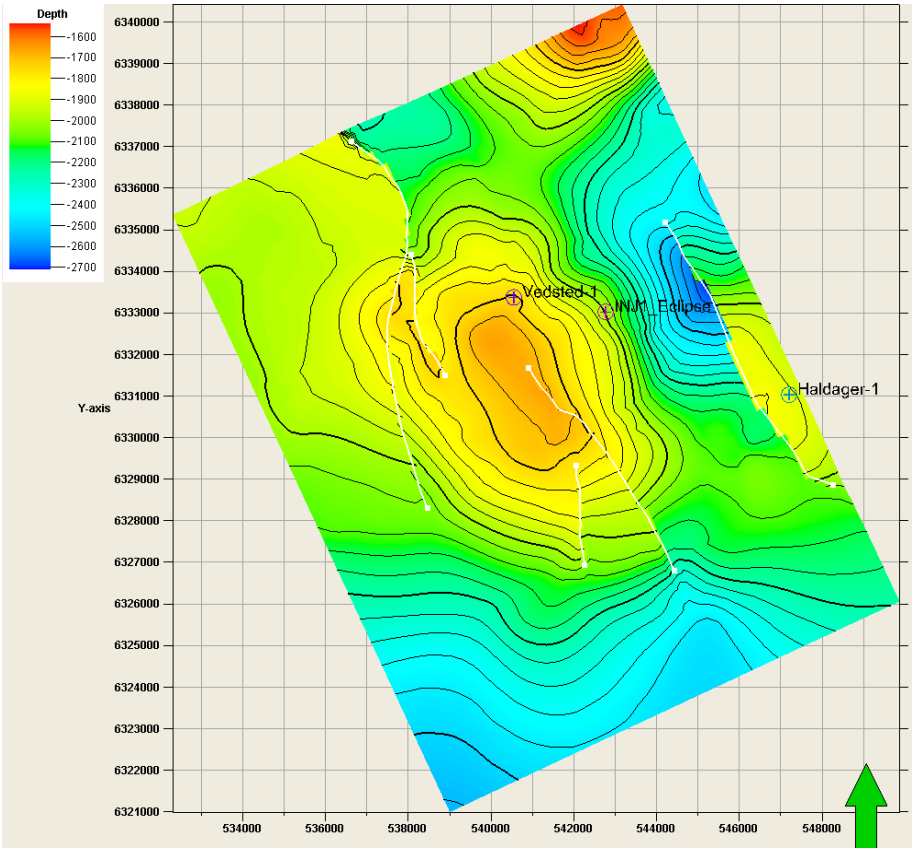

Figure 6-2 **Top Gassum reservoir map with faults. The existing old Vedsted-1 well and a suggested early stage injection well in simulation are shown.**

6.4 Well data

The Vedsted-1 has TD in the upper part of the Skagerrak Formation at 2068 m b.msl. The well was drilled in 1958, with the purpose of testing the presence of hydrocarbons in the Middle Jurassic and Upper Triassic sandstones. Hydrocarbons were not encountered and the well was plugged and abandoned.

From the Vedsted-1 well only an SP log and 3 resistivity logs are available.

A number of core plugs covering the Gassum and Haldager Sand Formations are available from the Vedsted-1 well and the nearby Farsø-1 and Børglum-1 wells. This material has recently been evaluated for analysis procedures and possible measurement errors, and a subset has been recommended for further use.

6.5 Porosity calculations

The porosity was calculated from the deep-reading resistivity log (64") and calibrated to core porosity data. Both the Haldager Sand and Gassum Formation are only partly cored and accordingly, the porosity evaluation outside the cored intervals is associated with considerable uncertainty.

The mud composition and salinity was changed at *c.* 1624 m, which affects the SP log readings. The shale volume is therefore calculated with two different sets of parameters.

6.6 Design and detail of geological model for the Gassum reservoir

For the Gassum reservoir model area we include the 2 wells (Vedsted-1 and Haldager-1) and an area around the structure, in total 12x16 km, and rotated at an angle of 25 degrees to align with most of the faults included in the model. Laterally the grid cells extend 200x200 m.

6.7 Lithology subdivision

To simplify the modelling procedure the sequence is viewed as only consisting of 2 main lithologies: "sand" and "shale". The subdivision separates into "shale" and "sand" at a threshold of 5% porosity on the log for PHIE (effective porosity). From an updated review of the geology and the sequence stratigraphic analysis, the reservoir is considered layered with long-range continuity of the both the sand and the shale layers. The sea-level changes have caused wide extent of the sandy deposits in blanket-like sheets, at least covering the 10's of km scale for the model area. Therefore high continuity has generally been assumed.

6.8 Assignment of physical properties to layers, Gassum reservoir

The porosity model has been converted with an equation for porosity/fluid-permeability relation: [PERMX3=20000*Pow(PHIE,3.4)]. Considering that the shale lithology might have thin silty or sandy intercalations that do not fully show up on the porosity log, we have assumed that if porosity is less than 6%, the permeability is assumed uniformly 1 mD.

As previously described, a number of air-permeability measurements are available from the Vedsted-1 cores, but fluid-permeability data do not exist in the Vedsted-1 database. Consequently, the air-permeabilities were transformed into assumed fluid-permeabilities by multiplying by 0.5, a factor derived from other studies. The modified Vedsted data along with some other selected data are also shown in Figure 6-3. For porosities greater than c. 20% it appears from the figure that the relationship actually used is slightly conservative compared to the limited Gassum Formation data presently available, if the air-fluid conversion is trusted.

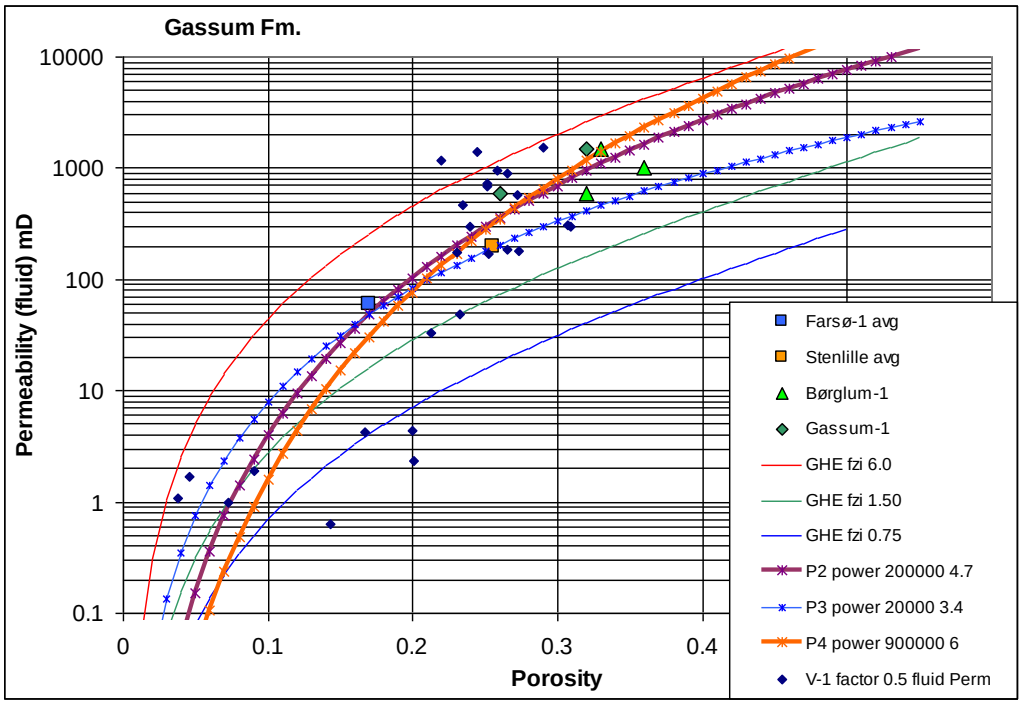

Figure 6-3 **Porosity vs fluid-permeability relation used for the modelling is shown as line P3 - in blue x. Core measurements from the Vedsted-1 well are plotted (dark blue); the original air-permeabilities have been re-calculated to fluid-permeabilities with a factor of 0.5. Furthermore, additional data from Gassum Formation samples from other wells are shown.**

The effective porosity and the permeability model are then exported for use in Eclipse.

6.9 Assignment of physical properties to faults

The fault model is incorporated in the Eclipse flow model by modifying the transmissibility values for the fault planes. For the faults have been used a transmissibility multiplier of 0.0099, and a setting for threshold pressure of 2 bar.

6.10 External boundary conditions

All external boundaries are no-flow boundaries. In order to moderate the pressure rise in the model, the pore volume of the outer grid cells is enlarged so that the CO_2 storage relevant volume can be considered surrounded by an infinite acting, constant pressure aquifer. To obtain this effect the pore volume of normal cells at the margin of the model was multiplied in Eclipse 10,000 times using the MULTPV keyword.

This boundary condition modification is to some degree simulating the condition if a family of water extraction wells were placed around the structure for managing the overpressure in the storage site and for moderating the pressure effects in the neighbouring region and any adverse effects on adjacent operations in the subsurface.

The pore volume compressibility is set to 6.96×10^{-5} 1/bar. This value has been adopted from previous studies (Frykman et al. 2009) and from other published studies, although a recent study by Mbia et al. (2013, 2014) has pointed out that caprock compressibility could be a factor 10 lower, i.e. more stiff than previously assumed. Initial hydrostatic conditions were assumed. Initial hydrostatic conditions were assumed.

6.11 Saturation functions

The curves (Figure 6-4) are inspired by analyses from Bennion and Bachu 2006(1). For the wells, linear relative permeability curves for brine and CO_2 phases were used.

For capillary pressure were used 2 different curves having 0.1 and 1 bar threshold pressure for the reservoir/shale respectively.

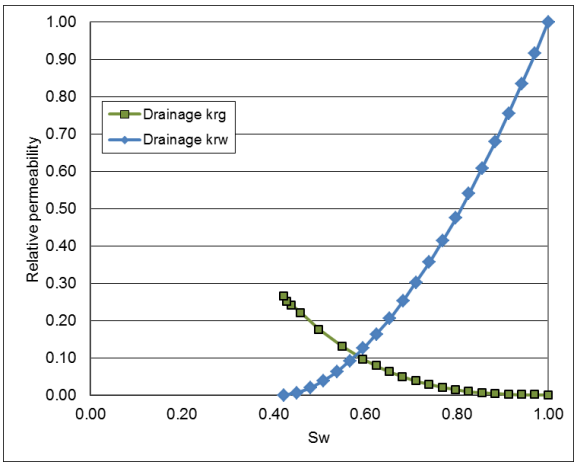

Figure 6-4 Relative permeability used for both lithologies.

6.12 Initial and injection conditions

The temperature at mid Gassum level is estimated as 49 Centigrade. From a general salinity/depth relationship a salinity of 16% is assumed.

Assuming hydrostatic pressure leads to a Gassum datum pressure of

$P_{D,Gassum}$ = 196 bar, at the datum depth $D_{D,Gassum}$ = 1724 m.

The PVT description is described in the input tables:

Brine_CO2_BO_PVT_data_vs3_P196bar_T66C_S25_PVTO.tab

CO2_PVT_T66C_P1-450bar.tab

By trial and error decision was reached for 4 wells to effectively fill most of the structure (Figure 6-5). The placement was considered in relation to faults and avoidance of spill points.

The CO_2 was injected at a constant rate of total of 3.1 Mt per year. The dynamic simulations account for the injection period of 40 years (Figure 6-6 and 6-7).

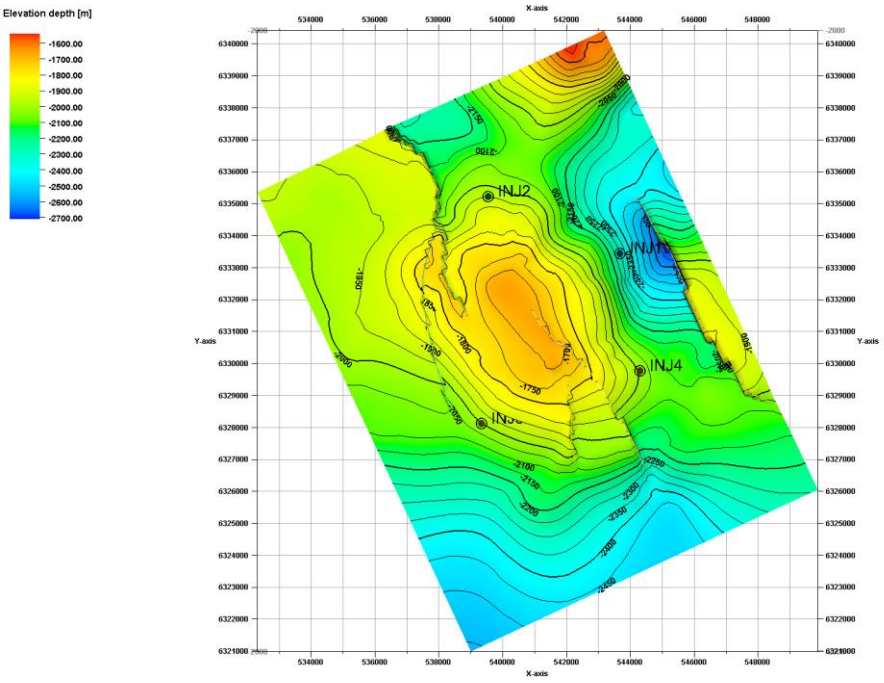

Figure 6-5 Map with depth contours for the top reservoir level and the position of the 4 injection wells.

6.13 Filling of structure

This described injection scenario results in a total injection mass of 125 Mtons = 0.125 Gt capacity.

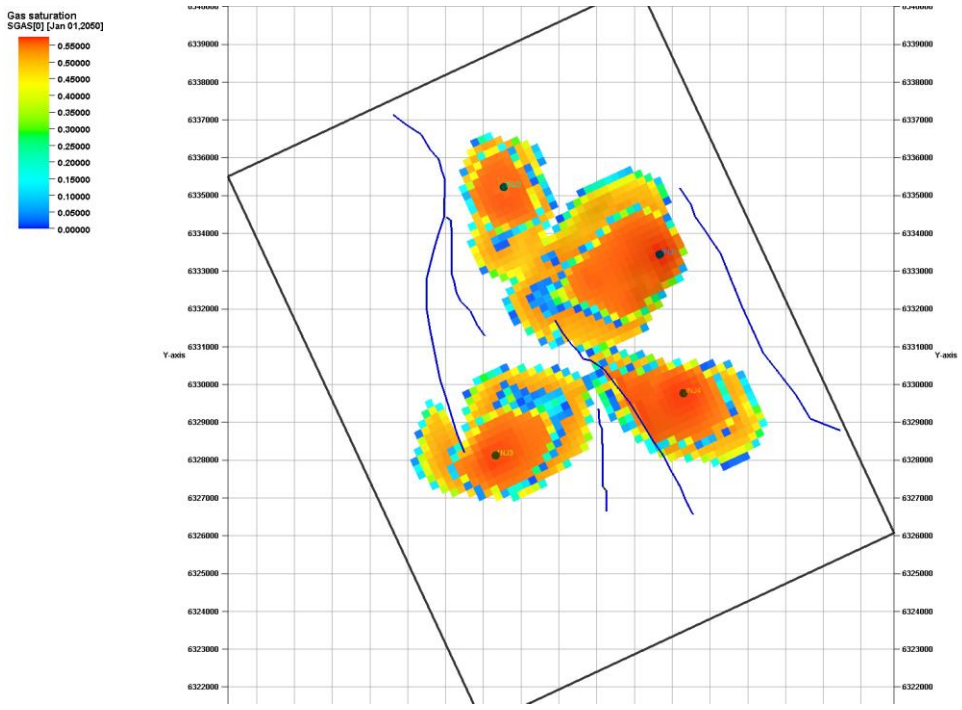

Figure 6-6 Map of extent of all layers with CO_2 saturation. Injection scenario at 40 years injection.

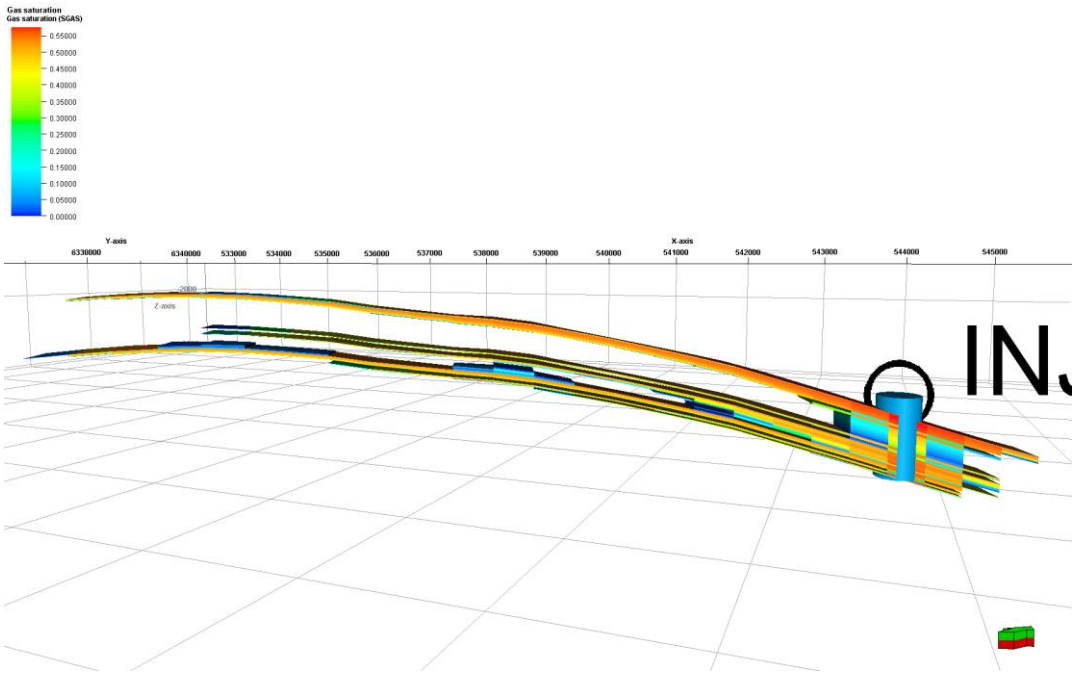

Figure 6-7 Vertical section West-East through injection well no. 1 showing the extent of the plume of 5 km laterally.

Without any geological information, it was considered that the engineering safety margin on the cap rock will allow a pressure increase up to about 85% the lithostatic pressure. Changing this safety rule will of course influence the evaluation of the storage capacity and has to be discussed in relation to risk factors regarding cap rock integrity (Figure 6-8).

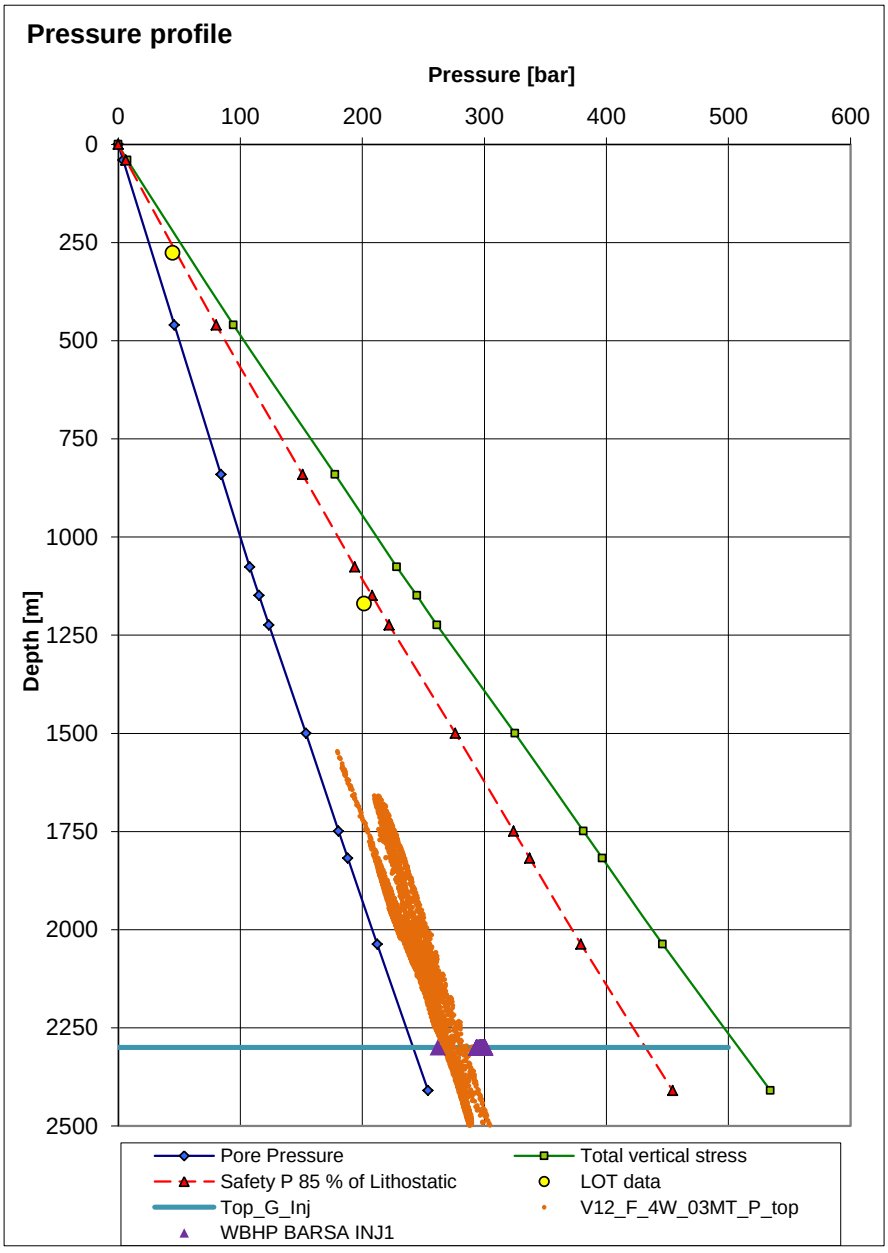

Figure 6-8 **Evaluation chart for pressure extracted from the uppermost reservoir layer at the 40 year time step (orange points) and the well BHP (purple points) at 2300 m depth. The hydrostatic and lithostatic gradients are calculated from brine and rock densities for the different formations overlying the reservoir. The safety margin for pressure at 85% of the lithostatic pressure is shown as red dashed line.**

6.14 Results

This described injection scenario results in a total injection mass of 125 Mtons = 0.125 Gt capacity. This can be compared to previous estimates based on the static model characteristics and an assumed efficiency factor, in this case 40% as described by Larsen et al. (2003), giving estimated capacity of 162 Mt (Figure 6-9).

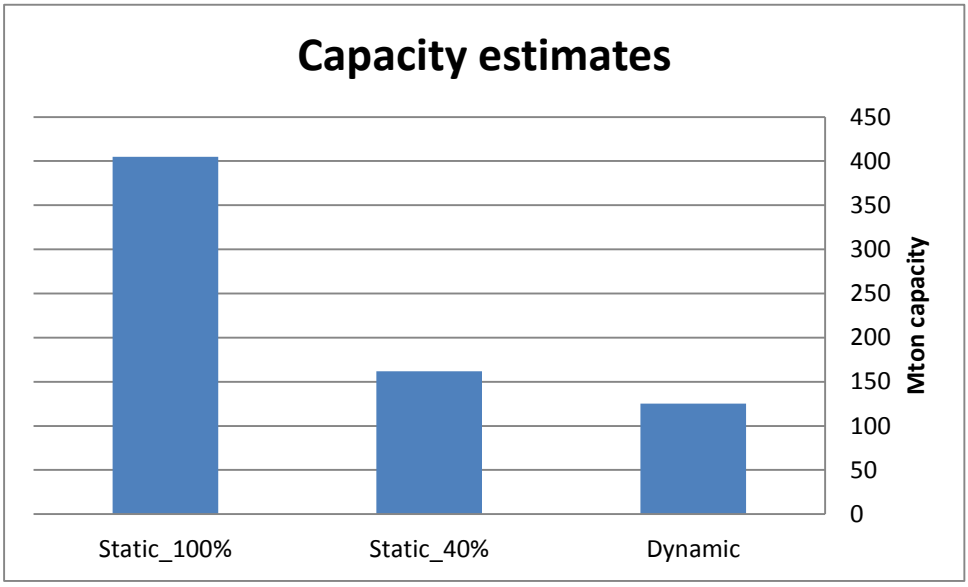

Figure 6-9 Comparison of different capacity estimates including value from dynamic simulation of optimum filling of the structure.

It should be obvious that the single scenario analysed here should be refined and subjected to various optimisation methods concerning injection strategy. The number of wells, location, operational injection rate over time, and other factor could be varied in order to optimise the estimate of capacity. Despite this treatment, it should also be noted that the underlying uncertainty for the geological model, maps, faults and their properties, often based on sparse data, will limit credibility of the capacity estimation study. Therefore this study should be seen as an example of a workflow which can be applied as a first-order treatment of structural closures for storage purposes.

7. Simulations of Faludden Sandstone, offshore Sweden

During the 1970-80s southern Sweden was commercially prospected for hydrocarbons by the Swedish Oil Prospecting Company (OPAB) and the Swedish Exploration Consortium (SECAB). Several seismic surveys with 2D technique were performed in the south-east Baltic Sea and south-west Scania. Most data are in analogue form, only limited degree of digitalization has been conducted recently. During the same investigations, a number of exploration wells were drilled, preferably onshore. All data from these investigations are public and stored at the Geological Survey of Sweden. Due to very limited findings, no further exploration was performed. Furthermore, the Geological Survey of Sweden has drilled five deep wells in Scania during 1940-1960s. Some core material and cuttings have been stored at the Geological Survey of Sweden.

Based on the NORDICCS ranking of storage sites (Aagaard et al. 2014), three of the eight Swedish identified storage aquifers are selected for further description:

- Faludden sandstone
- Arnager Greensand
- Höganäs-Rya sequence

In addition, dynamic modelling has been carried out for the Faludden sandstone and the Arnager Greensand (Figure 7-1).

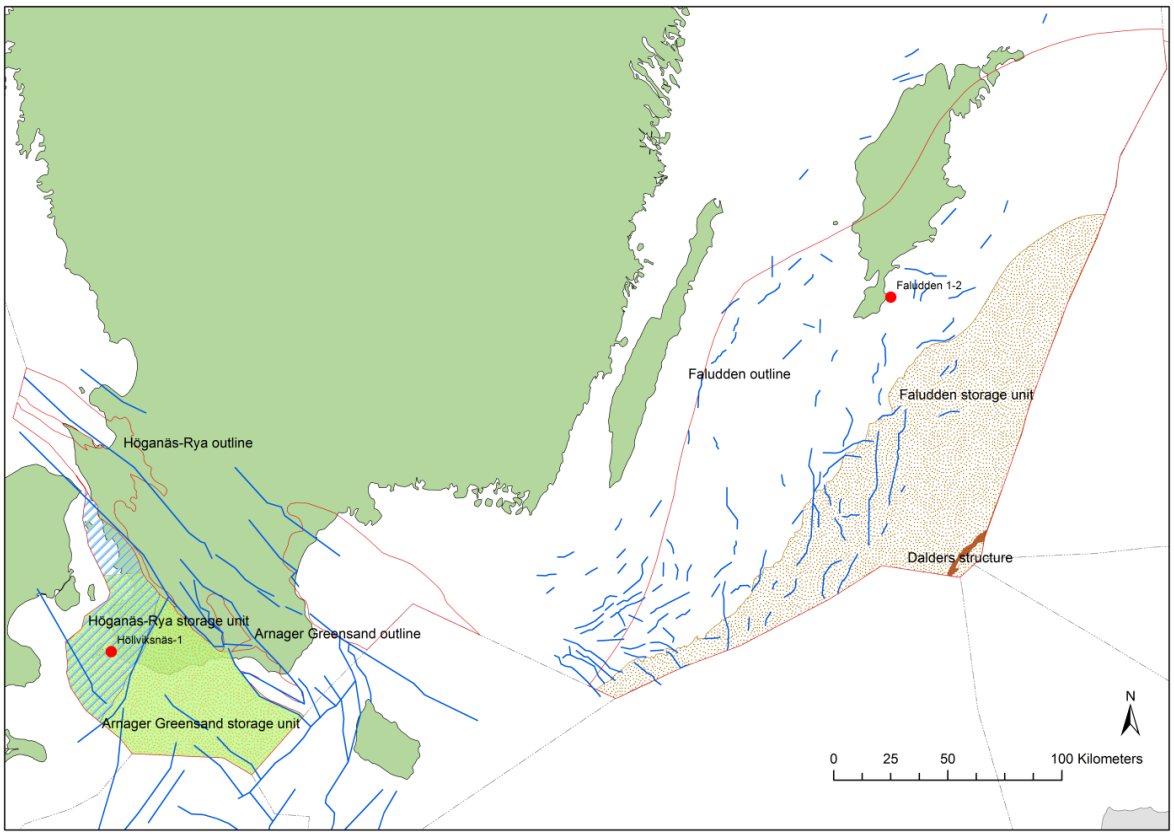

Figure 7-1 Map of the southernmost Sweden showing the assumed three best CO_2 storage sites in Sweden. Blue lines represent faults in the two areas; red dots mark the position of presented litho-stratigraphic logs (see Figure 7-2 and Figure 8-1).

7.1 Geological description of the Faludden sandstone

The Faludden sandstone is a member of the Borgholm Formation and is located in the south-east Baltic Sea. The sandstone was deposited in Middle Cambrian in the Baltic Syneclise which is the largest tectonic element within the south-western margin of the East-European Craton (Brangulis et al. 1993). Hence, the Faludden sandstone was deposited in a relative stable tectonic environment and sedimentation proceeded relatively slow and uniformly resulting in high homogeneity over a large area. The sandstone was deposited near shore and has a basin wards progradation from east to west. Minor variations represented by interbeds of shale and siltstone reflect distance to shore line, fluvial and deltaic influences and water depths (Erlström et al. 2011). To the south and south-west a shift in facies to more marine conditions is identified as finer grain size in an equivalent to the Faludden sandstone. The Faludden sandstone has a large lens shaped distribution weakly dipping (<1°) towards the east-south-east. The regional distribution of the sandstone unit covers an area of c. 33000 km² in Swedish territory. Towards the Baltic countries the Faludden sandstone continues as the Deimena Formation where it outcrops in Estonia, and is deeply buried at depths of more than 2000 m in Lithuania and more than 3000 m in Poland (Sliaupa et al. 2012). To the north-west the Faludden sandstone is pinching out in a north-east to south-west line between the islands of Gotland and Öland following the north-western margin of the Baltic Syneclise. The Faludden sandstone upper surface is relatively smooth except from small highs with amplitudes at 20—50 m and limited areal distribution (Erlström et al. 2011). In Swedish territory the Faludden sandstone is found on depth from 400 m below sea level beneath the island of Gotland to 1000 m below sea level in the deepest part offshore to the south-east. Thickness varies from 1—49 m increasing towards the Swedish economic zone to the south-east. Average thickness is 10 m onshore and 45 m offshore (OPAB 1976).

In terms of CO_2 storage the Faludden sandstone represents a stratigraphic confined open/semi-closed saline aquifer with a large lateral distribution where the part deeper than 800 m is covering an area of c. 11000 km² on Swedish territory (Mortensen 2014). The storage unit contains a structural trap, the Dalders structure, which has undergone commercial prospecting for oil, but the data is not available.

7.2 The CO_2 storage properties to Faludden sandstone

The Faludden sandstone consists of a clear, fine- to medium-grained, well sorted, calcite cemented quartz sandstone with local interbeds of shale and siltstone (Figure 7-2). In general, the upper 3-5 m of the sandstone is very hard and clayey with low porosity (OPAB 1976). The estimated net/gross sand is as high as 90% (Mortensen 2014). Chemical analyses performed by the Geological Survey of Sweden show silica oxide contents at 84,7-97,8% (Erlström et al. 2011) and densities at 2,65-2,67 g/ccm which further reflects the purity of the sandstone. Maximum bottom hole temperature at depth corresponding to the Faludden sandstone is in the range of 30-35°C with a gradient at 3-5°C per 100 m which is very high compared to crystalline bedrock in Sweden normally being in the range 2 °C per 100 m. Measurements on geophysical logs together with well cores show porosities in the range of 8.2-20% with an average of 14%, and permeabilities at 0,665-1255 mD, averaging 147 mD. Investigations by OPAB shows traces of oil and gas found in several wells on the island of Gotland and on geophysical logs from the offshore area (wells B-7 and B-9) indicate gas contents in the sandstone.

7.3 The caprock units

The Faludden sandstone sequence is followed by c. 80 m Ordovician limestone, with bentonitic limestone in the bottom c. 50 m, which is followed by c. 500 m Silurian marlstone (Figure 7-2).

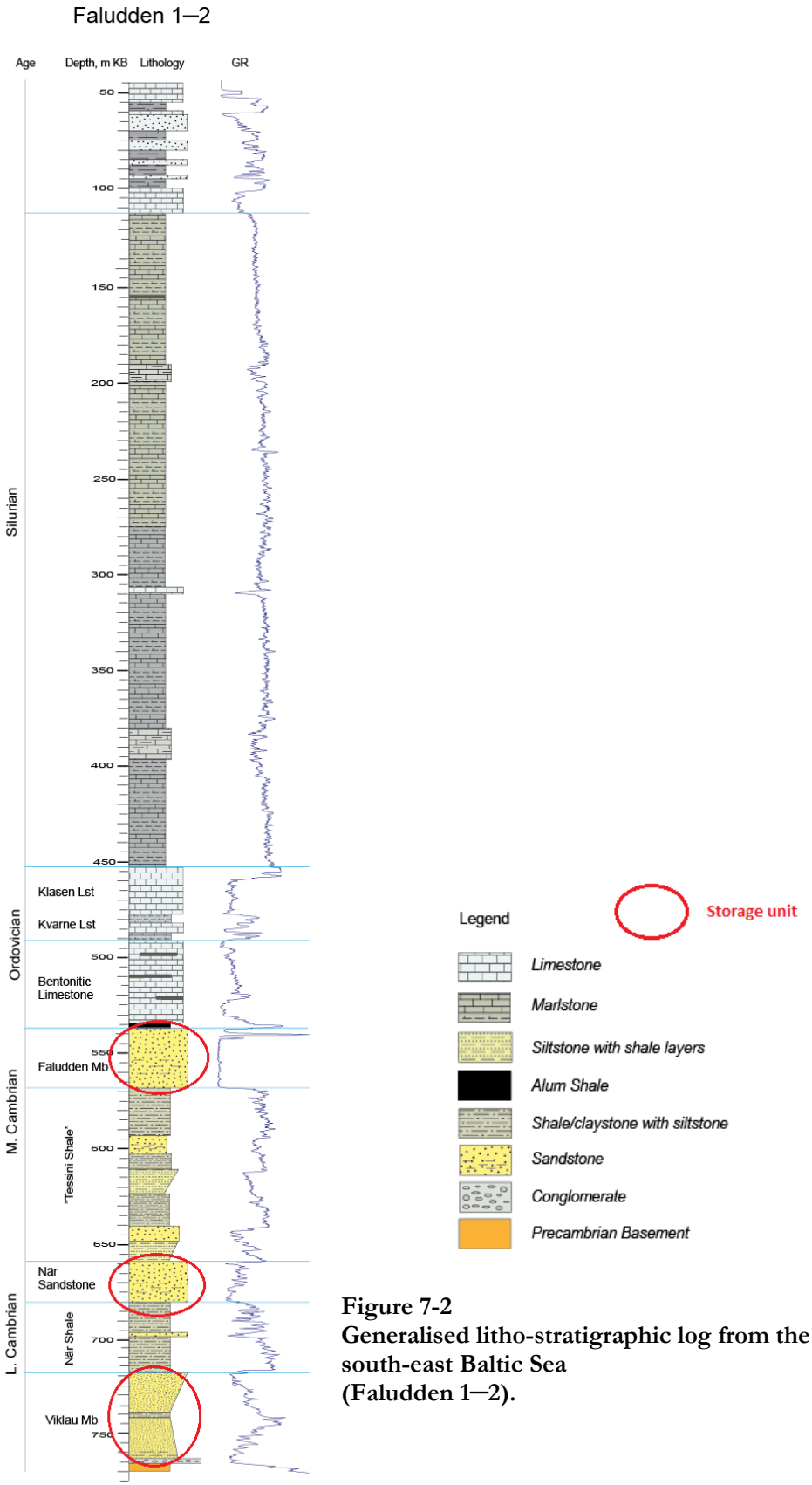

Figure 7-2
Generalised litho-stratigraphic log from the south-east Baltic Sea (Faludden 1–2).

7.4 Dynamic modelling of the storage capacities for the Faludden sandstone, south-east Baltic Sea

Based on the geological evaluation the Cambrian Faludden sandstone was selected for dynamic modelling of CO_2 storage capacity in the south-east Baltic Sea. Both, a basin modelling approach (SEMI) and a reservoir simulation (ECLIPSE 100) were performed (for a detailed description of the methods see chapter 4.3).

7.4.1 Modelling input data

Input parameters for the modelling approach are given in Table 7-1. Surfaces and fault maps were constructed from available interpreted seismic lines and well data (SGU and OPAB) (Figure 7-3). For the bathymetric maps we used data provided by the Baltic Sea Hydrographic Commission (2013). A thickness map for the Faludden sandstone was constructed and provided by Erlström et al. (2011) and further edited using Petrel.

Table 7-1 Parameters used for the basin modelling approach. The Baltic area fault map is constructed from the "Seismic Interpretations 1975, Baltic Sea, and Top Cambrian horizon made by OPAB.

Name	Depth [b.msl]	Thickness [m]	N/G	Porosity [%]	Thermal gradient [°C/km]	Surface temperature [°C]	Permeability [mD]
Faludden sandstone	Map seabed	Map	0.90	14	40	4	147

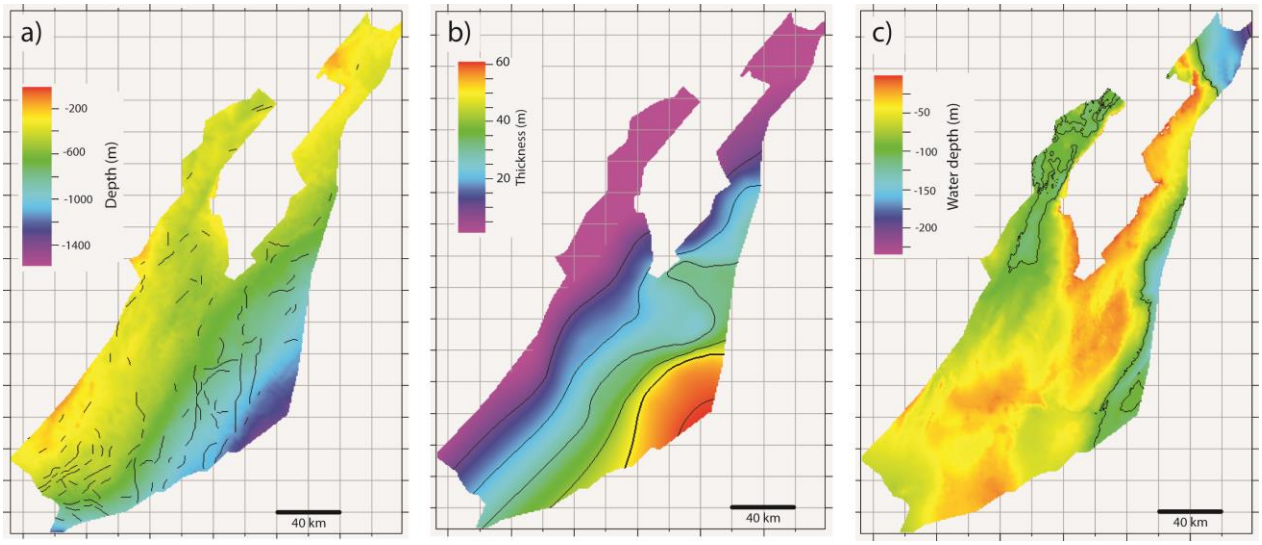

Figure 7-3 Input maps for the Faludden sandstone. a) Top of the Faludden sandstone with interpreted faults. b) Thickness map. c) Present day water depth.

7.4.2 Results from the basin modelling approach

a) Total trap storage capacity

The total trap storage capacity was calculated (methodology described in chapter 4.3) assuming two end-member scenarios, one as an open aquifer trap and one with sealing faults. The results are report for the whole stratigraphic unit and for the part below a depth of 800 m.

Modelling results indicate a total trap storage capacity of 561 Mt for the Faludden sandstone without faults. For the part below 800 m the modelled storage capacity in traps is reduced to only 10 Mt. If sealing faults are assumed, the total storage capacity increases to 602 Mt and for the part below 800 m the capacity increases to 70 Mt (Figure 7-4).

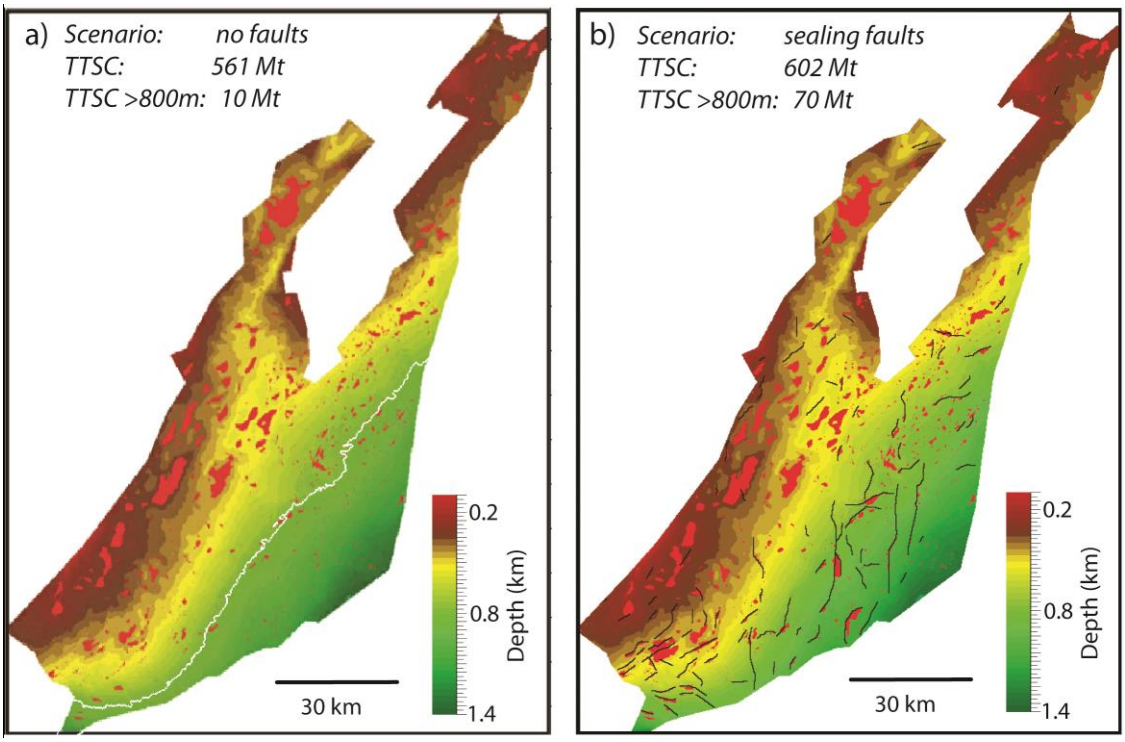

Figure 7-4 **Estimates of the total trap storage capacity (TTSC) for the Faludden sandstone (a, b). For the unit the total trap storage capacity depends on the sealing efficiency of faults. The maps are top surfaces of the Faludden units overlain by traps (red areas), black lines are faults (b) and the white line is (a) the 800 m depth isopach.**

b) Screening of safe injection sites

The basin modelling approach was used for a systemic screening for "safe injection sites" (see chapter 4.3). First, we injected CO_2 with a rate of 0.5 Mt/year over a period of 100 years. For the Faludden sandstone no safe injection site could be identified. CO_2 migration paths strongly depend on the fault distribution (Figure 7-5). For most of the tested injection sites, safe sites for the no fault scenario spilled out of the working area for the fault scenario or vice versa. Only by reducing the CO_2 injection rates to 0.23 Mt/year a safe injection site could be identified. The chosen site is located close to the south-eastern border within the deepest parts of the working area (Figure 7-5).

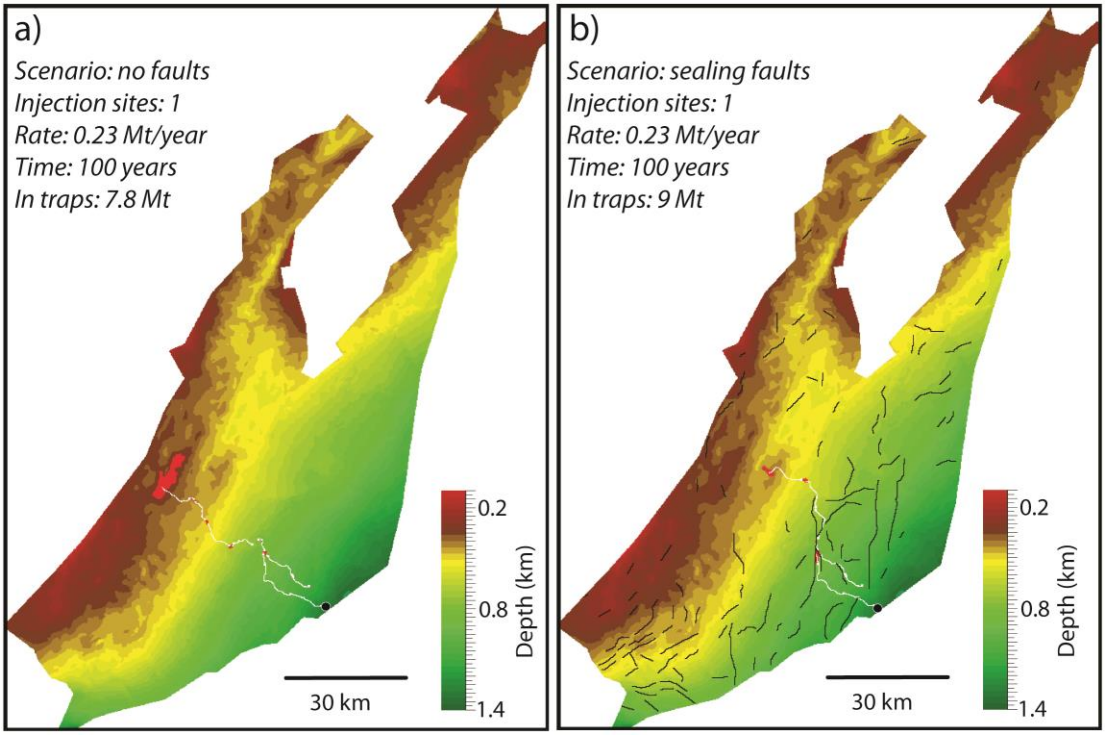

Figure 7-5 Results of screening for "safe injection sites". The maps are top surfaces of the Faludden unit overlain by traps (red areas). The black lines are faults (b) and the white lines indicate active spill-paths (a-b). Injection sites are marked with the black circle. In this modelling approach we used CO_2 dissolution during migration and in the trap entities.

7.4.3 Description of reservoir simulation model

Reservoir models for the mapped areas of the Faludden and the Arnager Greensand aquifer units have been constructed using Petrel. The reservoir models for Faludden and Arnager Greensand are described below. For both simulation models, temperature and formation water salinity have been set constant to 40°C and 6.3% total dissolved salts (TDS) respectively. The salinity and temperature are uncertain but the applied values are assumed representative for the injection depths in the two models and are on the conservative side with regards to CO_2 migration into the shallower regions. Saturation functions used are also the same for both models. The relative permeability functions are linear with residual gas saturation equal to 0.2 and residual water saturation equal to 0.07. Capillary pressure between CO_2 and water are set to zero (see Bergmo *et al.*, 2013).

a) Faludden simulation grid

A simulation grid with approximately 1.3 million grid blocks has been constructed based on the top Faludden depth surface, the Faludden isopach map and the interpreted fault lines received from SGU (see Figure 7-4). The lateral grid block resolution is 500 by 500 metres and the grid has four layers with the upper two layers refined to 1 m thickness. Figure 7-6 displays the outline of the modelled area with cell centre depth of the simulation grid top layer. Observe that the Dalder Structure is not included in the model.

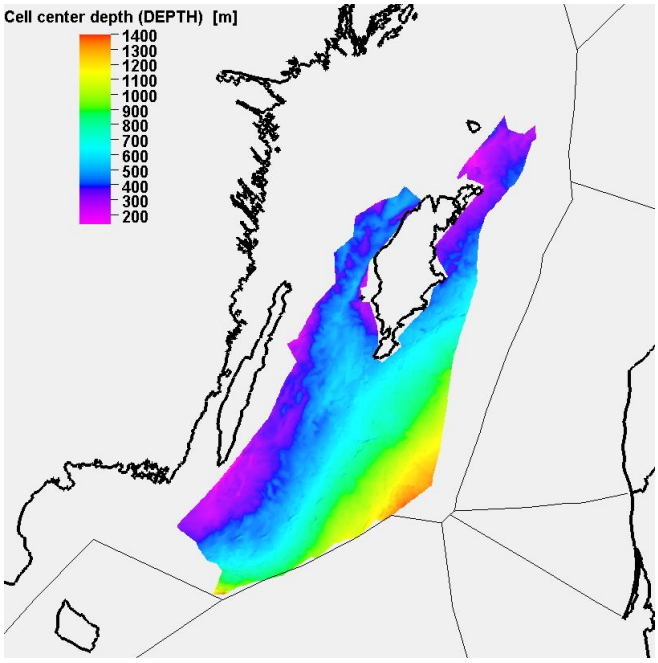

Figure 7-6 Outline of the model area showing the cell centre depth of the top layer in the simulation grid.

Average reservoir properties for Faludden are listed in Table 7-1. Based on interpretation from existing and available well logs (SGU) the reservoir model was populated using a stochastic Gaussian distribution function to add some heterogeneity into the model. Porosity varies between 8 and 20% with average value equal to 14% and permeability varies between 0.7 and 1255 mD with average value equal to 147 mD. Net to gross is set constant to 90%. Only one realisation with the given reservoir properties (porosity and permeability) has been generated. Figure 7-7 shows distribution of porosity and permeability in the top layer of the model.

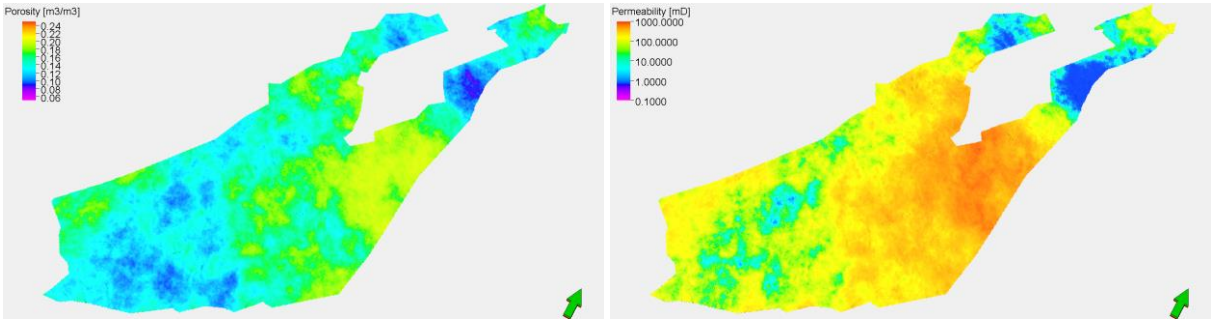

Figure 7-7 Petrophysical properties in the Faludden simulation model. Distribution of porosity (left) and permeability (right) in the top layer.

To represent the part of the formation not included in the model, pore volumes of the boundary grid blocks to the East and South-East has been increased by a factor of 500 (pore volume multiplier). This represents more than a doubling of the total pore volume of the formation. This will help dissipate the induced pressure from injecting CO_2 into the formation. However, to enable a relatively high injection rate and better utilisation of the storage resource, water production wells are required to keep the injection pressure below an assumed safe pressure limit (75% of lithostatic pressure). Figure 7-8 shows pressure distribution

below the cap rock initially, with and without modified aquifer and production wells and the assumed safe pressure. Lithostatic pressure at top Faludden is estimated using a constant overburden density of 2500 kg/m³ (from sea bed to top Faludden).

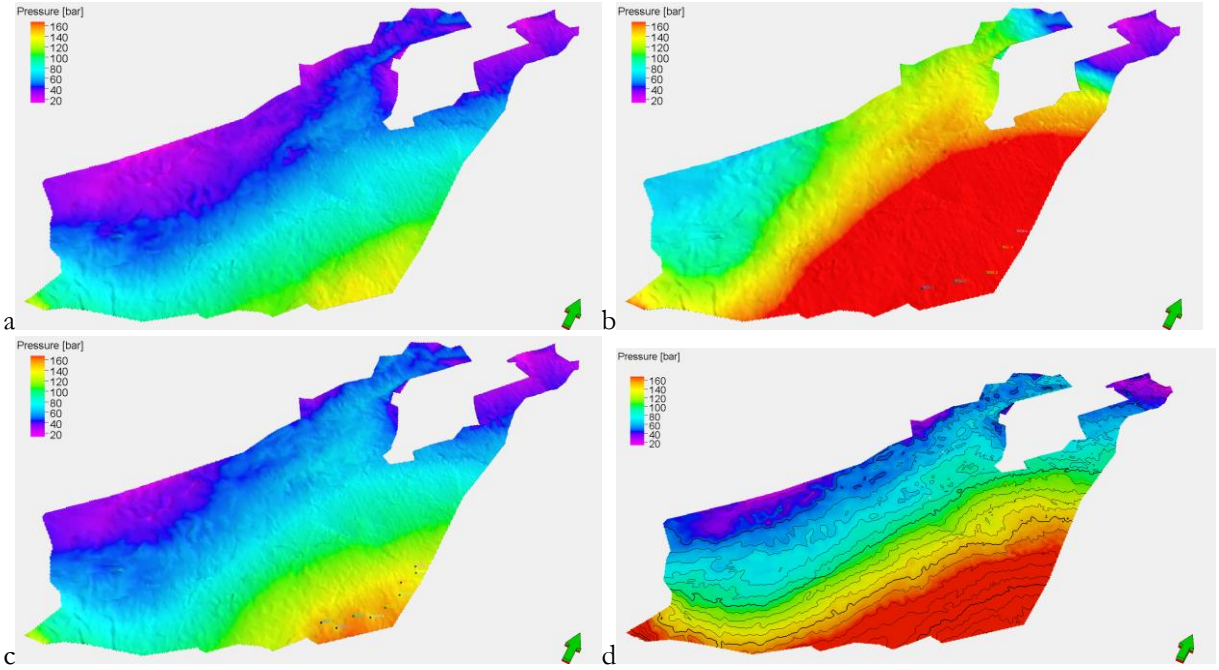

Figure 7-8 **a) Initial pressure distribution below the cap rock, b) pressure distribution at end of injection (500 Mt) without production wells and pore volume multiplier, c) pressure distribution at end of injection (500 Mt) with five production wells and pore volume multiplier and d) estimated safe pressure below the cap rock (75 % of lithostatic pressure).**

A series of tests to optimise the position, number and rates for injection wells resulted in six injection wells with injection rates between 0.5 and 1 Mt/year located in the deepest part of the formation. In addition, five production wells producing at constant bottom hole pressure (hydrostatic pressure) were positioned down-flank from the injectors. Figure 7-9 displays CO_2 saturation at the top after ten years injection indicating the positions of the injection and production wells. The northernmost and southernmost injection wells inject 0.5 Mt/year while the rest of the wells inject 1 Mt/year.

Figure 7-9 CO_2 distribution at top Faludden after 10 years injection showing position of injection and production wells.

As there are only smaller traps in the modelled area the main trapping mechanisms are capillary trapping as residual gas and trapping by dissolution into the formation water. As it is shown in the result section, parts of the injected CO_2 migrates to shallow depths (<600 m) and the amount are reported by indexing the regions shallower than 600 m, between 600 and 800 m and below 800 m in the model.

7.4.4 Results from dynamic reservoir simulations for the Faludden sandstone

To estimate a CO_2 storage capacity for the Faludden aquifer unit in the modelled area two final scenarios were simulated. One injecting 500 Mt CO_2 over a period of 100 years and one injecting 250 Mt CO_2 over a period of 50 years. The injection rates are the same in the two cases with 1 Mt/year for the four central wells and 0.5 Mt/year for the northernmost and southernmost wells. Figure 7-10 displays the CO_2 saturation after the injection period for the two cases.

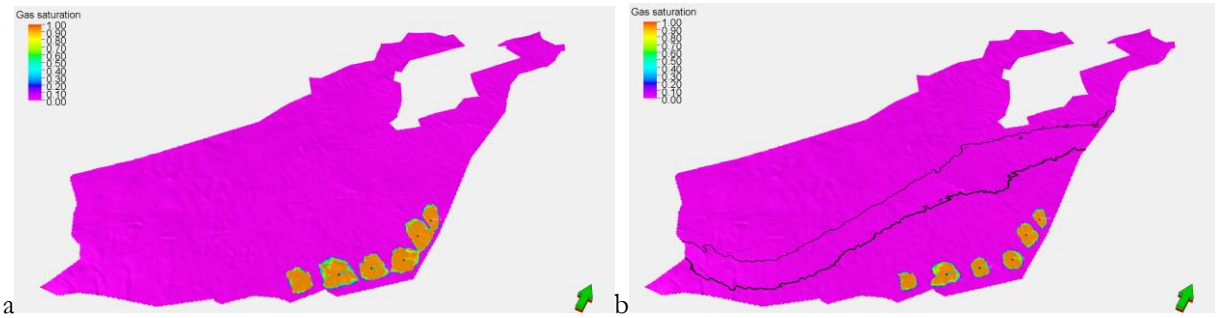

a b

Figure 7-10 CO_2 saturation at the end of the injection period, a) 100 years and b) 50 years. The iso-depth lines in figure b) shows the 600 and 800 meter depths.

After end of injection the simulation model is run for another 6000 years to model the migration of CO_2 towards the shallower regions. An evaluation of the storage capacity can then be performed based on how far the injected CO_2 migrates and how much of the CO_2 that will end up in the shallower regions (< 600 - 800 m).

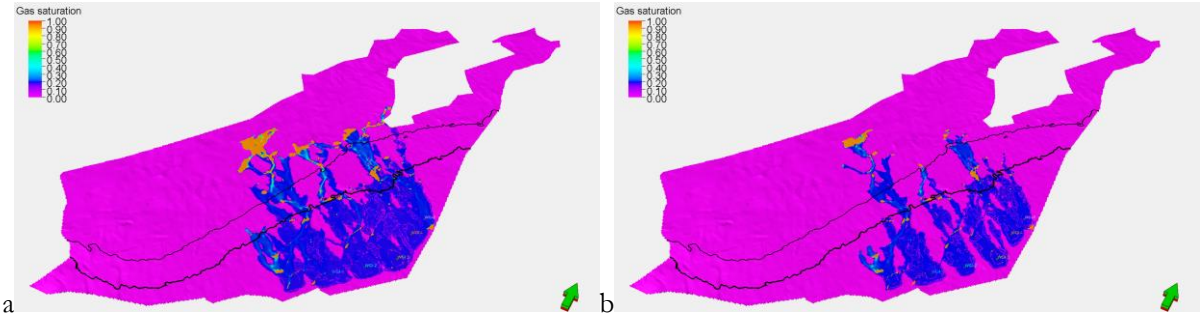

Figure 7-11 CO_2 saturation after 6000 years in the case with a) 500 Mt CO_2 injected and b) 250 Mt CO_2 injected. Iso-lines are at depth 600 and 800 meters.

Figure 7-11 shows that for both cases part of the injected CO_2 migrates to traps that are shallower than 600 meters. The CO_2 is at these depths no longer in dense phase (temperature dependent) but since it is retained in structural traps no further migration is expected. Figure 7-12 displays amount CO_2 in the different depth regions as function of time. For the case with 500 Mt CO_2 injected, 13% of the injected CO_2 ends up in traps shallower than 600 meters and 10.8% is located in the depth region between 600 and 800 meters. For the case with 250 Mt CO_2 injected the results are 4.1% and 9.1% respectively. Observe that a large part of the injected CO_2 is capillary trapped as residual gas (blue colour saturation)(Figure 7-11).

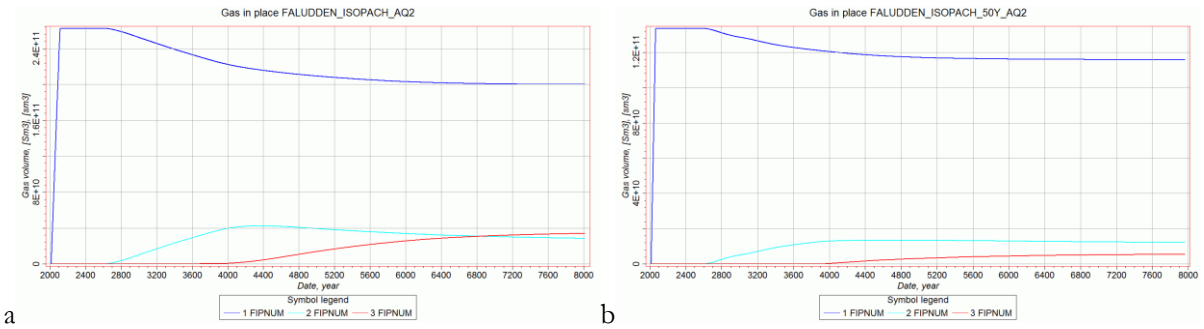

Figure 7-12 Volume CO_2 in the different depth regions as function of time for a) the 500 Mt CO_2 case and b) the 250 Mt CO_2 case. FIPNUM 1 is deeper than 800 m, FIPNUM 2 is between 600 and 800 m and FIPNUM 3 is shallower than 600 m.

Figure 7-13 shows the amount of dissolved CO_2 in the two cases. Total amount CO_2 dissolved after 6000 years is 39% (Figure 7-13a) and 42.5% (Figure 7-13b).

a)

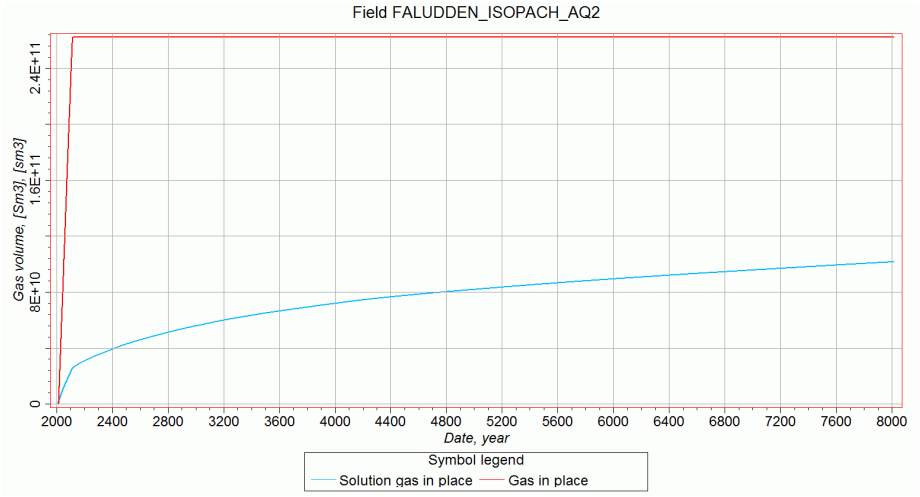

b)

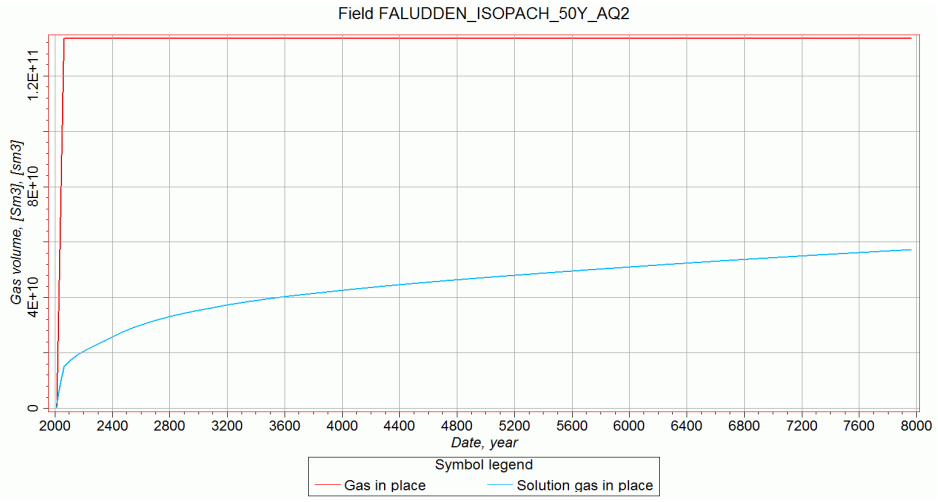

Figure 7-13 Total injected CO_2 volume (red) and dissolved CO_2 volume as function of time for a) the 500 Mt CO_2 case and b) the 250 Mt CO_2 case.

7.4.5 Summary from Eclipse simulations of the Faludden sandstone

The above described simulation results indicate a storage capacity for the Faludden sandstone in the order of 250 Mt CO_2. In the simulation approximately 4.1% migrated to depths shallower than 600 meters and approximately 42.5% of the injected CO_2 was dissolved into the formation water after 6000 years. The case simulated for the Faludden sandstone with injection of 500 Mt indicates that around 13% migrates to traps at depths shallower than 600 meters. This could pose a problem as the CO_2 at these depths are in gaseous phase experiencing much larger buoyancy forces and occupies much larger volumes. However, further migration of the CO_2 is not known.

It should be noted that there are large uncertainties in the models which will affect both the migration speed and distance, the residual trapping and the dissolution of CO_2 into the formation water. The results are, however, considered representative in giving an approximate estimate of storage capacity. The parameters are for the most cases considered conservative but further studies and more data is required to confirm this.

7.4.6 Discussion

Several studies have been published aiming to quantify the CO_2 storage capacity of the Faludden sandstone (Vernon et al., 2013; Anthonsen et al., 2013; Sopher et al., 2014). Different methodologies have been applied to different main target areas (Figure 7-14) giving a large spread in estimated CO_2 storage capacities (see Table 7.2). Thus, a direct comparison of these estimates is not possible and only results of similar approaches can be compared directly.

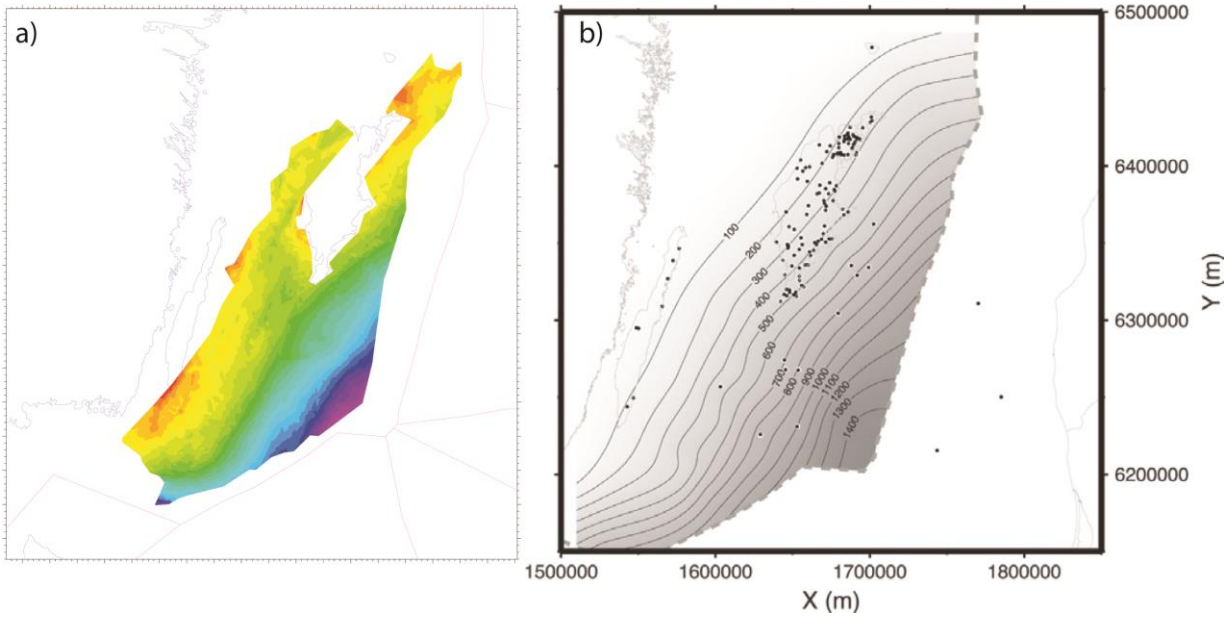

Figure 7-14 Comparison of the areas modelled in this study (a) and in Sopher et al. 2014 (b).

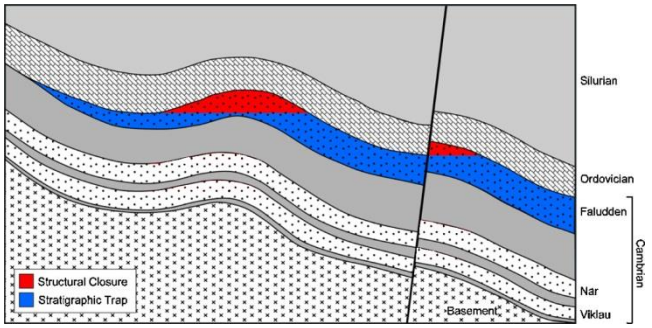

Figure 7-15 Definition of structural and stratigraphic traps illustrated on a schematic cross section through the Baltic Basin (from Sopher et al., 2014)

Following the definition of trap types (Figure 7-15) used by Sopher et al. (2014) all results from the basin modelling approach give estimates for structural traps. A further subdivision was made because the sealing behaviour/efficiency of the faults is unknown; by modelling two end member scenarios with open and sealing faults respectively. The results emphasize that the fault properties play an important role in the evaluation of storage capacities of structural traps, especially in the area below 800 m (Figure 7-4b; Table 7-2). However, our results are slightly lower compared to the estimates by the Sopher et al. (2014), SLR and the SGU reports (estimates number 3, 6 and 7 in Table 7-2). The logical reasoning for this is the different assumptions and modelled areas. The studies by Sopher et al. (2014), SLR and the SGU included:

- a larger area (Figure 7-8)
- larger traps in the deeper part of the Faludden sandstone (e.g., the Dalders structure)
- only sealing faults
- CO_2 dissolution in the trap entities

Because of a large variety of unknown parameters a simplified method was used, giving an estimate of how much CO_2 can be trapped if all traps are filled to a maximum capacity. In this approach do not model dissolution of CO_2 within the traps entities or during migration. The simulation results for the Faludden sandstone give estimates between ca. 602 Mt and 561 Mt depending on the fault sealing behaviour. The latter values can be regarded as a minimum trap storage capacity. However most of the larger traps are located at depth above 800 m (Figure 7-5) and below 800 m the capacity estimates are significantly lower ranging between 70 Mt and 10 Mt. These results indicate the importance of fault sealing efficiency on the final storage estimates.

Table 7-2 Comparison of different CO_2 storage capacity estimates for the Faludden sandstone. All models are based on different areas (size), modelling targets, different approaches, and/or used parameters (e.g., variable storage efficiency factor, porosities, temperature gradients, etc.).

ID	Author	Method	Comment	Storage capacity (Mt)
Structural traps - whole AOI				
1	This study	Basin Modelling	Structural traps (sealing faults)	602
2	This study	Basin Modelling	Structural traps (open faults)	561
3	SLR	Geocapacity	Structural traps	761
Structural traps below 800 m				
4	This study	Basin Modelling	Structural traps (sealing faults) below 800 m	70
5	This study	Basin Modelling	Structrural taps (open faults) below 800 m	10
6	SGU	USDOE	Structural traps below 800 m (?)	<100
7	Sopher et al. 2014	USDOE	Structural closures of Faludden, När and Viklau	74-26
Stratigraphic traps whole AOI				
8	SGU	USDOE	Stratigraphic traps	400-4500
9	SLR	Geocapacity	Stratigraphic trap below 800 m	1923
10	Sopher et al. 2014	USDOE	Stratigraphic trap	6962-4330
11	NORDICCS	USDOE	First estimates effective capacity	745
Dynamic reservoir model				
12	This study	ECLIPSE	Dynamic migration	250

The results for the screening of "safe injection sites" further point out the prominent influence of the fault distribution on possible CO_2 migration after injection (Figure 7-5). By using the basin modelling approach and injection rates of 0.5 Mt/year over a period of 100 years it was not possible to map safe injection sites (migration out of the working area for the open and/or the sealing fault scenario). Only by reducing the injection rate to 0.23 Mt/year the CO_2 stayed within the working area. The injection site is located within the deepest part of the Faludden sandstone (Figure 7-5). In the basin modelling approach migration is simulated using the ray-tracing (flow path) technique and migration loss is spatially very limited. In proper reservoir simulator software, CO_2 flows along a migration front and covers a larger area. This is included in the dynamic ECLIPSE modelling of the Faludden sandstone which indicates that 250 Mt CO_2 can be injected into the formation. Thereof, around 4.1% migrates to depths shallower than 600 meters and approximately 42.5% of the injected CO_2 is dissolved into the formation water after 6000 years.

8. Simulations of the Arnager Greensand Formation, south-western Scania

The Arnager Greensand Formation is situated in the south-western Scania in Sweden (Figure 7-1).

8.1 Geological description of the Arnager Greensand Formation

The Arnager Greensand Formation is confined to the north-east by the Romeleåsen Fault Zone continuing to the south-west across the Swedish economic zone. Presence in the Kristianstad Basin is not well documented even though the formation in this area is acknowledged. The sandstone is only known from deep drillings in Scania and surrounding offshore areas at depths from 1200 - 1700 m. In Denmark the Arnager Greensand Formation is outcropped at the island of Bornholm. Thickness varies in south-west Scania from almost 20 m in the north-western part of the area to c. 60 m in the southern part of the area. In the Kristianstad Basin thickness are maximum 20 m (Erlström, pers.com.). The Arnager Greensand was deposited in the Early Albian-Cenomanian in a marine setting.

8.1.1 The CO_2 storage properties to Arnager Greensand Formation

In terms of CO_2 storage the Arnager Greensand Formation represents a partly fault confined open saline aquifer with a regional distribution weakly dipping 1─2 degrees to the north-east. The part of the Arnager Greensand Formation suitable for CO_2 storage is located south-west from the Romeleåsen Fault Zone and covers an area of almost 5200 km² on Swedish territory (Mortensen 2014). The storage unit contains no traps or closures (Erlström et al. 2011).

The Arnager Greensand Formation is dominated by poorly consolidated fine- to medium-grained glauconitic quartz sandstone. Other components such as pyrite, micas, zircon and feldspars occur as associate minerals. Glauconite occurs very abundant, as grains as well as mineralization on other grains. Only minor amounts of carbonate occur and only in the northern part of the area, clay is occurring as a matrix. Porosity is very high, averaging 26%. Estimated average permeability is c. 400 mD, but more than 1 D has been measured (Erlström et al. 2011). The net/gross is very high and are estimated to 80% (Mortensen 2014).

8.1.2 The caprock unit

The Arnager Greensand Formation is followed by approximately 1000 m of Late Cretaceous to Palaeocene clayey limestone and chalk with interbeds of silt- and sandstone (Figure 8-1).

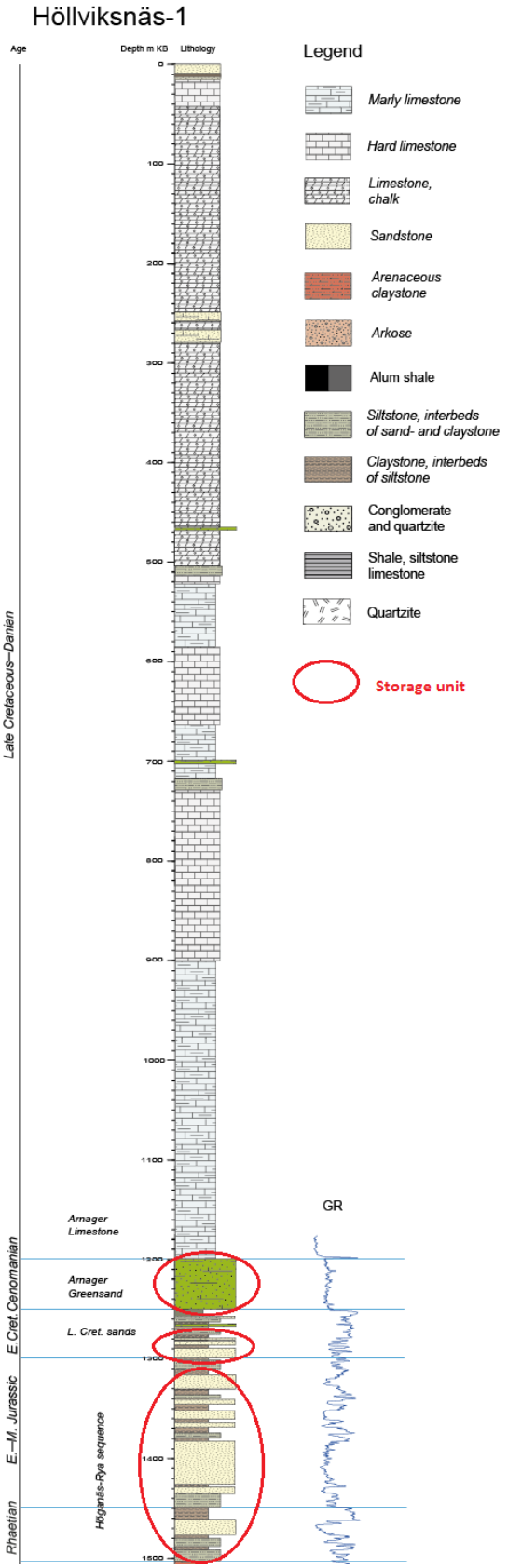

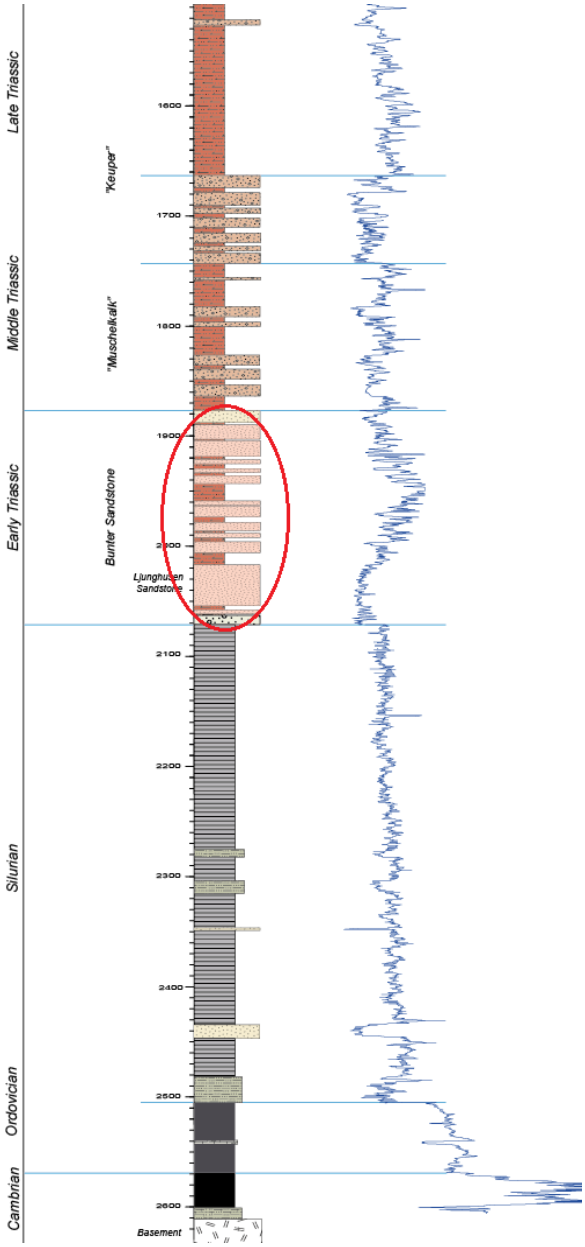

Figure 8-1 Generalized litho-stratigraphic log from the south-west Scania (Höllviksnäs-1).

8.2 Modelling input data

Input parameters for the modelling approach are given in Table 8-1 and shown in Figure 8-2. The unit surface and fault map were constructed from available interpreted seismic lines and well data (SGU and OPAB). The modelling work only concerned the part of the formation within the Swedish borders and is limited by the extent of seismic surveys. For the bathymetric maps we used data provided by the Baltic Sea Hydrographic Commission (2013).

Table 8-1 Parameters used for the basin modelling approach. Faults in the south-west Scania are identified by combining the SGU's digital bedrock map together with SGU's bedrock maps series Af nr 191 and 196.

Name	Depth [b.msl]	Thickness [m]	N/G	Porosity [%]	Thermal gradient [°C/km]	Surface temperature [°C]	Permeability [mD]
Arnager Greensand	Map seabed	40.5	0.80	26	35	4	400

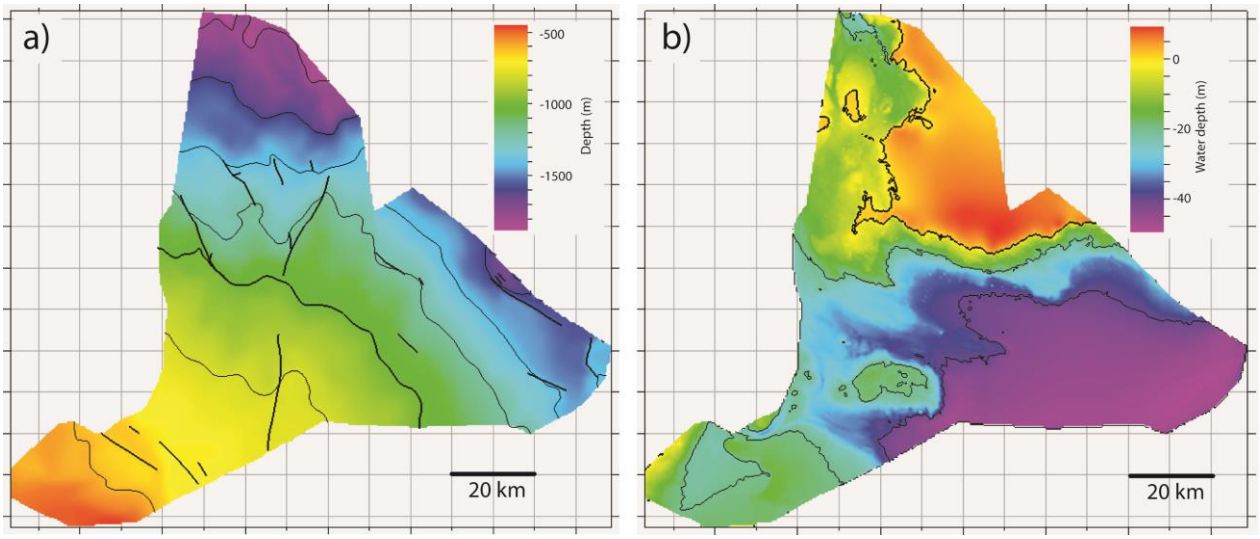

Figure 8-2 Input maps for the Arnager Greensand Formation. a) Top of the Arnager Greensand with interpreted faults. b) Present day bathymetry.

8.3 Results from the basin modelling approach

a) Total trap storage capacity

For the Arnager Greensand Formation the total trap storage capacity were calculated (methodology described in chapter 4.3) assuming two end-member scenarios with open and sealing faults. We report the results for the whole stratigraphic units and for the parts below a depth of 800 m.

For the Arnager Greensand Formation a scenario without faults gives a total trap storage capacity of 26 Mt whereby 10 Mt can be stored below 800 m. The sealing fault scenario gives higher capacities of 132 Mt and 115 Mt below 800 m depth (Figure 8-3).

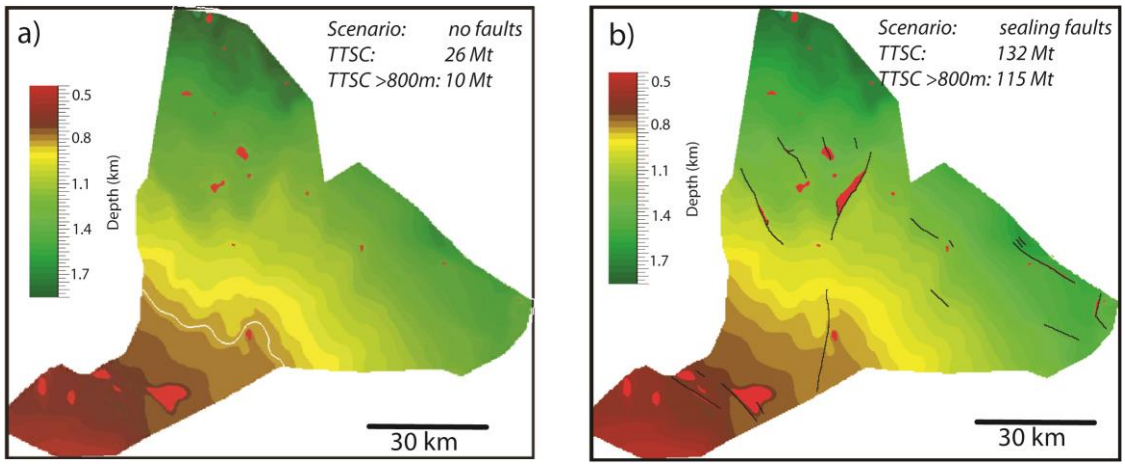

Figure 8-3 **Estimates of the total trap storage capacity (TTSC) for the Arnager Greensand Formation. The total trap storage capacity depends on the sealing efficiency of faults. The maps are top surface of the Arnager unit overlain by traps (red areas), black lines are faults (b) and the white line is (a) the 800 m depth isopach.**

b) Screening of safe injection sites

The basin modelling approach was used for a systemic screening for "safe injection sites" (see chapter 4.3). First, we injected CO_2 with a rate of 0.5 Mt/year over a period of 100 years. For the Arnager Greensand no safe injection site could be identified. CO_2 migration paths strongly depend on the fault distribution (Figure 8-4). Thus, for most of the tested injection sites safe sites for the no fault scenario spilled out of the working area for the fault scenario or vice versa. Only by reducing the CO_2 injection rates to 0.08 Mt/year a safe injection site could be identified. The chosen site is located close to the north-western border within the deepest part of the working area (Figure 8-4).

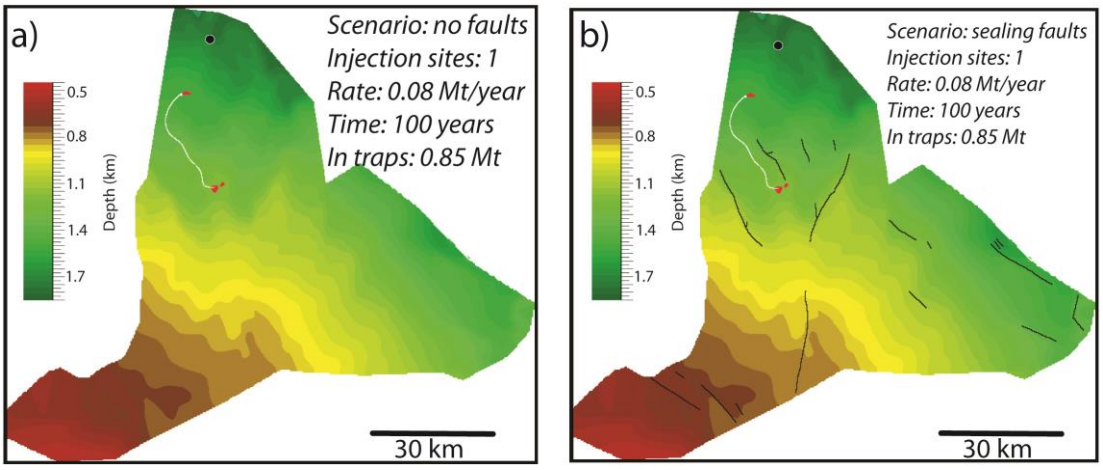

Figure 8-4 **Results of screening for "safe injection sites". The maps are top surfaces of the Arnager Greensand unit overlain by traps (red areas). The black lines are faults (b) and the white lines indicate active spill-paths (a). Injection sites are marked with the black circle. In this modelling approach we used CO_2 dissolution during migration and in the trap entities.**

8.4 Description of reservoir simulation models

Reservoir model for the mapped areas of the Arnager Greensand aquifer unit has been constructed using Petrel. For the simulation model, temperature and formation water salinity have been set constant to 40° C and 6.3% total dissolved salts (TDS) respectively. The salinity and temperature are uncertain but the applied values are assumed representative for the injection depths in the model and are on the conservative side with respect to CO_2 migration into the shallower regions. The relative permeability functions are linear with residual gas saturation equal to 0.2 and residual water saturation equal to 0.07. Capillary pressure between CO_2 and water are set to zero (see Bergmo *et al.*, 2013).

The simulation grid for the Arnager Greensand model has approximately 870 000 grid blocks with lateral grid resolution of 500 by 500 metres. The grid was constructed based on the depth map of the top Arnager Greensand, interpreted faults and an average thickness interpreted from existing and available wells. The thickness of the model is 40 meter and the model has 12 layers with refining layer thickness towards the top. The two upper layers have thickness 1 meter. Figure 8-5 shows the outline of the modelled area with depth of the top Arnager Greensand.

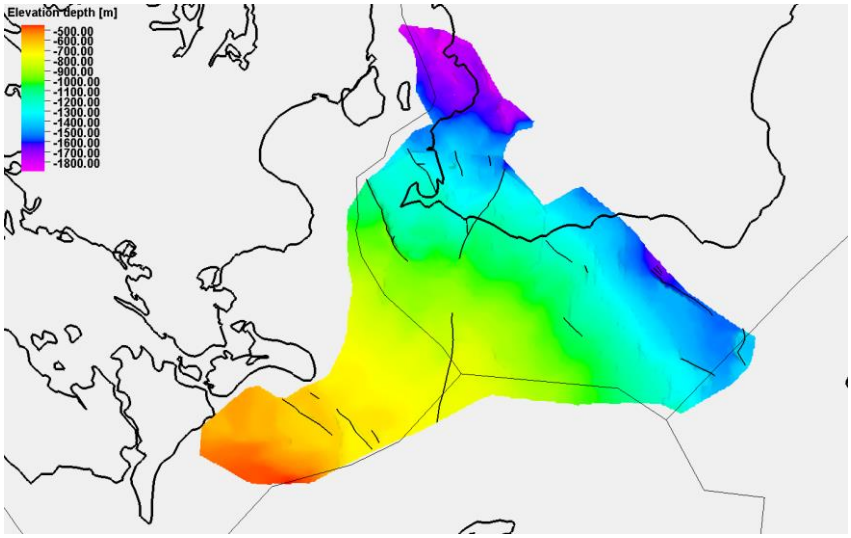

Figure 8-5 Outline of the modelled area for the Arnager Greensand aquifer unit. The figure shows top depth with interpreted faults. Observe that parts of the model extend into Danish and German territory.

Average reservoir properties for the Arnager Greensand are listed in Table 7-1. As for the Faludden model, the reservoir model was populated using a stochastic Gaussian distribution function based on interpretation from existing and available well logs (SGU). Porosity varies between 13 and 33% with average value equal to 26% and permeability varies between 30 and 1000 mD with average value equal to 400 mD. Net to gross is set constant to 80%. Only one realisation with the given reservoir properties (porosity and permeability) has been generated. Figure 8-6 shows distribution of porosity and permeability in the top layer of the model.

a) b)

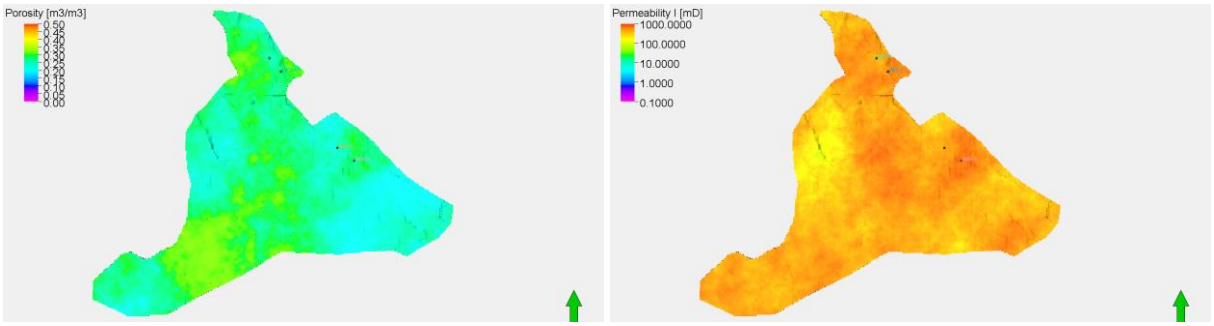

Figure 8-6 a) Porosity and b) permeability distribution in the top layer of the Arnager Greensand reservoir model.

To represent the part of the formation not included in the model, pore volume multipliers have been applied to the boundary grid blocks on all sides of the model. In addition, production wells are located down flank from the injection wells to constrain the induced pressure increase from CO_2 injection. A safety pressure limit below the cap rock is assumed to be 75% of the lithostatic pressure (average overburden density equal to 2500 kg/m^3 is assumed). A series of tests to optimise the position, number and rates for injection wells resulted in four injection wells with injection rates between 0.25 (southern wells) and 1 Mt/year (northern wells) located in the deepest part of the formation. In addition, five production wells producing at constant bottom hole pressure (hydrostatic pressure) were positioned down-flank from the injectors. Figure 8-7 displays CO_2 saturation at the top twenty years after injection indicating the positions of the injection and production wells.

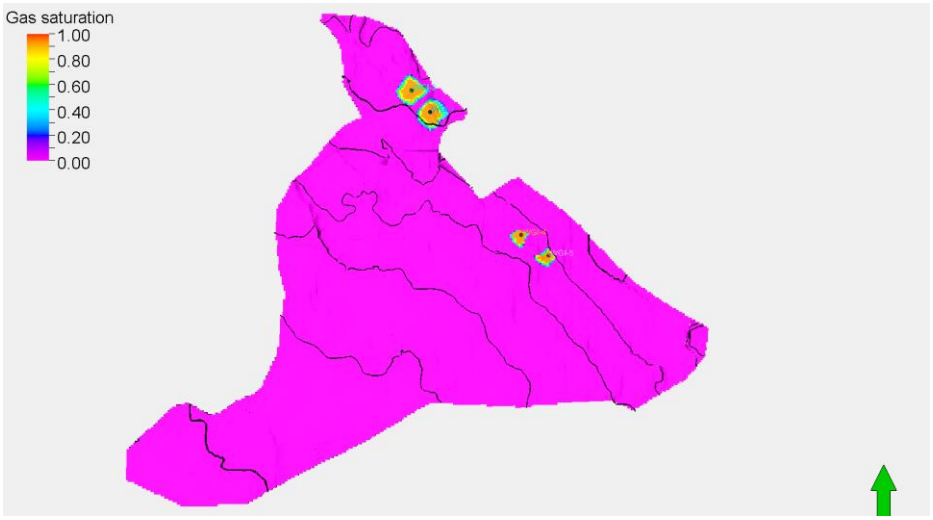

Figure 8-7 CO_2 distribution at top Arnager Greensand after 20 years injection showing position of injection wells. The iso-depth curves (black) starts at 600 m (south-west) and has a 200 m interval between them.

The model has very small and only a few structural traps and the main trapping mechanism is expected to be capillary trapping as residual gas and trapping by dissolution of CO_2 into the formation water.

8.5 Results from dynamic reservoir simulations for the Amager Greensand

As mentioned above there are almost no structural traps in the Arnager Greensand model and the amount of injected CO_2 is adjusted so that only a small fraction of the CO_2 migrates to areas shallower than 800 m and outside the Swedish territorial border. In the final simulation case a total of 225 Mt CO_2 was injected through four injection wells with rates 1 Mt/year (two northernmost wells) and 0.25 Mt/year (two southernmost wells). Figure 8-8 shows CO_2 saturation at the end of the injection period.

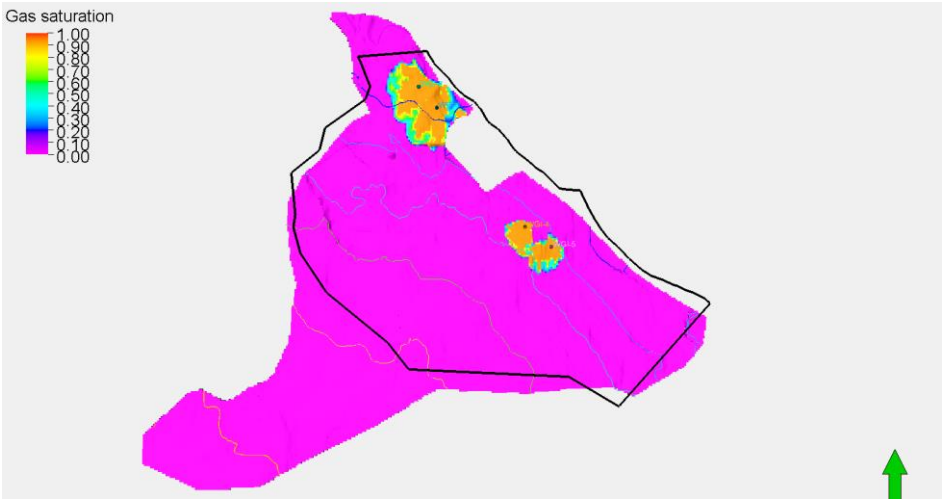

Figure 8-8 CO_2 saturation at the end of the injection period (100 years). Iso-depth curves are plotted on top of the model (200 meter intervals) and the defined storage area (Swedish territory) is indicated by the black polygon.

The model is simulated for 6000 years and shows the final distribution of CO_2 at the end of the simulation. Observe that a small fraction of CO_2 has migrated out of the Swedish territorial border and that a part of the CO_2 has migrated to a region shallower than 800 m.

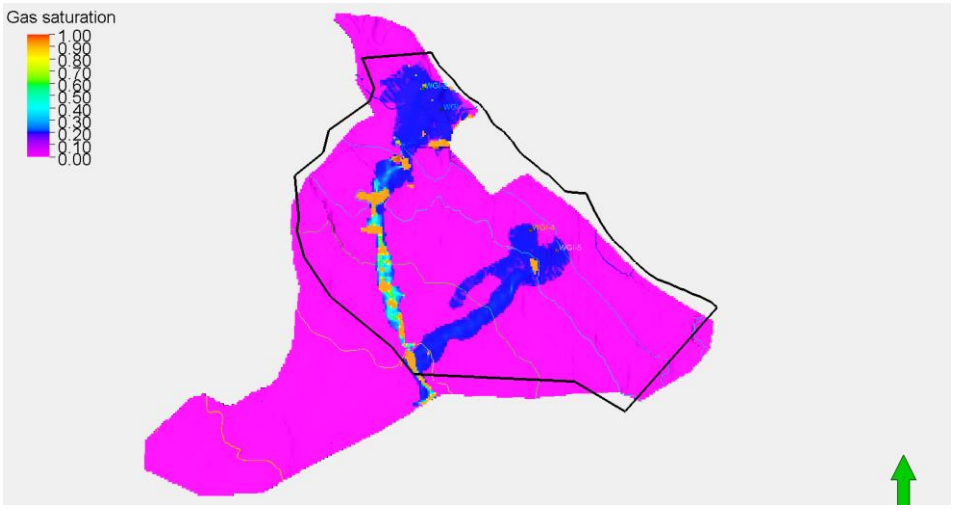

Figure 8-9 Final CO_2 distribution after 6000 years in the Arnager Greensand model.

Figure 8-9 shows the volume of CO_2 deeper than 800 meters and shallower than 800 meters after 6000 years. The amount of CO_2 that has migrated to the shallow region (<800 m) is approximately 7 Mt (3.3%). Tests where the southernmost wells had an injection rate equal to 1 Mt/year (total injected 400 Mt) showed

that approximately 14% of the injected CO_2 ended up in the region shallower than 800 meters indicating that the increased rate for those two wells will increase the migration to shallower areas by around 10% (Figure 8-10).

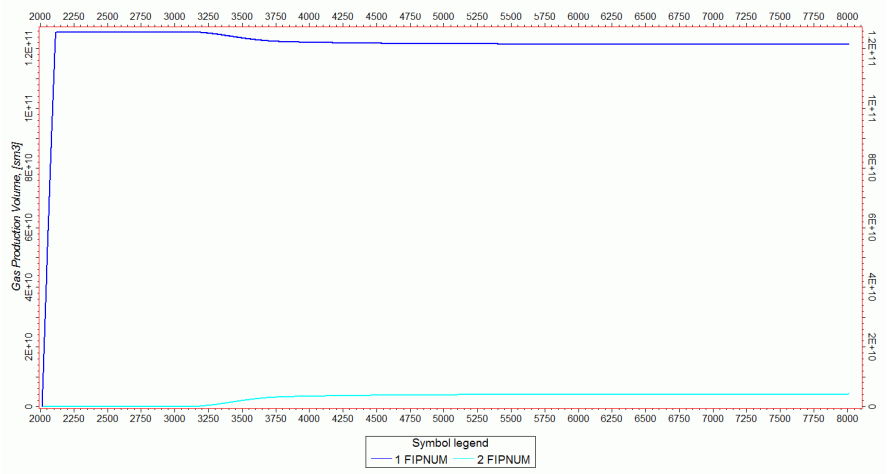

Figure 8-10 Volume CO_2 in the two different depth regions as function of time. FIPNUM 1 is deeper than 800 m, FIPNUM 2 is shallower than 800 m.

Simulation results show that approximately 26% of the injected CO_2 is dissolved after 6000 years. This is illustrated in Figure 8-11.

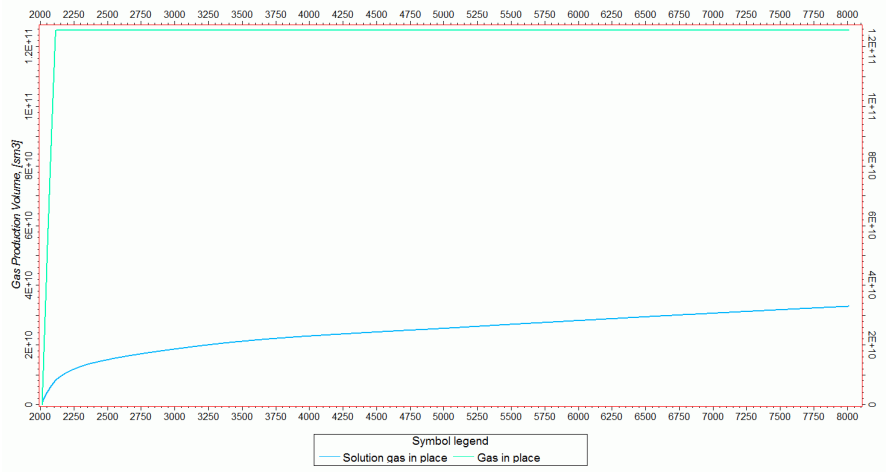

Figure 8-11 Total injected CO_2 volume (red) and dissolved CO_2 volume as function of time.

7.4.5 Summary from Eclipse simulations of the Arnager Greensand

The simulation results indicate a storage capacity for and the Arnager Greensand in the order of 225 Mt CO_2. Only 3.3% of the injected CO_2 migrates to shallower regions (<800 m) and approximately 26.2% of the CO_2 is dissolved into the formation water after 6000 years.

It should be noted that there are large uncertainties in the models which will affect both the migration speed and distance, the residual trapping and the dissolution of CO_2 into the formation water. The results are, however, considered representative in giving an approximate estimate of storage capacity. The parameters are for the most cases considered conservative and further studies with more data is required to confirm this.

8.6 Discussion

Previous studies indicated that the Arnager Greensand Formation in south-west Scania contains no structural traps or closures (Erlström et al. 2011). However, using the definition for structural traps given in Figure 7-15 several traps can be mapped (Figure 8-3). Using the basin modelling approach these traps can store 132 Mt to 26 Mt depending on the fault sealing efficiency. Thereby, 115 Mt to 10 Mt can be stored in parts of the formation located below 800 m (Figure 8-3, Figure 8-2). The higher estimates refer to the sealing fault scenario demonstrating also for the Arnager Greensand Formation the importance of the fault distribution and their sealing efficiency.

Similar to the Faludden sandstone, by injecting 0.5 Mt CO_2/year the CO_2 migrates beyond the boundaries of the working area. Only by reducing the injection rate to 0.08 Mt/ year "safe injection sites" could be mapped in the deepest, north-western part of the working area (Figure 8-4). However, the dynamic ECLIPSE model for the Arnager Greensand indicates that ca. 225 Mt (Figure 8-2) CO_2 can be injected and only 3.3% of the CO_2 migrates to shallower regions (<800 m). Approximately 26.2% of the CO_2 is dissolved into the formation water after 6000 years.

Table 8-2 Comparison of different CO_2 storage capacity estimates for the Arnager Greensand Formation.

ID	Author	Method	Comment	Storage capacity (Mt)
Structural traps - whole AOI				
1	This study	Basin Modelling	Structural traps (sealing faults)	132
2	This study	Basin Modelling	Structural traps (open faults)	26
Structural traps below 800 m				
3	This study	Basin Modelling	Structural traps (sealing faults) below 800 m	115
4	This study	Basin Modelling	Structrural taps (open faults) below 800 m	10
Stratigraphic traps whole AOI				
5	NORDICCS	USDOE	First estimates effective capacity	521
Dynamic reservoir model				
6	This study	ECLIPSE	Dynamic migration	225

9. Summary

There is a large spread in how "mature" CO_2 storage is in the three countries Denmark, Norway and Sweden. For Norway at one hand, a large amount of data exits, and there is a solid base for selecting storage sites, while for Sweden new ground braking work is carried out on mapping possible sites and also on the simulations to estimate the capacity.

In order to quantify the CO_2 storage potential dynamic modelling has been carried out for different formations including:

- the Gassum Formation in the Skagerrak area (Denmark)

- the Garn Formation at the Trøndelag Platform (Norway)

- the Faludden sandstone in south-west Scania (Sweden)

- the Arnager Greensand Formation in south-east Baltic Sea (Sweden)

For the Danish sector dynamic reservoir simulation was carried out on different scales and locations (Figure 3-1). (1) The open dipping Gassum Formation has an estimated pore volume of ca. $4.1 \cdot 10^{11}$ m^3. The pore volume of the simulation model is $1.1 \cdot 10^{11}$ m^3 and assuming the same storage efficiency for the larger area as in the simulation model would give a storage capacity of 3.7 Gt CO_2 for the north-eastern part of the Gassum Formation. This represent a storage efficiency of 1.6% (plus ~25% dissolved CO_2) in the open dipping aquifer. (2) Dynamic models for the Hanstholm structure, offshore Denmark give a storage capacity of ca. 1.17 Gt. (3) The capacities for the Vedsted structure is ca. 0.125 Gt.

The Garn Formation on the Trøndelag Platform offshore middle Norway (Figure 4-1) has in the structural closures a storage capacity of ca. 2.0 Gt to 5.2 Gt. This estimate is made assuming no migration loss and a very low dissolution rate in the traps. Scanning of safe injection sites revealed several locations where CO_2 with a rate of 1 Mt/year could be injected without migrating out of the working area. These sites were verified using different modelling approaches.

The Faludden sandstone in south-west Scania, Sweden (Figure 7-1) can store at least 561 Mt CO_2 in structural traps, but below 800 m with the capacity is just 10 Mt. The dynamic ECLPISE models indicate that 250 Mt CO_2 can be injected into the sandstone with only 4.1% migrating to shallow depth above 600 m.

Within the Arnager Greensand Formation in the south-east Baltic Sea, Sweden (Figure 7-1) structural traps could be identified. Within these traps at least 26 Mt CO_2 can be stored where the storage capacity below 800 m is reduced to only 10 Mt. The dynamic migration modelling suggests that c. 225 Mt CO_2 can be injected and only 3.3% would migrate to depths less than 800 m.

10. References

Aagaard, P., Anthonsen, K.L., Mortensen, G.M., Bergmo, P. & Snæbjörnsdottir, S.Ó. 2013. Screening and ranking of aquifer formations, storage units and traps. NORDICCS report D 6.2.1301.

Akervoll, I., Lindeberg, E. & Lackner, A. 2008: Feasibility of reproduction of stored CO_2 from the Utsira formation at the Sleipner gas field. Proceedings of the 9th International Conference on Greenhouse Gas Control Technologies, Washington, USA.

Allan, U.S. 1989: Model for hydrocarbon migration and entrapment within faulted structures. AAPG Bulletin 73(7), 803-811.

Anthonsen, K.L., Aagaard, P., Bergmo, P.E.S., Erlström, E., Faleide, J.I., Gislason, S.R., Mortensen, G.M.& Snæbjørnsdottir, S.Ó. 2013: CO_2 storage potential in the Nordic region. Energy Procedia, 37, 5080-5092.

Anthonsen, K. L., Aagaard, P., Bergmo, P. E., Gislason, S.R., Lothe, A.E., Mortensen, G. M., Snæbjornsdottir, S.O. 2014: Characterisation and Selection of the Most Prospective CO_2 Storage Sites in the Nordic Region. Energy procedia, 63, 4884-4896.

Bennion, D.B. and Bachu, S. 2006(1): Supercritical CO_2 and H2S – Brine Drainage and Imbibition Relative Permeability Relationships for Integral Sandstone and Carbonate Formations, Paper SPE 99326, SPE Europec/Eage Annual Conference and Exhibition, Vienna, Austria, 12 – 15 June, 2006.

Bergmo, P.E.S., Pham Van, T.H., Nielsen, L.H., Kristensen, L., Fawad, M., Faleide, J.I. & Aagaard, P. A. 2011: Potential CO_2 Storage Play in Skagerrak – Injection Strategy and Capacity of the Gassum Formation. Poster presentation at *TCCS-6*, Trondheim.

Bergmo, P. 2013: Memo: Method for ranking storage sites in NORDICCS WP6. NORDICCS dissemination.

Bergmo, P. E., Baig, I., Aagaard, P. & Nielsen, L. H. 2013: Estimation of storage capacity in the Gassum Formation in Skagerrak. Talk on the *7th Trondheim CCS Conference, 4th-5th of June 2013*.

Bergmo, P.E., Grimstad, A.-A., Lindeberg, E., Riis, F. & Johansen, W.T. 2009: Exploring geological storage sites for CO_2 from Norwegian gas power plants: Utsira South, Energy Procedia, vol. 1, issue 1, 2953-2959.

Bergmo, P.E., Lindeberg, E., Riis, F. & Johansen, W.T. 2009: Exploring geological storage sites for CO_2 from Norwegian gas power plants: Johansen formation, Energy Procedia, vol. 1, issue 1, 2945-2952.

Bergmo, P.E., Polak, S., Aagaard, P., Frykman, P., Haugen, H. A. & Bjørnsen, D. 2013: Evaluation of CO_2 storage potential in Skagerrak. Energy Procedia, vol. 37, 4863-4871.

Blystad, P., Færseth, R.B., Larsen, B.T., Skogseid, J. & Tørudbakken, B. 1995: Structural elements of the Norwegian continental shelf, Part II. *The Norwegian Sea Region. Norwegian Petroleum Directorate Bulletin*, 8, 44 p.

Brangulis, A.P., Kanev, S.V., Margulis, L.S. & Pomerantseva, R.A. 1993: Geology and hydrocarbon prospects of the Paleozoic in the Baltic region. Petroleum Geology '86 Ltd, 651-656.

Bøe, R., Magnus, C., Osmundsen, P.T. & Rindstad, B.I. 2002: CO_2 point sources and subsurface storage capacities for CO_2 in aquifers in Norway. NGU report 2002.010, 132 p.

Bøe, R., Zweigel, P., Polak, S. & Lindeberg, E. 2005: Potential risks associated with CO_2 storage, Case Study Mid-Norway, CO_2STORE project, NGU report: 2005.043/SINTEF report: 54.5272/01/05.

Corfield, S., Sharp, I., Häger, K. O., Dreyer, T., & Underhill, J. 2001: An integrated study of the Garn and Melke formations (Middle to Upper Jurassic) of the Smørbukk area, Halten Terrace, mid-Norway. In: Martinsen, O.J. and Dreyer, T. (Eds) Sedimentary Environments Offshore Norway - Paleozoic to Recent, 199-210.

Dalhoff, F., Klinkby, L., Sørensen, A.T., Bernstone. C., Frykman. P., Andersen, C. & Christensen, N.P. 2011: CCS demo Denmark: The Vedsted case, Energy Procedia, v. 4, p. 4704-4710, ISSN 1876-6102,

Dalland, A.G., Worsley, D. & Ofstad, K. 1988: A lithostratigraphic scheme for the Mesozoic and Cenozoic succession offshore mid-and northern Norway. *Norwegian Petroleum Directorate, 65*.

ECLIPSE 100., 2007, Schlumberger Information Solutions.

Eigestad, G. T., Dahle, H. K., Hellevang, B., Riis, F., Johansen, W. T.& Øian, E. 2009: Geological modeling of the Johansen formation, Computational Geosciences, 13(4), 435-450.

Elenius, M. & Gasda, S. E. 2012. Impact of tight horizontal layers on dissolution trapping in geological carbon storage. *XIX International Conference on Water Resources, CMWR 2012, June 17-22 2012*

Erlström, M., Frederiksson, D., Juhojuntti, N. Sivhed, U. & Wickström, L. 2011: Lagring av koldioxid i berggrunden - krav, förutsättningar och möjligheter. SGU, Rapporter och meddelanden 131.

Erlström, M. & Sivhed, U. 2012: Overview of existing data, Swedish sector. Geological Survey of Sweden/Dissemination of NORDICCS.

Fawad, M., Sassier, C., Jarsve, E.M., Aagaard, P., Faleide, J.I., Nielsen, L.H., Kristensen, L. & Bergmo, P.E.S. A. 2011: Potential CO_2 Storage Play in Skagerrak – Depositional Environment and Reservoir Geology of the Gassum Formation. Poster presentation at *TCCS-6*, Trondheim 2011.

Fenghour, A., Wakeham, W.A. & Vesovic, V. 1998: Viscosity of Carbon dioxide. *J. Phys. Chem. Ref. Data*, 27, 1.

Frykman, P., Bech, N., Sørensen, A.T., Nielsen, L.H, Nielsen, C.M., Kristensen, L. & Bidstrup, T. 2009: Geological modeling and dynamic flow analysis as initial site investigation for large-scale CO_2 injection at the Vedsted structure, NW Denmark, Energy Procedia, v. 1, Issue 1, , p. 2975-2982, ISSN 1876-6102,

Frykman, P., Nielsen, C.M., Dalhoff, F., Sørensen, A.T., Klinkby, L., Nielsen, L.H. 2011:Geological modelling for site evaluation at the Vedsted structure, NW Denmark, Energy Procedia, v. 4, p. 4711-4718, ISSN 1876-6102, http://dx.doi.org/10.1016/j.egypro.2011.02.433

Gjelberg, J., Dreyer, T., Høie, A., Tjelland, T. & Lilleng, T. 1987: Late Triassic to Mid-Jurassic development on the Barents and Mid-Norwegian shelf. In: Brooks, J. and Glennie, K. (eds), Petroleum Geology of North West Europe. Graham and Trotman, London, 1105-1129.

Grøver, A. Rinna, J., Lothe, A.E., Bergmo, P. & Wessel-Berg, D. 2013: How and when could basin modelling approaches be useful for CO_2 storage assessment? *Poster on the 7th Trondheim CCS Conference, 4th-5th of June 2013.*

Halland, E.K. et al. 2012: CO_2 Storage Atlas Norwegian North Sea.

Halland, E., K., Gjeldvik, I.T., Tjelta Johansen, W., Magnus, C., Meling, I.M., Mujezinović, J., Pham, V. T.H., Riis, F., Sande Rod, R., & Tappelet, I.M. 2013a: CO_2 Storage Atlas Norwegian Sea, 60p.

Halland et al. 2013b: CO_2 Storage Atlas Barents Sea.

Japsen, P. & Langtofte, C. 1991: Geological map of Denmark 1:400 000 "Top Trias" and the Jurassic–Lower Cretaceous. Danmarks Geologiske Undersøgelse Map series 30.

Kestin, J., Khalifa, H.E., Abe, Y., Grimes, C.E., Sookiazian, H. & Wakeham, W.A. 1978: Effect of pressure on the viscosity of aqueous sodium chloride solutions in the temperature range 20-150°C. J. Chem. Eng. Data, 23, 328–336.

Larsen, M., Bidstrup, T. & Dalhoff, F. 2003: CO_2 storage potential of selected saline aquifers in Denmark. Danmarks og Grønlands Geologiske Undersøgelse Rapport 2003/39, pp. 83.

Lindeberg, E., Vuillaume, J.F., Ghaderi, A. 2009: Determination of the CO2 storage capacity of the Utsira formation, Energy Procedia, vol. 1, issue 1, 2777-2784.

Lothe, A.E., Pluymaekers, M., Grøver, A., Shi, J-Q., Rinna, J. 2013: SiteChar Deliverable 6.2. CO_2 migration modelling on basin scale, Trøndelag Platform, 41 p.

Lothe, A.E., Emmel, B., Grøver, A., Bergmo, P.E. 2014: CO_2 Storage Modelling and Capacity Estimation for the Trøndelag Platform, Offshore Norway - using a Basin Modelling Approach. Energy Procedia, vol. 63, 3648-3657.

Lundin, E., Polak, S, Bøe, R., Zweigel, P. & Lindeberg, E. 2005: Storage potential for the CO_2 in the Froan Basin area of the Trøndelag Platform, Mid-Norway. Sintef report (54.5272.00/01/05) and NGU report (2005.027). 47 p.

Martinius, A.W., Ringrose, P.S., Brostrøm, C., Elfenbein, C., Næss, A. & Ringås, J.E. 2005: Reservoir challenges of hetrolithic tidal sandstone reservoirs in the Halten Terrace area, mid-Norway, Petroleum Geoscience, 11, 3-16.

Maurand, N., Le Gallo, Y. & Frykman, P. 2009: CO_2 injection simulation and statistical sensitivity analysis in an offshore saline aquifer. Presentation at IFP Scientific Conference "Deep Saline Aquifers for Geological Storage of CO_2 and Energy". 27-29 May 2009, IFP/Rueil-Malmaison, France.

Mbia, E.N, Frykman, P., Nielsen, C.M., Fabricius, I.L., Pickup, G.E., Bernstone, C.: 2013. Caprock compressibility and permeability and the consequences for pressure development in CO_2 storage sites. International Journal of Greenhouse Gas Control, Volume 22, Pages 139-153. Doi:10.1016/j.ijggc.2013.12.024.

Mbia, E.N., Fabricius, I.L., Krogsbøll, A., Frykman, P. and Dalhoff, F.: 2014. Permeability, compressibility and porosity of Jurassic shale from the Norwegian–Danish Basin. Vol. 20, pp. 257–281. doi:10.1144/petgeo2013-035

Michelsen, O. & Clausen, O.R. 2002: Detailed stratigraphic subdivision and regional correlation of the southern Danish Triassic succession. Marine and Petroleum Geology 19, 563–587.

Mortensen, G.M., 2014: CO_2 Storage Atlas for Sweden - a contribution to the Nordic Competence Centre for CCS, NORDICCS. Poster and abstract to the 31st Geological Winter Meeting 2014.

Nielsen, L.H. 2003: Late Triassic – Jurassic development of the Danish Basin and the Fennoscandian Border Zone, southern Scandinavia. In: Ineson, J.R. & Surlyk, F. (Eds.) The Jurassic of Denmark and Greenland. Geology of Denmark Survey Bulletin 38.

Nielsen, C.M., Frykman, P.& Dalhoff , F. 2013: Synergy Benefits in Combining CCS and Geothermal Energy Production, Energy Procedia, ISSN 1876-6102, http://dx.doi.org/10.1016/j.egypro.2013.06.146, v. 37, 2622-2628.

Nielsen, L.H. & Japsen, P. 1991. Deep wells in Denmark 1935–1990. Lithostratigraphic subdivision. Geological Survey of Denmark, DGU Series A 31, 179 pp.

OPAB, 1976: Baltic Sea, Exploration activities 1971-1976. Geology and Petroleum prospects.
OPAB, 1976: Gotland, Exploration activities 1972-1976. Geology and Petroleum prospects.
Peneloux, A., Rauzy, E. and Fréze, R.: A consistent correction for Redlich-Kwong-Soave volumes, Fluid Phase Equilibria 8, 7-23, 1982.
Rinna, J., Grøver, A., Frykman, P., Pluymaekers, M., Shi, J.-Q., Volpi, V. & Lothe, A.E. 2013:Characterization of a potential CO_2 storage site offshore mid Norway using migration modelling tools on a basin-wide scale. Talk on the 7th Trondheim CCS Conference, 4th-5th of June 2013.
Sliaupa, S., Sliaupiene, R., Nulle, I., Nulle, U., Shogenova, A., Shogenov, K., Jarmo, K., Wickström, L. & Erlström, E. 2012: Options for geological storage of CO_2 in the Baltic Sea region. Contribution to the ENeRG network and the CGS Europe project.
Sopher, D., Juhlin, C., Erlström, M. 2014. A probabilistic assessment of the effective CO_2 storage capacity within the Swedish sector of the Baltic Basin, International Journal of Greenhouse Gas Control, 30, 148-170.
Span, R. & Wagner, W.1996: A new equation of state for carbon dioxide covering the fluid region from the triple-point temperature to 1100 K at pressures up to 800 MPa. J. Phys. Chem. Ref. Data, v. 25, no. 6, 1509-1596.
Spivey, J.P., McCain, W.D. Jr. & North, R. 2004: Estimating density, formation volume factor, compressibility, methane solubility, and viscosity for oilfield brines at temperatures from 0 to 275°C, pressures to 200 MPa, and aalinities to 5.7 mole/kg. *JCPT*.
Spycher N, Pruess, K., Ennis-King, J. 2005: CO_2-H_2O Mixtures in the Geological Sequestration of CO_2. II. Partitioning in Chloride Brines at 12−100°C and up to 600 bar. *Geochimica et Cosmochimica Acta*, v. 69, no. 13, 3309–3320.
Storvoll, V. & Bjørlykke, K. 2004: Sonic velocity and grain contact properties in reservoir sandstones. Petroleum Geoscience, 10, 215-226.
Sylta, Ø. 2004: Hydrocarbon migration modelling and exploration risk. *Ph.D. thesis, NTNU Trondheim.*
The Baltic Sea Hydrographic Commission, 2013, Baltic Sea Bathymetry Database version 0.9.3. Downloaded from http://data.bshc.pro/ downloaded on 01.10.2014.
Wessel-Berg, D. 2013: Upscaling of dissolution of CO_2. Poster at the 7th Trondheim CCS Conference, 4th-5th of June 2013.
Zweigel, P., Arts, R., Lothe, A. E. & Lindeberg, E. B. G. 2004: Reservoir geology of the Utsira Formation at the first industrial-scale underground CO_2 storage site (Sleipner area, North Sea). Geoloigcal Society, London, Special publications 2004, v. 233,165-180.